

**V/STOL AND STOL GROUND EFFECTS**

**AND**

**TESTING TECHNIQUES**

**by R. E. Kuhn**

**PREFACE**

The contract under which this report was prepared is a part of the NASA Ames Research Center effort to improve our understanding of the ground effects associated with V/STOL operation and to develop the equipment and testing techniques needed for this effort. Primary emphasis is on future experimental programs in the 40 by 80 and the 80 by 120 foot test sections and in the outdoor static test stand associated with these facilities.

Task I of the present contract covers a review of the commonly used experimental techniques and a comparison of data obtained by various techniques with each other and with available estimating methods. These reviews and comparisons provide insight into the limitations of past studies and the testing techniques used and identify areas where additional work is needed.

Task II will examine and recommend testing methods appropriate to the 40 by 80, 80 by 120 and static test stand facilities.

This contract work is being conducted under guidance of James Eshleman (contract monitor), David Koenig and Richard Christiansen of the 40 by 80 staff. Their help and advice is gratefully acknowledged.

# SYMBOLS

A	Aspect ratio
$A_j$	Jet area, $m^2$
b	Wing span, m
c	Wing chord, m
$C_L$	Lift coefficient
$\Delta C_L$	Lift coefficient increment
$\Delta C_m$	Pitching moment coefficient increment
$C_p$	Pressure coefficient
D	Plate diameter, m
$\bar{D}$	Planform angular mean diameter, m
d	Jet diameter, m
$d_e$	Equivalent single jet diameter, m
e	Jet spacing, m
h	Height, m
L	Lift, N
$\Delta L$	Induced lift increment, N
$\Delta L_f$	Fountain induced lift increment, N
NPR	Nozzle pressure ratio
$P_T$	Total pressure, $N/m^2$
$P_a$	Ambient pressure, $N/m^2$
$\Delta P$	Pressure increment, $N/m^2$
$q_\infty$	Free stream dynamic pressure, $N/m^2$
$q_n$	Jet dynamic pressure at nozzle, $N/m^2$

$q_{w,max}$	Maximum dynamic pressure in wall jet at a radial station, $N/m^2$
$R$	Radius of plate, m
$R_G$	Radius of ground board, m
$r$	Radial distance or corner radius, m
$S$	Total planform area, $m^2$
$S_L$	Area contained within LIDs, $m^2$
$T$	Thrust, N
$t$	Time, sec
$\Delta T$	Inlet temperature rise, deg
$T_a$	Ambient temperature, deg
$T_j$	Jet temperature at nozzle, deg
$u$	Vertical velocity in fountain, m/sec
$V$	Velocity, m/sec
$V_e$	Effective velocity ratio $V_e \approx \sqrt{q_\infty/q_n}$
$V_j$	Jet velocity at nozzle, m/sec
$V_w$	Velocity in wall jet, m/sec
$V_{w,max}$	Maximum velocity in wall jet at a radial station, m/sec
$x$	Longitudinal distance, m
$X$	Distance to leading edge of ground vortex flow field, m
$X_V$	Distance to ground vortex, m
$X_0$	Distance to zero pressure point, m
$z$	Vertical distance, m
$Z$	Depth of ground vortex flow field, m
$\alpha$	Angle of attack, deg
$\epsilon$	Downwash angle, deg
$\delta_j$	Jet or jet sheet deflection

## INTRODUCTION

The development of equipment and testing techniques for investigating the ground effects of V/STOL aircraft must be based on the available understanding of the flow phenomena involved. Our current understanding of the flow mechanisms involved in hovering and in transition in and out of ground effect is discussed under several categories in the main body of this report. The paragraphs that follow give a brief overview in an attempt to put the flow mechanisms in broad perspective.

The basic flow fields associated with hovering, transition and STOL operation of jet powered V/STOL aircraft are depicted in figure 1. The flow fields induce forces and moments on the aircraft which must be known in order to make accurate predictions of the performance and stability and control characteristics of the aircraft.

When hovering out of ground effect (upper left hand corner of fig. 1), the jet streams that support the aircraft entrain air and induce suction pressures on the lower surfaces. These pressures produce a small download, usually about 1 to 2 percent or less of the jet thrust. Because these downloads are small, the available empirical methods for estimating them (ref. 1) are adequate.

As the hovering aircraft descends into ground effect, the jet stream (or streams) impinge on the ground and form a radial wall jet flowing outward from the impingement point(s). These wall jets also entrain air and significantly increase the induced suction pressures and the resulting down load as the configuration approaches the ground. There have been many investigations of the jet induced suckdown for single jet configurations, and while the basic phenomena is well understood, there are significant differences in the results obtained by various investigators. These will be presented and discussed in later sections.

With multiple jet configurations, the radial wall jets flowing outward from their respective impingement points meet and form an upflow or "fountain". The impingement of the fountain on the aircraft produces an upload which usually partially offsets the suckdown created by the entrainment action of the wall jets. Unfortunately, the fountain flow also induces higher suction pressures between the jets and the fountains. The mechanisms involved are poorly understood and the present method for estimating the jet induced ground effects on multiple jet configurations are inadequate.

In the transition between hover and conventional flight, there are several flow mechanisms that induce forces and moments on the aircraft. The flow into the inlet produces an inlet momentum drag force and usually a nose up pitching moment. The exiting jet flow is deflected rearward by the free stream and rolls up into a pair of vortices. These vortices plus the blockage and entrainment action of the jets induce suction pressures behind and beside the jets and positive pressures ahead of the jets. The net effect for most jet V/STOL configurations is usually a loss in lift and a nose up pitching moment. However if the jets are at or near the trailing edge of the wing (particularly if they have appreciable spanwise extent as in a jet flap configuration) they induce positive lift and a nose down moment. The jet wake system also induces significant increases in the downwash at the tail.

In ground effect at transition speeds (STOL operation) all the above flow phenomena are present, but modified by the presence of the ground. In addition a ground vortex is formed by the action of the free stream in opposing the wall jet flowing forward from the impingement point(s) of the front jet(s). This ground vortex creates and defines the dust cloud produced when operating over loose terrain. It is also one of the hot gas ingestion mechanisms and it induces an additional lift loss and associated moment. Our knowledge of the factors that control the position and strength, and therefore the effects, of the ground vortex is incomplete at this time.

Both the ground vortex and the fountain flow are involved in hot gas reingestion. In hover the fountain flow provides a direct path to bring hot gasses into the vicinity of the inlet where they can be inhaled. The severity of this part of the hot gas problem can be controlled to some extent by the placement of the inlet, by the arrangement of the jets and by the use of suitable flow deflectors. At forward speed the ground vortex provides an additional path to bring the hot gas in the forward flowing wall jet back to the vicinity of the inlet. Our ability to design for minimum ingestion is compromised by our limited understanding of both the fountain flows and ground vortex.

The following sections will review each of these flow phenomena in more detail, present and compare the results of key investigations and make recommendations for the next steps in improving our understanding of the factors involved and in improving our ability to predict the aerodynamic and stability and control characteristics of V/STOL aircraft.

## SINGLE JET SUCKDOWN

### DATA BASE:

The first definitive work on jet induced suckdown in ground effect was done by Wyatt (ref. 2). He showed (fig. 2) that when the suckdown for plates of different sizes was plotted against the height divided by the plate diameter minus the jet diameter all the data would fall on a single curve. He also showed that the suckdown for noncircular plates would follow the same curve when the effective angular mean diameter,  $\bar{D}$ , of the planform is used.

A few years later Hall used a J-85 engine in a setup to measure the jet induced suckdown at large scale (ref. 3). His results (fig. 3) are in good agreement with the estimate based on Wyatt's work and appeared to indicate that any scale or real jet effects were negligible. However, the small scale results of reference 4 indicated somewhat more suckdown than either Wyatt's or Hall's work. There is considerable scatter in the data of reference 4 and most of the data were taken at higher nozzle pressure ratios than those for Wyatt's (ref. 2) data.

Other data also showed departures from Wyatt's and there have been several attempts to resolve these differences. One of these is presented in reference 1 (section 2.2.1) and attempted to examine the effects of pressure ratio by reanalysing available data. Excerpts from that study are presented in figures 4 and 5. In figure 4 Wyatt's data are compared with other data taken at low nozzle pressure ratios. There is considerable scatter in the data but it was found that if the exponent and the intercept value in Wyatt's expression are changed slightly most of the data falls within  $\pm 1$  percent of the new correlation line. Similar correlations at other nozzle pressure ratios showed that the effects of pressure ratio could be accounted for (within the data scatter) by making the exponent in Wyatt's expression a function of nozzle pressure ratio (fig. 5).

More recently Christiansen (ref. 7) conducted another large scale investigation. He used a J-97 engine to cover a wider range of nozzle pressure ratios than Hall's work. His results (fig. 6) show considerably higher values of suckdown at low heights than are predicted by any of the available modifications of Wyatt's method for estimating suckdown. They also show no effect of nozzle

pressure ratio (fig. 7). Clearly there are factors at work than have not been identified.

#### DISCUSSION:

There are several factors that could contribute to the differences shown in the results presented above. These include jet turbulence and the temperature, exit velocity distribution, cross gusts in the room in which the tests were conducted and the effects of ground board size. Few of the reports on jet suckdown give information on any of these factors. All of these and perhaps others need to be investigated. The following discussion is offered in hopes of providing some guidance for future investigations of these factors.

It should be useful to examine some of the basic mechanisms of jet induced suckdown. Figure 8 shows a pictorial sketch of the flow between the planform and the ground and some pressure distributions measured on the lower surface of the planform. The suckdown is created by the entrainment action of the vertical part of the jet and of the wall jet on the ground. This entrainment action draws air into the space between the planform and the ground and lowers the pressures on the lower surface of the planform. As long as the planform is above the critical height the pumping action should be relatively constant and the velocity of the entrained air must increase as the height is reduced. If the height is reduced by half, the velocity will be doubled. The suction pressures and therefore the download should be a function of the square of the height. In practice the exponent is a little over two because the gap is in reality the distance between the planform and the effective upper edge of the wall jet; not the distance to the ground.

When the planform is lowered to the height where it intersects the upper edge of the wall, jet entrained air can no longer be drawn in from around the planform but must be drawn from the wall jet itself. A trapped vortex condition is created and the pressure distribution is radically altered. The data of figure 8 are for a very large ratio of plate area to jet area and, fortunately, the "below critical height" condition is not encountered in practical aircraft configurations.

Under normal operating conditions, the flow field corresponds to the "above critical height" depiction shown at the right on figure 8. In this region both the wall jet and the vertical jet are entraining air. The amount of entrainment

should be proportional to the surface area of these surfaces. Figure 9 shows that at low heights where the suckdown is most serious the vertical surface area is small compared to the surface areas of the wall jet under the planform. Attention should, therefore, be focused on the characteristics of the wall jet and its effects on the suckdown. There have been numerous studies of the wall jet but none on the effect of the proximity of the planform on the wall jet or of the effects of the characteristics of the vertical jet before impingement on the characteristics, entrainment (pumping) ability or decay rate of the wall jet in the presence of the planform. This is where future work should be focused.

Reference 9 presents some data that indicate that the characteristics of the vertical portion of the jet may not have much effect on the wall jet characteristics (fig. 10). Reference 9 was concerned with the dust and debris problems of hovering helicopters and effect of the roughly triangular velocity distribution found in the slipstreams of these configurations on the development of the wall jet. Figure 10 compares the velocity decay and growth in thickness of the wall jet with distance from the impingement point for uniform and nonuniform nozzle exit velocity distributions. With the nonuniform velocity distribution, a trapped "doughnut shaped" vortex was generated centered on the impingement point. This trapped vortex flow was absent with the uniform velocity distribution. Beyond a radial station of about 2 exit diameters, the growth in thickness and decay in velocity in the wall jet created by the two exit velocity distributions were essentially the same indicating no difference in their entrainment action. This, however, leaves unanswered the questions of the effects of the changes in the velocities and shape in the region of the conversion from vertical to wall jet and the possible effect of planform proximity.

The effect of ground board size should also be investigated. The data of reference 7 were obtained with a ground board that was only about 50 percent greater in diameter than the planform. The earlier discussion has assumed that only the wall jet directly under the planform is important in determining the entrainment and suckdown. However, when the wall jet reaches the edge of the ground board, it suddenly has a mixing and entrainment surface on both the top and bottom (fig. 11). It will decay much faster and this decay will be felt upstream, perhaps thickening the wall jet under the planform. A rough estimate indicates that the wall jet would have to be thickened by about 50 percent to account for the higher suckdown exhibited at low heights by the configuration of reference 7. The effect of ground board size should be investigated.



Most of the data on single jet suckdown has been taken indoors but few of the reports indicate the size of the room in which the tests were run. Nor do they say anything about any obstructions that may have been near the experimental setup. One case in which the chamber where the static suckdown data were taken was clearly of inadequate size is reported in reference 10. The tests were run in a wind tunnel because the primary purpose was to investigate STOL ground effects. Two of the static "end points" taken at zero tunnel speed are presented in figure 12. The model in this case consisted of a 2 inch diameter nozzle to which various size planforms could be attached. The model was mounted at the center of an approximately 14 by 16 foot test section with a ground board that spanned the tunnel and could be raised and lowered to vary the height above the ground.

The experimental data presented in figure 12 show greater suckdown than the estimates, particularly for the larger plate. It was possible to enter the test chamber while the static tests were in progress and it was observed that the wall jet on the ground board flowed up the side wall of the test section and across the ceiling. In addition, and more importantly, there were strong and random gusts throughout the chamber and in the vicinity of the model. It is these gusts that are believed to be responsible for the larger than expected measured suckdown.

The data of reference 4 were taken using a 1 inch diameter jet in a room that was 18.5 feet wide by 10 feet high and 42.5 feet long. It was, therefore, relatively larger than the test chamber of reference 10 but was it large enough? Figures 13 and 14 were prepared to offer some perspective on the problem.

Figure 13 presents the decay in the velocity of the wall jet with distance from the impingement point. If the path from the nozzle to the ground, across the floor, up the wall, across the ceiling and back to the model were "unrolled" the distance for the tests of reference 10 would be 195 diameters. If this distance were traversed on a flat surface, the downward velocity at the model would be less than 1 percent of the jet velocity. However it is not the down flow depicted in the sketch on figure 13 that is important but the random gusts. It is probable that these gusts are much stronger than the velocity the wall jet would have at a radial distance of 195 diameters (or 450 diameters for the configuration of reference 4).

Figure 14 presents the effect of a small crossflow velocity on the suckdown (estimated by the method of reference 10). It can be seen that it takes a cross flow velocity of only about 1 percent of the nozzle velocity to produce incremental changes in apparent suckdown of the magnitude seen in figure 3 for example. These estimates are for a steady crossflow. Gusts would produce an unsteady increment but there is no compensating effect. A gust from any direction will increase the download and the average of the unsteady readings will be higher than the suckdown would be if there were no crossflow gusts. These observations suggest that some of the differences between the suckdown data obtained by different investigators could be due to the inadequate size of the room in which the tests were made. The effects of test chamber size should be investigated.

#### RECOMMENDATIONS:

It is doubtful that additional force tests could uncover the reasons for the differences in suckdown discussed above. What is needed are investigations to probe the fundamentals of the flow. Two investigations are recommended, one related to test chamber size and the other to study the effects of various factors on the development of the wall jet and in turn the effects on the suckdown.

1) A schematic of the test chamber size investigation is shown in figure 15. It would have to be conducted in a large high-bay area with a small model to obtain "gust free" data as the anchor point. The dimensions in figure 15 assume a 1 inch diameter jet. A jet/plate combination would be mounted so that the height could be varied and the suckdown force and pressure distribution measured on several plate sizes. The set up would be surrounded with strategically located hot wires to measure the gust velocities. Care would have to be taken to fair and streamline the mounting struts so that they did not reflect any of the wall jet to create gusts.

Following tests in the large room, chambers of successingly smaller sizes would be constructed around the test setup using plywood and 2 by 4's and the tests repeated to determine the effect of chamber size on the gust environment and suckdown.

If the tests show, as expected, that the gusts in the small chambers are the problem, studies of the use of strategically located damping "screens" and/

or venting would be used to see if they can reduce the gust effects to an acceptable level. It would be extremely helpful if such a "fix" could be found that would permit static tests in wind tunnel test sections so that hovering "end point" data could be obtained for configurations being tested in the STOL mode.

2) A schematic of the wall jet effects investigation is presented in figure 16. The heart of the investigation would be measurements of the growth in thickness and the velocity decay in the wall jet for various jet exit conditions and planform heights and the correlation of the suckdown with the observed changes in wall jet characteristics. The investigation should be run in a very large high-bay area to minimize gust effects due to chamber size. The jet size would have to be chosen to provide a thick enough wall jet for acceptable measurements, probably about a 4 inch diameter jet would be adequate but this would require a very large room. Tests should cover a range of ground board sizes and jets of varying pressure ratio, turbulence and exit distribution.

Because the ground effect suckdown is a fundamental problem for most jet VTOL configurations and the estimate of the single jet suckdown is the starting point or a significant factor in the estimation of more complex ground effects, a resolution of these problem areas is very important.

## MULTIPLE JET GROUND EFFECTS

### DATA BASE AND DISCUSSION:

#### Fountain Lift and Additional Suckdown:

When the wall jets from two jets of equal size and thrust meet, a fan shaped upwash or "fountain" is formed between the jets as shown in figure 17. If there are more than two jets, a fan shaped fountain is formed between each pair and a fountain "core" is formed where the fountain fans meet. The impingement of the fountain flow on the configuration produces an upload which partially offsets the suckdown induced by the wall jet entrainment action.

The result is not always a reduction in suckdown as shown in figure 18. Lummus (ref. 11) ran a two jet configuration and measured a suckdown greater than expected for a single jet configuration of the same planform to jet area ratio. He then ran a single jet with half the planform (thus maintaining the same planform to jet area ratio and nearly the same planform aspect ratio) and found less suckdown than for the two jet case. Thus the fountain lift increment  $\Delta L_f$  is negative. He ran similar tests with other jet spacings and with 3 and 4 jet configurations (fig.19) and found negative fountain lift increments for the other two jet configurations and nearly zero fountain lift for 3 jet configurations.

The probable cause of this additional suckdown is shown in figures 20 and 21 (from ref. 12). A vortex-like flow is formed between the fountain flow and each of the adjacent jets (fig. 20). Figure 21 shows that, as expected, the impingement of the fountain flow produces high lifting pressures on the center region of the plate between the jets, but the vortex-like flows between the fountain and the jets induce equally strong suction pressures. The estimated suckdown for a single jet configuration with the same planform to jet area ratio would correspond to an average suction pressure coefficient about equal to the outer contour line shown in figure 21 ( $C_p = -0.004$ ). Thus both the lifting pressures and the additional suckdown pressures are much greater than the pressures induced on a single jet configuration and the question of whether there is a net lift gain or loss depend on which predominates. Unfortunately there is no other pressure data of the type shown in figure 21 on which a method for estimating multiple jet ground effects can be based.

Yen, in reference 13, developed a theoretical framework for estimating the fountain lift contribution and recognized the additional suckdown term but offered no method to estimate it. Kuhn in reference 14 used Yen's fountain jet contribution and the estimated suckdown from an equivalent single jet configuration to back the additional suckdown contribution out of the available experimental data and developed an empirical method for estimating multiple jet ground effects. The method works reasonably well for configurations similar to those in the data base on which it was derived (fig. 22), but badly misses on some other configurations (fig. 23).

Additional pressure distribution data of the type shown in figure 21 are needed to more fully explain the effects of multiple jet interactions. Such pressure distribution data appear at this time to provide the best hope of developing a reasonable method for estimating multiple jet ground effects.

#### Turbulence:

Lummus, in reference 11, also investigated the effect of jet turbulence. A grid of wires was placed in the nozzle slightly upstream of the exit to change the turbulence of the jet stream. The turbulence intensity was defined as the RMS values of the fluctuating total pressures (fig. 24) as measured by a total pressure survey across the exit divided by the average gage total pressure. The turbulence intensity for the base line nozzles, as well as the nozzles with turbulence generators, were found to decrease with nozzle pressure ratio (fig. 25).

The effect of turbulence and pressure ratio for a two jet configuration is presented in figure 26. The suckdown is shown to increase with turbulence level. However, there is no way of knowing whether this increase is due to turbulence increasing the entrainment action of the wall jet or the strength of the fountain itself. Carefully controlled single jet tests as discussed above could provide a partial answer to this question and are needed.

Foley, in reference 16, investigated the turbulence in the fountain between two jets and its sensitivity to "trips" on the stagnation line where the wall jets meet to form the fountain. Unfortunately the study did not include measurement of the effects on the suckdown (the setup did not include a plate or planform on which suckdown could be measured). The study showed that the upward velocity in the fountain was increased and the turbulence in the fountain

decreased (fig.27) by obstructions at the stagnation line. Even a 1/8 inch "trip" (about the thickness of the boundary layer under the wall jet) had a noticeable effect. These results suggest that there is an appreciable energy exchange between the wall jet flows across the stagnation line and that turbulence in the main jets may be affecting the fountain and its associated vortex flows more than the wall jet flowing outward away from the fountain. These effects need further investigation.

#### Other Configuration Variables:

The previous discussion has concerned only flat plate configurations. The fountain and additional suckdown effects on these simple cases must be understood to provide a solid base for isolating the other effects of real airplane configurations such as wing height, fuselage lower surface contour and devices to increase the fountain lift (LIDs). An attempt was made in reference 14 to develop methods for estimating some of these effects.

Figure 28 presents some data on the effect of fuselage contour on the fountain lift contribution. If the fuselage lower surface is flat with sharp corners and wide enough to intercept all of the fountain flow, all the fountains vertical momentum will be converted to lift. If, however the fuselage lower surface has rounded corners, some of the fountain flow will adhere to this curved surface, retain some of its vertical momentum and less than full fountain lift will be realized. Three sets of data were found for the case of two jets, one on either side of a body with a longitudinal fountain between them. The reduction in fountain lift was found to correlate reasonably well with the ratio of the fuselage corner radius to the jet spacing. However, there is no data on fore and aft jet arrangements and little on 3 and 4 jet configurations. Additional work is needed in this area.

Reference 14 also attempted to develop a method for estimating the additional lift contributed by LIDs (lift improvement devices). An example is shown in figure 29 for a Harrier-type configuration (one of the configurations used in developing the method). LIDs attempt to "trap" some of the fountain flow and turn it downward to increase the lift. The LID contribution is therefore assumed to be some fraction of the fountain life that would be achieved on a flat plate and should be proportional to the area contained within the LIDs,  $S_L$ . This was found to be the case at intermediate heights but at the lowest

heights an expression using the inverse of the square root of the LIDs area (which appears illogical) had to be used.

Other configuration variables that will affect the fountain formation and the ground effect of multiple jet configurations include non-circular jets, jets canted inward or outward, jet deflection fore and aft, differential jet size and thrust and model attitude. There is some specific configuration data on some of these and the work of Kotansky and associates at McDonnell Douglas has provided a solid data base on the wall jets and fountains produced by vertical and deflected noncircular jets. The related data on the additional suckdown pressures induced by the vortex-like flows between the jets and the fountain are needed to provide a good foundation for developing estimating methods.

#### Pitching Moments:

The ground effect induced pitching moments have not received any attention. With practical aircraft configurations, such as that sketched in figure 30, a nose up moment will be experienced as the aircraft settles into ground effect. The positive pressures induced by the fountain flow will be experienced between the lifting jets and negative or suckdown pressures will be experienced on most of the rest of the lower surface area. A large part of the area subject to download will be aft of the center of gravity thus contributing a nose up moment. It should be possible to estimate these moments if the distribution of induced pressures are known. The fountain flow induced pressure distribution investigation recommended above could and should be structured to include some nonsymmetrical flat plate configurations which would provide pressure as well as force data on which to begin building a method for estimating pitching moments.

#### RECOMMENDATIONS:

The recommendations with respect to multiple jet suckdown can be divided into four areas.

- 1) The most important investigation in the multiple jet ground effects area is a study to better understand the effects of the flow field between the jets, including the fountain and the associated vortex type flows between the fountain and the jets. This investigation should start with two jet configurations investigating the effects of height and jet spacing on the suckdown and

pressure distribution of selected flat plates. The study should include flow visualization to better understand the flow fields involved.

A proposed method for isolating the fountain and additional suckdown terms is shown on figure 31. The pressure distribution measured on a plate for a given jet spacing and height would be compared with the pressure distribution measured at the same height with single jet. Integration of the single jet pressures would be the single jet suckdown and should be equal to the measured suckdown. The fountain lift would be determined by integrating the portion of the distribution that shows a positive increment relative to the single jet case and the additional suckdown would be determined by integrating the excess negative pressures.

The flat plates used would have to be heavily instrumented with pressure taps, particularly between the jets (fig. 32), where the pressure gradients are steep. Only one quadrant of the plate would have to be fully instrumented for those configurations with a symmetry about two axes but a couple extra rows of pressure taps should be included in the other quadrants of the plate to ensure symmetry.

The study should investigate the effects of:

- Jet spacing
- Height
- Planform size and shape
- Jet pressure ratio and turbulence
- Wall Jet and fountain characteristics

The study should begin with two jet configurations and be extended to 3 and 4 jet configurations after the experimental techniques have been developed with the two jet configurations.

2) A revised method for estimating the ground effects of multiple jet configurations, including the fountain term and the additional suckdown term should be developed from the data obtained from the above study.

3) A method for estimating the pitching moments of multiple jet configurations hovering in ground effect should be developed. This will require including planforms that are nonsymmetrical fore and aft in the fashion of aircraft planforms in the pressure distribution studies of the first investigation.

4) Work should be extended to the items listed below after the first three studies are completed:



- Body contour
- LIDs
- Noncircular jets
- Canted jets
- Jets deflected fore and aft
- Differential jets size
- Differential jet thrust
- Wing height
- Model attitude

There is some data in the literature on most of these items and these data should be reexamined in the light of the findings of the above three studies to see if and where additional work is needed before embarking on new studies.

## GROUND VORTEX IN STOL OPERATIONS

### DATA BASE AND DISCUSSION:

In STOL operation the wall jet flowing forward ahead of the configuration is opposed by the free stream and rolled up into a horseshoe shaped ground vortex as depicted in figure 33. When operating over loose terrain this ground vortex creates and defines the dust cloud that can reduce visibility and damage engines. It is also one of the primary mechanisms of hot gas ingestion and can cause lift loss and pitching moments.

The ground vortex contribution is most significant at low speeds and heights and its significance decreases rapidly with increasing height and speed (fig. 34). Reference 10 presents the most complete database on these effects available at this time.

A ground vortex type of flow is also associated with jet flap configurations. Williams and Wood, in reference 20, found a trapped vortex under the high aspect ratio full span flap configuration when they approached the ground (fig. 35). The problems of the ground board boundary layer and jet flap configuration testing will be discussed in a later section.

### Vortex Strength:

The ground vortex associated with jet impingement has been studied in several investigations (refs. 10 and 21-24). Two of these (ref. 10 and 24) measured the pressure distribution induced on the ground board by the ground vortex. Figure 36 illustrates a typical distribution on the center line through the impingement point. The jet is swept aft by the free stream and produces high positive pressures in the impingement region. The pressure decreases rapidly under the wall jet flowing forward from the impingement point and reaches a maximum negative pressure under the vortex. Ahead of the vortex the pressure rises and there should be a stagnation point where the wall jet and free stream are in balance. However the pressure coefficient never reaches a value of 1.0, probably because of unsteady mixing in this region. In reference 10 the point at which the pressure coefficient was zero was used as an indication of the effective leading edge of the vortex flow field.

The effect of jet exit height on the ground board pressure distributions along the center line through the jet impingement point is presented in figure 37. The data are from reference 10 at a velocity ratio of  $V_e = 0.1$ . The first clear evidence of the ground vortex occurs at a height of 15 jet diameters. At this height the jet impinges on the ground about 5 diameters behind the projected jet center and the maximum negative pressure, indicating the approximate position of the ground vortex, also occurs behind the projected jet centerline. As the height is reduced the ground vortex moves forward as expected and the increasing magnitude of the negative pressure coefficients indicates the vortex is gaining strength. The forward movement stops at a height of about 4 diameters (probably when the jet potential core reaches the ground) and the maximum negative pressure appears to have stabilized at a value of almost -3.0.

Figure 38 presents similar data from reference 24 on the effect of forward velocity on the ground vortex pressure distribution with the nozzle at a height of 4 diameters. At the highest velocity ratio (free stream almost half of the jet velocity) the pressure coefficients are small and the ground vortex is close to the jet centerline. As the velocity ratio decreases the ground vortex moves upstream as expected and the maximum negative pressure coefficient again stabilizes. However in this investigation the maximum negative value is only about -1.7.

The vortex strength in the investigation of reference 10 appears to be greatly different than that in the investigation of reference 24. At a height of 4 diameters and a velocity ratio of 0.1, the maximum negative pressure ratio coefficient has stabilized in both investigations but at a level of -1.7 in reference 24 and almost -3.0 in reference 10. The difference is believed to be associated with the nozzle pressure ratios at which the tests were conducted. The data of figure 37 (ref. 10) were taken at a nozzle pressure ratio of about 1.8 whereas a jet velocity of only about 80 meters per second (indicating a nozzle pressure ratio of less than 1.05) was used in reference 24. An investigation to study the effects of pressure ratio at several constant levels of velocity ratio is needed.

#### Vortex Position:

The five investigations of the ground vortex show a wide variation in the forward projection of the ground vortex flow field (fig. 39). Some of this variation may be due to the manner in which the forward edge of the flow field was defined (some measured the leading edge from photographs of dust clouds and some, like reference 10, used the position of the zero pressure coefficient (fig. 36). Also they were run at different pressure ratios. However, it is believed that the boundary layer on the ground board may be the biggest factor. With a boundary layer the high velocities in the wall jet, which are very close to the ground (fig. 40), can penetrate further against the relatively lower velocities in the ground board boundary layer than they would be able to penetrate against the free stream. The investigation of reference 21 set out to simulate the boundary layer of the atmosphere and thus had a thick boundary layer. It is seen to indicate the most forward penetration (fig. 39). Reference 22, on the other hand, used the moving model technique and thus there was no boundary layer. It shows the smallest penetration. Little is known about the boundary layer in the other investigations other than that the investigation of reference 24 was made at a relatively low Reynolds number and thus probably had a relatively thick boundary layer. Because of the importance of the ground vortex to both the aerodynamic characteristics and hot gas ingestion, a special investigation to determine the independent effect of the ground board boundary layer and pressure ratio is needed.

#### Thrust Reversers and the Effects of Jet Deflection:

Up to this point the illustrations used have considered vertical jets. The thickness of the wall jets and the strength and position of the ground vortex are strongly influenced by jet inclination (ref. 10). If the jet is inclined aft, more of the mass flow is directed aft and the wall jet flowing forward is thinner and the ground vortex is closer to the impingement point. Thrust reversers direct more of the flow forward, thicken the wall jet, move the ground vortex forward and increase its strength. Reference 25 shows that large lift losses and pitching moments can be generated (fig. 41).

The work reported in reference 25 also encountered a phenomena which may indicate a serious problem for thrust reverser equipped fighter aircraft. Close

to the ground the model experienced a severe rolling oscillation. Flow studies indicated that the ground vortex flow field was not fixed but moving rapidly fore and aft when these roll oscillations were encountered and that the forcing frequency full scale would be about 2 hertz. The stability and control implications for operational aircraft are unclear but these results suggest that investigations of the ground vortex should include instrumentation to study the dynamics of the wall-jet/free-stream interaction and the formation of the ground vortex.

#### RECOMMENDATIONS:

Because of the importance of the ground vortex effects on STOL performance, stability and control and hot gas ingestion the uncertainties and discrepancies discussed above must be resolved. The primary need at this time is to determine the effects of jet pressure ratio and the ground board boundary layer on the position, depth, strength and dynamic motion of the ground vortex flow field at various velocity ratios.

Figure 42 illustrates the key elements that should be included in this investigation. A body-jet combination that can be tested at various heights, pressure ratios and free stream velocities should be tested over a fixed and a moving ground board. Pressure distributions should be measured on the fixed ground board to correlate with previous studies and on the body to determine the effects of the ground board boundary layer and correlate with the flow field surveys. Some dynamic flow survey and high response pressure instrumentation measurements should be included to determine the dynamic movement of the ground vortex and the stagnation flow region.

## JET FLAP GROUND EFFECTS STUDIES

### DATA BASE AND DISCUSSION:

#### Ground Board Boundary Layer Effects:

Jet flap configurations operating at very high lift coefficients suffer a lift loss when operating within ground effect. Williams et al. (ref. 20) showed that when the jet sheet from the jet flap impinges on the ground a ground vortex-like flow was generated between the wing and the ground plane (fig.35). Turner, in reference 26, showed that the lift loss measured in a wind tunnel with a fixed ground board (with a boundary layer on the ground board) was considerably greater than the lift loss measured on the same model using the moving model technique (no boundary layer). And Werle, in reference 27, using the ONERA water tunnel to show the flow, demonstrated (fig. 43) that the interaction of the boundary layer with the wall jet flowing forward from the point where the jet sheet impinges on the ground caused a major alteration in the flow under the model.

These results lead to the development of several moving-belt ground-board installations, first in England and later in the United States and elsewhere. The installation shown in figure 44 illustrates the principal features. A slot is installed ahead of the belt to remove the boundary layer up to that point and the belt, by running at the same speed as the air in the test section, prevents the regeneration of the boundary layer. Turner, in references 28 and 29, showed that this technique gave essentially the same result as the moving model technique used earlier (fig. 45).

#### Alternate Ground Board Concepts:

The use of a moving belt ground board in the 40 by 80 and 80 by 120 foot test sections is impractical on two counts. First the development and installation of a large enough belt system would be excessively complex, time consuming and costly and second, belt materials compatible with the exhaust temperatures of the jet engines that are frequently used are not readily available.

The use of suction and/or blowing on the ground board has been suggested but the problem is where and how much to suck or blow. Hackett (refs. 30 and

31) investigated a blowing BLC system on the ground board using both a jet flap and vertical lifting jet model. He used measurements of pressures on the lower surface to determine the amount and location of blowing required with similar data measured over a moving belt as the control. He developed a criteria for blowing that would work well for most conditions tested. Figure 46 presents the blowing BLC design he proposed for the 40 by 80 test section.

A concern with blowing is the possibility of over blowing. Turner, in reference 29, investigated belt over-speed conditions and showed that if the belt was run faster than the air velocity a "negative" boundary layer was created and the lift continued to increase (fig. 47). With a blowing BLC system, the blowing slot must be ahead of the location of the model, a small boundary layer will be developed under the blowing air and an over velocity will be present above it to provide the overall momentum balance.

The French claim to have minimized this problem by using two blowing slots (ref. 32). Both slots ahead of the model with the first slot providing the bulk of the BLC flow required and the second providing a trimming flow to produce a nearly planer velocity distribution at the model station. The operating conditions are determined by adjusting the flow from each slot to achieve as near a planer velocity distribution at the model station with the model out (or at zero lift) and holding this BLC flow throughout the test program. The system was stated to work well for jet flap models but has not been used with jet lift models.

Hackett points out (ref. 31) that some over blowing is desired. With a belt ground board, the air at the surface of the belt is carried with the belt as show in figure 48. That is, the air in the boundary layer of the forward flowing wall jet is retarded and the wall jet boundary layer is thickened. (In the case of the aircraft moving forward over the fixed ground the air at the surface is retarded by the surface with the same result, the wall jet boundary layer is thickened and the wall jet loses energy). With a fixed model and fixed ground, this extra energy loss in the wall jet is not experienced and some over blowing is needed to compensate and achieve the correct ground vortex flow field. The question is how to determine where and how much to blow. Hackett used skin friction gages to set up the condition of zero skin friction under the model.

A major concern is the proper location of the BLC slot. Obviously the BLC slot, either suction or blowing, should not be placed under or aft of the ground

vortex location where it would do violence to the wall jet and the generation of the ground vortex that should be there. Figures 49 and 50 present estimates of the position of the leading edge of the ground vortex flow field with and without the ground board boundary layer. In order to cover a wide range of operating conditions, it would be desirable to be able to move the BLC slot location in accord with the operating conditions.

Figure 51 presents a schematic of a method that could be used to position the BLC slot (blowing or suction). The ground board would be raised above the tunnel flow to avoid the larger boundary layer on the floor and minimize the BLC requirements. The entire ground board would be translated fore and aft to position the BLC slot. Thus it should be possible to cover a wide range of operating conditions.

It is suggested that the ground vortex pressure distribution could be used as a "signature" to position the ground board (fig.52). As indicated above, the BLC slot must be kept ahead of the ground vortex flow field but there is no data to tell us how to locate it. An experimental program to investigate the feasibility of this approach is recommended.

#### Jet Flap and Direct Jet Lift Ground Effects Comparison:

If vertical jets are placed at or near the wing trailing edge, they induce a favorable lift out of ground effect similar to that produced by a jet flap. In reference 10 the effect of ground proximity on the induced lift produced by a jet flap configuration and a direct jet lift configuration were measured on the same wing-body configuration. A comparison of the results is presented in figure 53. The round jet and the slot jet had different areas and pressure ratios so a direct comparison is difficult but the conditions chosen in figure 53 were those that give about the same induced lift/thrust ratio out of ground effect. The resulting comparison is interesting in that the round jets show a favorable ground effect whereas the slot jets show the expected adverse ground effect associated with jet flap configurations. The reason for the different behavior appears to be associated with the differences in the ground vortex position and probably strength. The ground vortices, as determined from the ground board pressure distributions, were much further forward and had a much greater spanwise extent for the slot jets (jet flap) than for the round jets.



The large favorable ground effect for the round jets is not very helpful (the configuration still has to fly out of ground effect) but the adverse behavior shown by the slot jet configuration is to be avoided. Some place between these configurations, a better compromise should be possible. An investigation of the effects of jet size, shape and spanwise extent should be initiated.

#### Dynamic Ground Effects:

The preceding discussion has assumed steady state operation in ground effect. In practice, an aircraft does not fly at a constant height but is either descending during landing or climbing after take-off. The ground effects are, therefore, transient. Stevens and Wingrove, in reference 33, present the lift history during a landing approach and wave-off of the augmentor wing aircraft (fig. 54). In this case the lift coefficient out of ground effect was only about 2.5 and ground effects are favorable. The data show a significant hysteresis with lower lift during the climbout after wave-off indicating a lag in the development of the effects of ground proximity.

Turner, in reference 26, investigated this lag using the moving model technique. The model was suspended from a carriage and brought up to speed before reaching the platform which represented the ground. Figure 55 shows that, for the flat ground board, the lift loss started to develop at the edge of the ground board but did not develop fully until it had traversed the ground board a distance of 4 or 5 chords. In a second series of tests, the forward edge of the ground board was inclined at an angle to represent a landing approach. A comparison of the lift measured with that expected for steady operation at each height shows a lag in the development of the lift corresponding to a flight distance of about 3 chords.

Techniques for investigating these rate-of-height change effects on the ground effects are needed. Conceptually, it might at first be thought possible to insert rapid actuators into a conventional support system to produce the dynamic height and angle of attack changes needed to simulate a landing approach and touchdown. However, a review of reference 34 suggests that achieving adequate stiffness in a conventional support system to ensure position accuracy while keeping them light enough to permit the rapid movements required will be extremely difficult. On the other hand, the support system shown in figure 56

(from ref. 34) places the support strut in the ground effect flow field and may compromise the results aerodynamically. It may be necessary to invert the entire system; mount the dynamic support drive on a solid foundation as shown in figure 56 but turn the model over and bring the support into the model from the top. This would require mounting the ground board above the model. The entire area of dynamic testing and the needed support system must be subject to more study.

#### RECOMMENDATIONS:

There are three recommendations with regard to jet flap research and testing techniques.

1) The moving belt ground board is not practical for the 40 by 80 and 80 by 120 foot test sections and an alternative must be developed. Boundary layer control, either blowing or suction, will have to be used. The problem is how to position the BLC slot for the relatively wide range of possible test conditions. It is recommended that the possibility of using the ground vortex pressure distribution signature to locate the BLC slot be investigated.

A sketch of the principal features to be included in such an investigation is presented in figure 57. A body containing a 1 inch diameter nozzle (one twelfth scale of the J-97 engine exhaust in the 80 by 120 foot test section) would be mounted over a ground board that is raised above the floor of the test section to avoid the floor boundary layer. A row of pressure orifices on the ground board centerline would be used to measure the pressure distribution generated by the ground vortex created by the flow from the 1 inch nozzle. The ground board would be translated fore and aft to determine the effect of BLC slot location on the ground vortex pressure signature and determine the sensitivity of the ground vortex flow field to BLC slot location. The model would first be tested over a moving belt ground board and the pressure distribution of the body measured so that it could be used for evaluation of the BLC ground board effectiveness. If initial tests with a simple jet model were successful, the program should be repeated with a jet flap wing configuration with pressures measured on the wing to ensure adequacy of the concept.

Consideration should be given to combining this investigation with the investigation suggested in the previous section to determine the effects of pressure ratio and ground board boundary layer on the ground vortex strength and

position. Or at least the two investigations should be coordinated so that they support each other.

2) An investigation of the effects of jet configuration bridging the gap between the jet flap and the direct lift jet at the wing trailing edge should be undertaken. Figure 58 presents the principal elements. A common wing body should be designed to incorporate full span and half span jet flaps and a series of jet shapes ranging from circular to very high aspect ratio slots as shown in figure 58 so that the effects of jet configuration can be fully explored. A range of jet and jet sheet deflection angles, from 90 degrees to about 45 degrees should be covered as well as a full range of momentum coefficients and velocity ratios.

3) It appears doubtful that the model support system that would be chosen for standard research investigations could be made suitable for the studies of transient ground effects. Also a support system that uses a strut from below the model will adversely affect the flow under the model and the ground effects experienced. The possibility of inverting the entire set-up for transient tests so that the model could be supported from its top rather than the bottom should be considered.

## DOWNWASH AT THE TAIL

### DATA BASE AND DISCUSSION:

#### Jet Flap Configurations:

Lift is produced by deflecting the flow around the aircraft downward. The slower the flight speed, the greater the deflection of the flow. Powered lift systems are designed to achieve this high deflection of the flow and, as a consequence, produce high downwash angles behind the wing (for example, fig. 59). The presence of the ground interrupts this downward deflection of the flow and, therefore, would be expected to affect not only the lift, but also the downwash behind the wing.

There is a useful data base on the downwash behind the wing of jet flap configurations out of ground effect, but there is relatively little data on the effects of ground proximity. Stewart, in reference 10, presents a curve for the ratio of the downwash in ground effect to the out-of-ground-effect downwash (fig. 60). Unfortunately, the curve is based on only two sets of data. Additional data are needed to determine the range of its validity.

#### Jet Lift Configurations:

There is even less data on the downwash behind direct jet lift configurations either in or out of ground effect. Figure 61 presents out-of-ground-effect downwash for a two jet configuration for three tail heights. As expected the downwash is seen to increase as the velocity ratio is reduced (as the dynamic pressure of the jet increases relative to the free stream dynamic pressure) and to decrease as the position of the tail is raised. On the other hand, much of the data for a Harrier-type configuration (fig. 62) show the opposite trend; the downwash decreases with decreasing velocity ratio. It is speculated in reference 10 that this trend reversal is due to the fact that the lift loss induced on the wing is increasing as the velocity ratio decreases and that this changes the spanwise load distribution on the wing in a manner so that the wing contribution to downwash overpowers the direct jet effect.

Figure 63 presents the effect of ground proximity on the downwash for the Harrier-type model of reference 39. The data indicate the surprising result

that at low speed, high power conditions ( $V_e = 0.1$ , fig. 63b), the downwash is negative; that is, an upwash is experienced close to the ground. Again the reason is not known but it is speculated in reference 10 that this upwash may be due to the fountain flow generated by the rear pair of jets on the configuration. Additional data are needed to clarify these data and to provide a better data base estimating downwash both in and out of ground effect.

#### RECOMMENDATIONS:

Specific investigations to study the downwash of powered lift configurations in ground effect could be developed, but in view of the large number of other ground effect studies that need attention, it is recommended that additional data in this area be obtained by seizing every opportunity presented by tests of complete configurations to extend them to obtain downwash data.

Care must be taken to see that the proper runs are included in the test program. Too often the basic data needed to extract downwash data are not obtained in test programs on complete configurations. Emphasis must be placed on obtaining both tail-on and tail-off data as well as stabilizer effectiveness data for each power and flap configuration tested. And, of course, these data should be obtained out of ground effect and at as many heights as practical.

## HOT GAS INGESTION

### DATA BASE AND DISCUSSION

The ingestion of hot gases into the engine inlet depends on the flow field under and around the aircraft. There are three basic mechanisms involved. Far field ingestion is illustrated in figure 64. The wall jet flowing outward from the impingement point under a single jet decreased in velocity with distance. Eventually the velocity has decreased to the point where the wall jet separates from the ground under the influence of buoyancy. The entrainment action of the wall jet causes an induced downward and inward flow that carries hot gases back to the vicinity of the inlet. The inlet temperature rise associated with the far field flow is small because there is considerable mixing before the flow reaches the inlet and the time required for the flow field to develop is such that this mechanism is seldom a problem in normal operations.

The fountain flow (fig. 65) is a more serious hot gas ingestion mechanism. When the wall jets flowing outward from the impingement points of adjacent jets meet, they are projected upward in a fountain flow. This flow can bring hot gases into the vicinity of the inlet. The path from the jet exit is short and the velocities are high, therefore, high temperatures can be brought to the vicinity of the inlet very quickly. The factors involved in determining the temperature rise from this source and what can be done to minimize it will be discussed further in later sections.

The ground vortex flow field (fig. 66) is the third basic mechanism. In STOL operation the wall jet flowing forward from the front jets is opposed by the free stream and rolled up into a horseshoe shaped ground vortex. This flow field transports the hot gases back to the vicinity of the inlet and can increase the inlet temperature.

#### Effect of Inlet Flow:

The inlet is a sink and in hovering draws air in from all directions. The extent to which this sink action influences the ingestion of hot gasses depends on the direction and energy of the hot flow. Hall, in reference 12, measured the effect of inlet flow on the temperature rise for two isolated lift engine simulators (fig. 67). In this case the fountain transports hot gases upward

between the simulated engines, but the temperature at the inlet face is not changed by the inlet flow. The air above and between the inlets is heated by mixing with the fountain flow and brought back to the inlet face by the induced downflow. Apparently, the sink effect of the inlet is not strong enough or close enough to the fountain to draw fountain air directly into the inlet.

Figure 68 on the other hand shows a case where the inlet flow is significant. In this case, the fountain flow impinges on the bottom of the configuration. Some hot air flows upward around the body and is in turn stopped and redirected by the wing and/or canard. Boundary layers are generated on the various surfaces over which the fountain flows and leaves low energy hot air in the vicinity of the inlet where the sink effect can draw it in. In this case, the inlet flow is very important but the full mass flow does not have to be simulated.

#### Flow Control Devices:

Hall, in reference 40, investigated the effectiveness of various devices to control the flow and minimize hot gas ingestion. The most significant result of that work is shown in figures 69 and 70. The basic approach was to try to intercept the fountain flow and keep it from getting near the inlets. Flow diverters or "shields" were tried at the top of the body near the inlets and at the bottom of the body between the jets. Figure 69 shows that shields placed at the bottom of the body in the plane of the jet exits almost eliminated ingestion. On the other hand, shields at the inlet plane had almost no effect. The inlet temperature rise is the same as with the shields off. Apparently, the flow loses a lot of energy in flowing up around the sides of the body and there is a significant amount of dead hot air near the top of the body that the inlets can draw in.

With exit plane shields, however, the fountain flow is redirected before significant energy is lost and the laterally deflected flow (the "deflected upwash boundary" in fig. 69) carries the hot fountain flow away laterally. It also appears to contain sufficient energy to act as an entrainment mechanism and draw ambient air down from above, thus, insulating the inlet from the hot fountain flow. The inlet temperature rise shown with shield on in figure 69 is probably due to far field ingestion.

Tolhurst and Kelly show similar results in reference 41. Time histories of the operating conditions and inlet temperature for a six engine (J-85 engines) configuration are shown in figures 71 and 72. With the wing in the high position, low energy hot gas can easily be sucked into the "cruise engine" inlets and apparently large quantities of hot air find their way to the lift engine inlets. The time histories are for engine no. 3 and show very high and rapidly varying inlet temperatures that lead to compressor stall a few seconds after the jets are deflected to the vertical (fig. 71). With the wing in the low position, the fountain is apparently intercepted and redirected before it loses significant energy and low energy hot air is not left where it can be drawn into the inlets.

Kaemming and Smith in reference 42 present related results. In their flow visualization tests of a four jet configuration, they found that the impingement of the forward flowing wall jet on the nose gear created a nearly stagnant bubble of hot air immediately under the inlet from where it was drawn, by the sink effect, into the inlet.

From an aircraft design point of view, the lesson from the the above findings is to design the configuration so that the fountain is intercepted and redirected in a harmless direction before significant pockets of low energy hot air, that can be drawn into the inlets, are created.

From a testing point of view the lesson is that the space below and around the model must be kept clear of everything except legitimate parts of the model. The support system must be designed so that it does not affect the flow field under and near the model.

#### Effect of Forward Speed or Wind:

The ground vortex flow field is the principal additional mechanism that comes into play at forward speeds. The free stream that opposes the forward flowing wall jet and rolls it up into the ground vortex also carries hot gases from the top of the wall jet back to the inlet (fig. 73). As the speed is increased the distance from the impingement point back to the inlet and the time for mixing with the ambient air are reduced and the inlet temperature rises. Eventually a speed is reached where the ground vortex has been blown behind the inlet or has been reduced in depth so that all the hot flow is below the inlet and there is no temperature rise.



These trends are shown for a two-jet configuration in figures 74 and 75. With the jets in line with the free stream direction only the wall jet from the front jet is projected forward. Both the shields on and shields off cases show about a 5 or 6 degree increase in inlet temperature rise in the 5 to 8 knot speed range due to the free stream bringing heated air back to the inlet. At a speed of about 25 knots the ground vortex flow is blown aft and reduced in depth to the point that all the hot air is below the inlet.

However, with the jets side by side (fig. 75), the fountain flow between them is projected forward and upward and much more hot gas is available to be transported back to the inlet. The temperature is still rising at a speed of 25 knots, the highest speed investigated.

In this case the shields have no effect at forward speed, probably because part of the fountain flow the shields have deflected is projected directly into the oncoming free stream which carries it back to the inlet. Clearly the design of flow control devices must avoid this situation.

This problem of minimizing the forward projection of hot gas flow has been addressed in the development of the AV-8B Harrier (ref. 43) by incorporating a spanwise fence at the forward end of the LIDs installation (fig. 76). Figure 77 shows that this fence greatly reduced the inlet temperature rise at low heights relative to that on the AV-8A (which uses the same engine/nozzle arrangement) but which did not have the spanwise fence. The higher rise experienced by the AV-8B model at intermediate heights is not explained.

Kuhn, in references 44 and 45, made an attempt at correlating the maximum inlet temperature rise experienced at forward speed. Figure 78 presents data for the four-jet, in-line configuration of reference 46. This model was designed so that either top or side inlets could be used and the wing could be placed in either a high or low position. The correlation (right side of figure 78) shows that the inlet temperature rise can be correlated with the inlet height for all four configurations. For the side inlets the height is measured to the lowest point on the inlet.

In reference 45 an attempt was made to correlate the inlet temperature rise data taken from several sources for configurations with side-by-side front jets (fig. 79). There is considerable scatter in hot gas ingestion data but the bulk of these data follow the same trend as the in-line configuration data of figure 78. However, because of the forward projecting fountain flow, these data show

maximum temperatures about four times as high as the configurations of figure 78 which had only a simple wall jet projected forward.

The D0-31 configuration (ref. 48) experienced a much higher inlet temperature rise than the other configurations including the XV-6A (ref. 47) which used the same engine. On the XV-6A (predecessor to the Harrier), the inlet temperature rise is dictated by the fan flow from the front nozzles. The rear nozzles are canted outward about 7 degrees more than the front nozzles so that the relatively cool fan air from the front nozzles shields the inlet from the hot rear exhaust. The cruise engines on the D0-31 are the same as the engine used in the XV-6A but the D0-31 also used the lift engine pods at each wing tip. These lift engines were canted aft to facilitate transition. As a result the nozzles of the lift cruise engines had to be deflected forward of the vertical in hovering to balance the thrust component of the lift engines. It is believed that this forward deflection of the cruise engine nozzles brought some of the hot rear exhaust forward where it could be ingested and caused the very high inlet temperature rises shown in figure 79. A more complete discussion of the D0-31 data is presented in references 45 and 49.

Additional data on a configuration with a forward projected fountain and with four inlet/wing-height combinations is presented in figure 80. The bulk of the data follow the trend presented in figure 79 (the side inlet high wing data are also used in figure 80) but the data for the top inlets with the high wing show considerably higher inlet temperature rises at the higher height than the rest of the data. It is speculated that the low energy hot air associated with the fountain flow up around the body may be responsible for these higher temperatures.

#### The Speed Required to Avoid Ingestion:

To avoid ingestion the inlet must be ahead of or above the hot gas cloud created by the interaction of the free stream with the wall jet and/or fountain flow projected ahead of the aircraft. Data on the forward projection of the ground vortex flow, which creates and defines the hot gas cloud, are presented in figure 39. These data are repeated in figure 80 along with the corresponding data on the depth of the cloud. All the investigations which attempted to determine the depth of the ground vortex flow field indicate the depth to be about half the forward projection. As with the forward projection Abbott's

moving model data (ref. 22) (no ground board boundary layer) showed the least depth. Th Schwantes investigation (ref. 24), which set out to simulate the boundary layer that would be present with atmospheric winds, showed the greatest depth. One can consider two boundaries then, one for hovering in a wind ( $z/d = .45/V_E$ ) and one for STOL operation with no wind ( $z/d = .27/V_E$ ). These boundaries are for single jet or in-line jet configurations.

The data from reference 46 on the speed at which the inlet temperature rise went to zero for the configuration with four jets in line are compared with these boundaries in figure 82. Because the data were taken in the wind tunnel with a ground board boundary layer they should correlate with the "wind" boundary. The estimated boundary appears to be about right but the investigation was not carried to high enough speeds or heights to be conclusive.

With two jets side by side a fountain flow will be projected forward and upward ahead of the configuration. This will increase the depth of the ground vortex flow field. Abbott, in reference 22, found that the depth was about doubled for the spacing he used. Unfortunately, there is no data on the effect of spacing ratio. (For very closely spaced jets it would be expected that the flow would approach that of a single jet of twice the area and the depth would only be increased by  $\sqrt{2}$ . Similarly, if the jets are very widely spaced they would be expected to produce two isolated flow fields with no increase in depth). More study of this area is needed.

The reference 46 data for the speed at which the inlet temperature rise went to zero for the configuration with two side-by-side jets forward are presented in figure 83 and compared with the estimated boundary for hovering in a wind (the data were taken in a wind tunnel with a boundary layer on the ground board). Again the estimated speeds appear about right, but the investigation was not carried to high enough speeds to be conclusive.

#### Time and Temperature Scaling:

The preceding discussion has considered mostly steady state data. In practice it takes some time for the flow field to develop. McLemore, in reference 50, presented a sequence of photographs (fig. 84) showing the development of the hot gas cloud. The model is a J-85 powered rig with a top inlet and at an exit height of two jet diameters in an outdoor facility. The concrete ground plane had a radius of 25 feet or about 25 jet diameters. A deflector was

attached to the exit so that the engine could be started and brought up to speed with the exhaust deflected aft of the vertical to avoid ingestion. At time zero the deflector was removed to bring the exhaust to the vertical. Simultaneously, at time zero a pulse of smoke was injected into the upward side of the jet and photographs were taken at .2 second intervals to record the development of the hot gas cloud. About 1 second was required for the cloud to develop to the point that smoke is brought back to the vicinity of the inlet and at this point the temperature was observed to begin to increase.

The photographs of figure 84 indicate that at 1 second the hot gas cloud had grown to a radius of about 25 diameters. The data of figure 80 would indicate that the fully developed hot gas cloud should have a radius of over 50 diameters with the stated cross wind condition. Apparently hot gas ingestion begins long before the hot gas cloud is fully developed.

Figure 85 presents a sketch of the developing hot gas cloud and a plot of the radius/diameter ratio as a function of time as measured from the photographs of figure 84. Abbott measured a similar time history of the hot gas cloud development for a 1 inch jet (ref. 22) but at about twice the effective velocity ratio. At one second Abbott's cloud had almost reached steady state size. This is to be expected because for the same exit velocity the distances involved in a scale model are reduced by the scale and the relative growth would be increased by the scale.

Although the hot gas cloud has reached a radius of 25 feet by the time ingestion starts, the ingestion apparently does not arise from the hot gases flowing out to the ground vortex and then being transported back to the inlet. The flow from the ground vortex back to the inlet should be moving at about the free stream velocity and it would take about 2 seconds (at 13 fps) for the hot gases to traverse the 25 feet back to the inlet even if they got to the ground vortex instantaneously. The time required is probably related to the height of the inlet and the speed at which the air mixing with the top edge of the wall jet rises to the height at which it can be blown back to the inlet. This appears to be an area where our basic understanding of the flow mechanisms is very weak and additional research is required.

Some observations with regard to time scaling in large and small scale hot gas testing are presented in figure 86. Two ingestion paths are considered. Path I involves fountain flow and Path II the hot gas cloud blown back at forward speeds or by winds. For Path I the distance from the exit to the inlet

is short, perhaps 8 to 12 feet for a 1 foot diameter nozzle. The velocity of the hot gases over most of this distance is large, approaching jet velocity in the wall jet before it enters the fountain, and the time required for the hot gases to reach the vicinity of the inlet is very short even at full scale. Hot gas ingestion will be almost instantaneous, or put another way, the inlet temperature should follow the build up of thrust and exit temperature with negligible delay. Measuring the time delays in this class of flow at small scale would require very high response instrumentation.

For Path II the velocities vary from almost jet velocity in the wall jet near the impingement point to free stream velocity in the return path to the inlet. The data of figures 84 and 85 indicate that the path effective length must be about 10 to 15 feet. At one-tenth scale time lag in the build-up of the hot gas cloud would be one-tenth of those full scale and if the conditions involved in a landing approach representing, say 3 fps sink speed, at full scale are to be duplicated the model sink rate must be 30 fps (assuming full scale exhaust velocity and temperature). This results in the incremental angle of attack at the wing due to sink speed being 10 times that full scale! This indicates the problems of simultaneously matching the hot gas flow fields and those for lift development. Small scale testing requires scaling velocities, temperatures and times in combinations dictated by the importance of the parameters to be matched. The British (ref. 51) are wrestling with these problems and have developed sophisticated test apparatus (fig. 87) to study these areas.

Bore, ref. 51, has also pointed out that the temperature scaling law used until recently needs to be revised. It has generally been assumed that the inlet temperature rise is proportional to the excess of exit temperature over ambient temperature. And this assumption has been used in the present paper. Milford (refs. 53 and 54) has postulated that the temperature rise should be related to the heat flux and developed the revised expression for inlet temperature rise shown at the top of figure 88 (from ref. 51). The experimental data appear to confirm that the temperature rise is a function of the jet to ambient temperature ratio, but Bore suggests that the exponent may be different. Again the British are working on this problem.

## Thrust Reversers:

Thrust reversing probably creates the most difficult hot gas ingestion control problem. In order to develop a high deceleration force, the flow from the engine exhaust must be deflected forward as much as possible. This increases the forward projection of the hot gas cloud and increases the speed at which the thrust reverser must be turned off to avoid ingestion.

Amin and Richards investigated the hot gas ingestion problem for a fighter-type aircraft (ref. 55) and found that the lateral cant (outward splay) angle of the reverser flow was an important parameter. Without cant their results indicated that ingestion would occur at about touchdown speed. By canting the flow out 40 degrees, the speed for ingestion was almost halved (fig. 89).

## RECOMMENDATIONS:

The recommendations with respect to hot gas ingestion research can be grouped into three areas, hot gas cloud development at forward speeds, fountain control and time and temperature scaling problems.

1) Primary emphasis should be placed on the rate of growth and the character of the hot gas cloud to develop a better understanding of the mechanisms that bring hot gases to the inlet. Figure 90 illustrates the key elements to be included in the study. Time histories of the temperature and velocity distribution in the developing hot gas cloud should be made for single and side-by-side jet arrangements through a range of jet pressure ratios, effective velocity ratios and heights. Jet deflection angles and outward cant angles should also be included to cover thrust reverser configurations. Accurate determination of the character of the developing hot gas cloud will require tests at moderate to large scale.

The flow surveys should be supplemented by inlet temperature measurements for various inlet locations and inlet flow rates. The free stream velocities should be chosen to accurately determine the speed needed to avoid hot gas ingestion.

2) A separate program to expand the data base and understanding of the fountain flow and means of its control (LIDs, shields, etc.) in hover flight should be undertaken. This program should also contain both flow field studies and inlet temperature rise measurements.

3) The problems of dynamic testing and temperature scaling are being studied by the British. It is recommended that the possibility of a cooperative program with them to continue the work in this area be explored.

## PROPULSION SYSTEM SIMULATION

A variety of techniques have and are being used for simulating the jet exhaust and inlet flow of the propulsion system in model testing. These range from simple high pressure jets through ejectors to the use of small jet engines. There are advantages and disadvantages connected with each. Koenig, in reference 56, presents an excellent review of the equipment and techniques available and the pros and cons of their use. There is no need to duplicate that review here. Instead this section will draw on that review and present some suggestions and observations on the equipment that should be used in connection with the investigations recommended above.

### Single Jet Suckdown Investigation:

The direct use of high pressure air will be the best way to simulate the jet for the two investigations (figs. 15 and 16) recommended with respect to single jet suckdown. Typically the air supply at most facilities is stored at pressures of from 20 to 300 atmospheres and the pressure must be reduced to the nozzle pressures of 1.5 to 4 needed for the tests. Usually, a series of perforated plates and screens are used to reach the desired pressure and achieve good quality nozzle flow. Typical designs are shown in figure 91. Where space is available, as it is for the single jet suckdown investigations being considered here, the concept shown in figure 91-b will be preferred (but without the jet deflection and tunnel floor).

The "turbulence screens" shown in figure 91-b should be of fine mesh and chosen to achieve a uniform velocity distribution at the nozzle, as well as to achieve as low a turbulence at the nozzle as possible. For the investigations of the effect of turbulence and non-uniform exit distribution, the nozzle should be designed so that grids to produce the desired turbulence and the "screens" of non-uniform density, or similar device, to produce the desired changes in exit velocity profile can be inserted a short distance upstream of the nozzle exit. Devices similar to those used in the investigation of reference 11 may be suitable. The schedule of the investigation must include adequate time for the development and documentation of the desired jet characteristics.



#### Multiple Jet Ground Effect Investigation:

The direct use of high pressure air is also recommended for the multiple jet investigation suggested in figures 31 and 32. And again the large plenum chamber design of figure 91-b should be used, this time with provision to interchangeably mount twin and other multiple nozzle configurations with various spacings on the basic chamber.

#### Ground Vortex Investigation:

High pressure air is also preferred for the ground vortex (fig. 42) investigation. In this case, however, the nozzle should be installed in a body so that the body pressures can be used to evaluate the effects of the ground board boundary layer (tests with belt running and stopped). In order to install the nozzle in the body a design of the type shown in figure 91-a will be needed. A certain amount of 'cut and try' is required to get such a nozzle assembly to give a good flow particularly for several jet deflections. Again the schedule must provide adequate time for the development and documentation of the nozzle flow.

#### BLC Ground Board Development:

The same body/nozzle model (or a similar model) could be used to produce the ground vortex flow field needed in the development of the boundary layer control ground board concept suggested in figures 49 and 57. The 7 by 10 foot tunnel could be used as a 1/12 scale model of the 80 by 120 foot test section and this would indicate a nozzle diameter on the model of about 1 inch to represent a single J-97 exhaust in the big tunnel.

#### Jet Configuration Effects Investigation:

A different model would be required for this study which is sketched in figure 58. Again direct use of high pressure air would be the choice and the nozzles would have to be of the type shown in figure 91-a and very carefully designed and developed.

### Downwash Investigation:

In as much as it is suggested that down wash data should be obtained by taking advantage of and expanding slightly complete model tests that come available for other purposes, special development of propulsion simulators for this purpose is not required. The characteristics of the flow from the propulsion units used should, however, be carefully documented including, if possible, the trajectory that the jets take under the influence of the free stream because the position of the jet wake is important to the downwash.

### Hot Gas Ingestion Study:

This investigation requires heated exhaust flow, and for part of the study a sucking inlet is needed. In order to be able to vary the inlet and exit locations, a remote source of hot flow and a remote pump to power the inlet are desirable. Also the accuracy of the flow field studies will be improved if the nozzles, and, therefore, the associated wall jet flow is not too small. These considerations suggest that jet engines such as the J-97's should be used - one to power the exit(s) and one to pump the inlet.

### Tests of Specific Aircraft Configurations:

The previous sections have discussed the propulsion units needed for the several general research investigations recommended above. As such they are concerned only with improving our understanding of the ground effect flow fields and some of the considerations of testing complete models of specific configurations could be ignored. Notably the inlet flow need not be simulated in any of the above investigations except the hot gas ingestion study.

The inlet flow imposes forces and moments on the configuration due to the momentum of the inlet mass flow. If the inlet is on the axis through the center of gravity and the model is at zero side slip, only a drag force is generated. In the more general case the inlet flow can contribute force and moment increments on all three axes. However, there is no evidence nor any reason to believe that ground proximity will change these inlet effects.

Ejectors and high pressure air driven fans have been used to power complete models in small scale testing but corrections have to be made for the fact that

the inlet mass flow was less than it should be and the nozzle pressure ratios are often not duplicated. At large scale, small jet engines are often used but the engines are often larger than a scale model of the full scale engine would be with the result that the aerodynamic lines of the configuration are often violated.

Figure 92 presents the results of a preliminary examination of the possibility of powering a complete model with remotely mounted jet engines. In this case the aerodynamic line of the Kestrel (predecessor to the Harrier V/STOL aircraft) were used and it was assumed that two J-97 engines would be employed - one to pump the inlet and one to supply hot exhaust to the exits. As can be seen the hot ducting takes up all the available space in the fuselage in the vicinity of the wing and nozzles and it would be necessary to duct the inlet flow out the top of the fuselage ahead of the wing. Thus the aerodynamic lines of the top of the fuselage from ahead of the wing aft are violated and the vertical tail is eliminated. Some jet induced interference investigations in and out of ground effect might be attempted with this type of model but it could not be used for any lateral/directional investigations and even the downwash at the tail would be affected. Another problem with the concept shown in figure 92 is that all the jets would operate at the same temperature and pressure ratio. Many aircraft configurations have mixed propulsion systems with part of the thrust from the hot exhaust and part from fan flow or a remotely mounted auxillary unit. A more versatile propulsion simulation system is required for large subscale models.

The Compact Multimission Aircraft Propulsion Simulator (CMAPS) (fig. 93) is being developed to fill part of this role. The concept and characteristics of CMAPS are reviewed in reference 57. Four of these units could be used to power the model show in figure 92 and the inlet flow and nozzle pressure ratios could probably be matched. However, there is no provision for heating the exhaust and, therefore, a CMAPS powered model could not be used for hot gas ingestion studies.

Another possibility that should be investigated is the use of ejectors with provision to add heat to the exhaust flow. It would not be possible to simulate the full inlet flow but the available data (fig. 67 and 68) suggests that full inlet flow is not required. Part of the hot gas ingestion investigation recommended above should be designed to further explore the level of inlet flow required to obtain reliable inlet temperature rise data.

## MODEL SUPPORT SYSTEM CONSIDERATIONS

The primary consideration with regard to the support system is to prevent the support system from altering the flow under and around the model. This suggests that the model should be supported from above and behind as sketched in figure 49.

The presence of obstructions under the model can alter the flow. Two extreme examples are shown in figures 93 and 94 (refs. 58 and 59). In reference 58 the upwash velocities in the fountain between two jets was measured with and without a reflection plate at the "plane of symmetry". With the reflection plate installed the flow adheres to the reflection plate and reaches higher values near the plane of symmetry than when the reflection plate is removed (fig. 94). Apparently the reflection plate prevents the exchange of energy across the plane of symmetry that is normally present. The same result was observed by Folley (ref. 16) who found that a vertical trip only as high as the thickness of the wall jet flowing outward from the impingement point of the jet would produce the same result.

In reference 59 the inlet temperature rise due to fountain flow was measured with and without a reflection plate at the plane of symmetry between two jets. The results (fig. 95) are dramatically different. Without the reflection plate the temperatures are very high with the jets close to the ground but drop off rapidly and go to zero when the inlets are raised above the top of the fountain flow. With a reflection plate the inlet temperature rise is much smaller at the low heights but increases as the height is increased. Apparently, the fountain flow adheres to the plate and is carried to much higher heights.

Obviously, struts or obstructions on the plane of symmetry between jets are to be avoided. Nothing is known about the effects of struts or obstructions at other points in the flow but, in general, obstructions to the wall jets flowing outward from the impingement points should be avoided or faired to minimize their effect on the flow. A useful addition to the multiple jet fountain investigation and to the hot gas ingestions suggested above would be to investigate the effects of realistically located model support struts.

## CONCLUDING REMARKS

The basic flow mechanisms that produce the ground effects experienced by V/STOL and STOL aircraft are known but there are apparently details of the mechanisms that are not adequately understood. Even for the simplest case, the suckdown on a single centrally located jet, there are differences in the data from various investigators that cannot be explained. In other areas such as the ground vortex and hot gas cloud formation experienced in STOL operation there is circumstantial evidence to indicate that parameters such as pressure ratio and the ground board boundary layer have a major impact on the result but there is no data base for quantifying these effects.

It is doubtful that additional force tests alone will be of much help in clarifying the picture in most areas. A more fundamental approach is needed. Carefully structured investigations to isolate and document the effects of key parameters on the flow field under and around the configuration as well as on the forces and moments induced are required. Additional comments on a few of the most important of the several areas discussed above are given below.

- 1) Resolution of the anomalies in the single jet suckdown area should be given first priority because the factors involved are fundamental to some of the other more complex areas. Both of the investigations sketched in figures 15 and 16 and discussed on page 8 should receive high priority.

- 2) The fountain flow produced by multiple jet configurations in hover and how to control it and its attendant side effects, are important because of the effects they have on lift and hot gas ingestion. The problem is complicated by the myriad of variables, jet arrangement and spacing, body contour, LIDS, etc. There are scraps of data on the effect of most of these variables but before these data can be put together to form a good basis for estimating the multiple jet induced lift and moments, a better understanding of the flow field between the jets and the fountain is needed. The approach sketched in figures 31 and 32 and discussed under item 1 on page 13 is the recommended next step in this area.

- 3) The ground vortex flow field is important to jet lift V/STOL and jet flap configurations as well as thrust reverser operation on conventional aircraft and STOL fighters. It also creates a problem in STOL testing if precautions are not taken to remove the boundary layer on the ground board. There is some evidence to indicate that interaction of the ground vortex flow, the approaching boundary layer on the ground board and the flow around the wing

can lead to fluctuating rolling moments with thrust reversers activated. A fundamental investigation such as that sketched in figure 42 and discussed on page 19 is needed to better understand the factors involved.

4) A moving belt ground board, such as is used in small wind tunnels is not practical for the 40 by 80 and 80 by 120 foot test sections because of size and because of the hot exhaust from the jet engines used in these facilities. A boundary layer removal system will be required. It is suggested that the ground vortex signature could be used to position the BLC slot for varying test conditions. The general concept is illustrated in figure 51 and discussed on pages 20-21. An experimental setup to investigate and develop the concept is sketched in figure 57 and discussed on page 24.

5) The ground vortex flow field is also one of the primary mechanisms involved in hot gas ingestion. A better understanding of the development of the hot gas cloud created by the ground vortex flow field is needed. A sketch showing the elements and features of a recommended investigation of developing hot gas cloud is presented in figure 90 and discussed on page 36.

## REFERENCES

1. Henderson, C., Clark, J. and Walters, M., "V/STOL Aerodynamics and Stability and Control Manual", NADC-80017-60, Jan. 1980.
2. Wyatt, L. A., "Static Tests of Ground Effect on Planforms Fitted With a Centrally-Located Round Lifting Jet", Ministry of Aviation CP749, June 1962.
3. Hall, G. R., "Scaling of VTOL Aerodynamic Suck-down Forces", AIAA Journal of Aircraft, July-August 1967, pp. 393-394.
4. Spreeman, K. P. and Sherman, I. R., "Effects of Ground Proximity on the Thrust of a Simple Downward-Directed Jet Beneath a Flat Surface", NACA TN 4407, Sept. 1958.
5. Gentry, G. L. and Margason, R. J., "Jet-Induced Lift Losses on VTOL Configurations Hovering In and Out-of-Ground Effect", NASA TN D-3166, Feb. 1966.
6. Vogler, R. D., "Interference Effect of Single and Multiple Round and Slotted Jets on a VTOL Model in Transition", NASA TN D-2380, Aug. 1964.
7. Christiansen, R. S., "A Large Scale Investigation of VSTOL Ground Effects", AIAA-84-0366, Jan. 1984.
8. Yen, K. T., "An analytical Solution of Lift Loss for a Round Planform with a Central Lifting Jet", AIAA-81-0011, 1981.
9. Ludwig, G. R., "An Investigation of the Flow in Uniform and Nonuniform Jets Impinging Normally on a Flat Surface", AIAA-ICAS-64-796, AIAA-CASI Joint Meeting, Ottawa, Canada, Oct. 1964.
10. Stewart, V. R. and Kuhn, R. E., "A Method for Estimating the Propulsion Induced Aerodynamic Characteristics of STOL Aircraft in Ground Effect", NADC-80226-60, Aug. 1983.
11. Lummus, J. R. and Smith, E. W., "Flow-Field Characteristics and the Effect of Jet-Exhaust Simulation for V/STOL Vehicles Near the Ground", Proceedings of the NADC V/STOL Aircraft Aerodynamics Symposium, Naval Postgraduate School, Monterey Calif., May 1979, pp. 293-313.
12. Hall, G. R. and Rogers, K. H., "Recirculation Effects Produced by a Pair of Heated Jets Impinging on a Ground Plane", NASA CR-1307, May 1969.
13. Yen, K. T., "On the Vertical Momentum of the Fountain Produced by Multi-Jet Vertical Impingement on a Flat Ground Plane", NADC-79273-60, Nov. 1979.

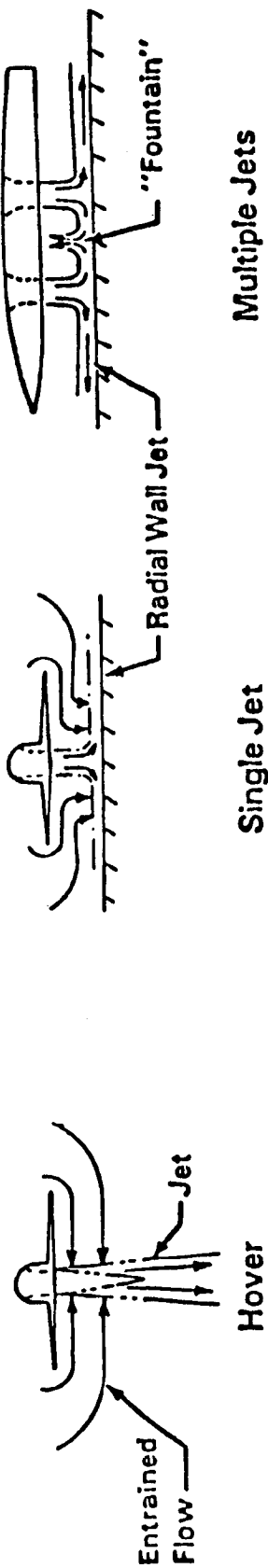
14. Kuhn, R. E., "An Engineering Method for Estimating the Induced Lift on V/STOL Aircraft Hovering in and out of Ground Effect", NADC-80246-60, Jan. 1981.
15. Foley, W. H. and Sansone, J. A., "V/STOL Propulsion-Induced Aerodynamic Hover Calculation Method", NADC-78242-60, Feb. 1980.
16. Foley, W. H. and Finley, D. B., "Fountain Jet Turbulence", AIAA-81-1293, June 1981.
17. Spong, E. D. et al., "V/STOL Jet-Induced Interactions", Proceedings of NADC Workshop on V/STOL Aerodynamics, Naval Post Graduate School, Monterey, Calif., May 1979, pp. 440-508.
18. Wohllebe, F. A. and Migdal, D., "Some Basic Test Results of V/STOL Jet-Induced Lift Effects in Hover", AIAA-79-0339, Jan. 1979.
19. Johnson, D. B. et al., "Powered Wind Tunnel Testing of the AV-8B: A Straightforward Approach Pays Off", AIAA-79-0333, Jan. 1979.
20. Williams, J., Butler, S. F. J. and Wood, M. N., "The Aerodynamics of Jet Flaps", RAE R & M No. 3304, Jan. 1961.
21. Schwantes, E., "The Recirculation Flow Field of a VTOL Lifting Engine", NASA TT F-14912, June 1973.
22. Abbott, W. A., "Studies of Flow Fields Created by Vertical and Inclined Jet When Stationary or Moving Over a Horizontal Surface", RAE CP No. 911, 1967.
23. Weber, H. A. and Gay, A., "VTOL Reingestion Model Testing of Fountain Control and Wind Effects", Prediction Methods for V/STOL Propulsion Aerodynamics, Vol. 1, Naval Air Systems Command, pp. 358-380, 1975.
24. Colin, P. E. and Olivari, D. "The Impingement of a Circular Jet Normal to a Flat Surface with and without Cross Flow", AD688953 European Research Office, United States Army, Jan. 1969.
25. Joshi, P. B., "Generic Thrust Reverser Technology for Near Term Application", Northrop Study for the USAF, to be published.
26. Turner, R. T., "Ground Influence on a Model Airfoil with a Jet-Augmented Flap as Determined by Two Techniques", NASA TN D-658, Feb. 1961.
27. Werle, Henri, "Simulation de L'Effet de Sol au Tunnel Hydrodynamique (Ground Effect Simulation at the Water-Tunnel)", La. Rech. Aérospatiale, no. 95, July-Aug. 1963, pp. 7-15.



28. Turner, T. R., "A Moving-Belt Ground Plane for Wind-Tunnel Ground Simulation and Results for Two Jet-Flap Configurations", NASA TN D-4228, Nov. 1967.
29. Turner, T. R., "Endless-Belt Technique for Ground Simulation", NASA SP-116, April 1966, pp. 435-446.
30. Hackett, J. E. and Boles, R. A., "High Lift Testing in Closed Wind Tunnels", Proceedings of the AIAA 8th Aerodynamic Testing Conference, Bethesda, Md., AIAA 74-641, July 8-10, 1974.
31. Hackett, J. E. et al., "Ground Simulation and Tunnel Blockage for a Jet-Flapped Basic STOL Model Tested at Very High Lift Coefficients", NASA CR-137857, March 1976.
32. Private discussions with Ph. Poisson-Quinton.
33. Stevens, V. C. and Wingrove, R. C., "STOL Ground Effect Determined from Flight Data", AIAA-77-576, June 1977.
34. Crowder, J. P., Goldhammer, M. T. and Smyth, D. N., "STOL Aircraft Transient Ground Effects. Pt. II. Experimental Techniques Feasibility Study", NASA CR-137,767, Nov. 1975.
35. Lowry, J. G., Riebe, J. M. and Campbell, J. P., "The Jet Augmented Flap", IAS Preprint No. 715, Jan. 1957.
36. McCormick, B. W., "Aerodynamics of V/STOL Flight", Academic Press, 1967.
37. Vogler, R. D., "Wind Tunnel Investigation of a Four Engine Externally Blowing Jet-Flap STOL Airplane Model", NASA TN D-7034, Dec. 1970.
38. Mineck, R. E. and Schwendamann, M. F., "Aerodynamic Characteristics of a Vectored-Thrust V/STOL Fighter in the Transition-Speed Range", NASA TN D-7191, May 1973.
39. Margason, R. J. et al., "Wind-Tunnel Investigation at Low Speed of a Model of the Kestrel (XV-6A) Vectored-Thrust V/STOL Airplane", NASA TN D-6826, July 1972.
40. Hall, G. R., "Model Tests of Concepts to Reduce Hot Gas Ingestion in VTOL Lift Engines", NASA CR-1863, July 1971.
41. Tolhurst, W. H., Jr. and Kelly, M. W., "Characteristics of Two Large-Scale Jet-Lift Propulsion Systems", NASA SP-116, April 1966, pp. 205-228.
42. Kaemming, T. A. and Smith, K. C., "Techniques to Reduce Exhaust Gas Ingestion for Vectored-Thrust V/STOL Aircraft", AIAA-84-2398, Oct. 1984.
43. Clark, R. S. and Vasta, S. K., "Development of the AV-8B Propulsion System", AIAA-84-2426, Oct. 1984.

44. Kuhn, R. E., "Design Concepts for Minimizing Hot-Gas Ingestion in V/STOL Aircraft", *Journal of Aircraft*, Vol. 19, Oct. 1982, pp. 845-850.
45. Kuhn, R. E., "Hot Gas Ingestion and the Speed Needed to Avoid Ingestion for Transport Type STO/VL and STOL Configurations," AIAA-84-2530, Oct. 1984.
46. McLemore, H. c. and Smith, C. C., Jr., "Hot-Gas Ingestion Investigation of Large-Scale Jet VTOL Fighter Models", NASA TN D-4609, 1969.
47. McKinzie, G. A. et al., "P-1127 (XV-6A) VSTOL Handling Qualities Evaluation", Air Force Flight Test Center FTC-TR-68-10, Aug. 1968.
48. Holzhauser, C. A. et al., "A Flight Evaluation of a VTOL Jet Transport Under Visual and Simulated Instrument Conditions", NASA TN D-6754, March 1972.
49. Gittner, U. et al., "Interaction Between Airframe Powerplant Integration and Hot Gas Ingestion for Jet-Lift V/STOL Transport Aircraft", AGARD 31st Flight Mechanics Panel Meeting on Integration of Propulsion System in Airframe, Sept. 1967.
50. McLemore, H. C., "Considerations of Hot-Gas Ingestion for Jet V/STOL Aircraft", NASA SP-116, April 1966, pp. 191-204.
51. Bore, C. L., "Ground Based Testing Without Wind Tunnels", AGARD Report No. R-710, Special Course on V/STOL Aerodynamics, May-June 1984.
52. Abbott, W. A., "Estimation of Intake Temperature During V/STOL Operation from Model Tests." NGTE Note NT.600, March 1966.
53. Milford, C. M., "Scaling Factors for Hot Gas Recirculation", BAe-KAD-N-GEN-2787, Aug. 1981.
54. Milford, C. M., "Further Consideration of Recirculation Temperature Scaling Laws", BAe-KAD-N-GEN-2844, June 1982.
55. Amin, N. F. and Richards, C. J., "Thrust Reverser Exhaust Plume Reingestion Model Tests", *Journal of Aircraft*, Vol. 21, June 1984, pp. 401-407.
56. Koenig, D. G., "V/STOL Wind Tunnel Testing", AGARD-R-710, Special Short Course on V/STOL Aerodynamics, May-June 1984, pp. 9-1 to 9-71.
57. Fearn, R. L. and Weston, K. P., "Induced Velocity Field of a Jet in a Cross Flow", NASA TP-1087, 1978.
58. Hertel, H., "Wandströmungen und Aufströme aus der Umlenkung von Freistrahlguppen (Wall Flows and Up-Streams Due to the Diversion of Free Jet Groups)", *Fortschritt Berichte VDI Zeitschrift Fortschr*, Vol. 12, No. 11, pp. 1-72, June 1966.

59. Ryan, P. E. et al., "A Generalized Experimental Investigation of Hot-Gas Recirculation and Ingestion for Jet VTOL Aircraft", NASA CR-1147, 1968.



### Out-of-Ground-Effect      Hover In-Ground-Effect

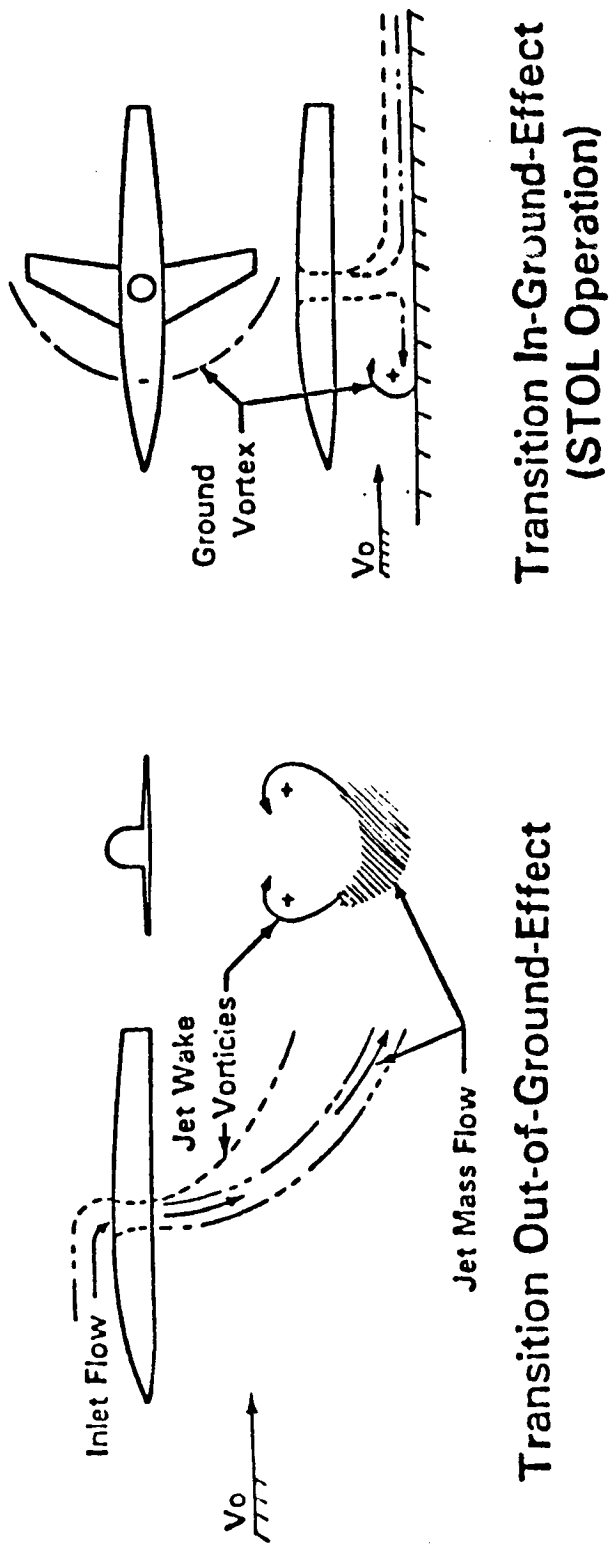


Figure 1.- Basic Flow Fields.

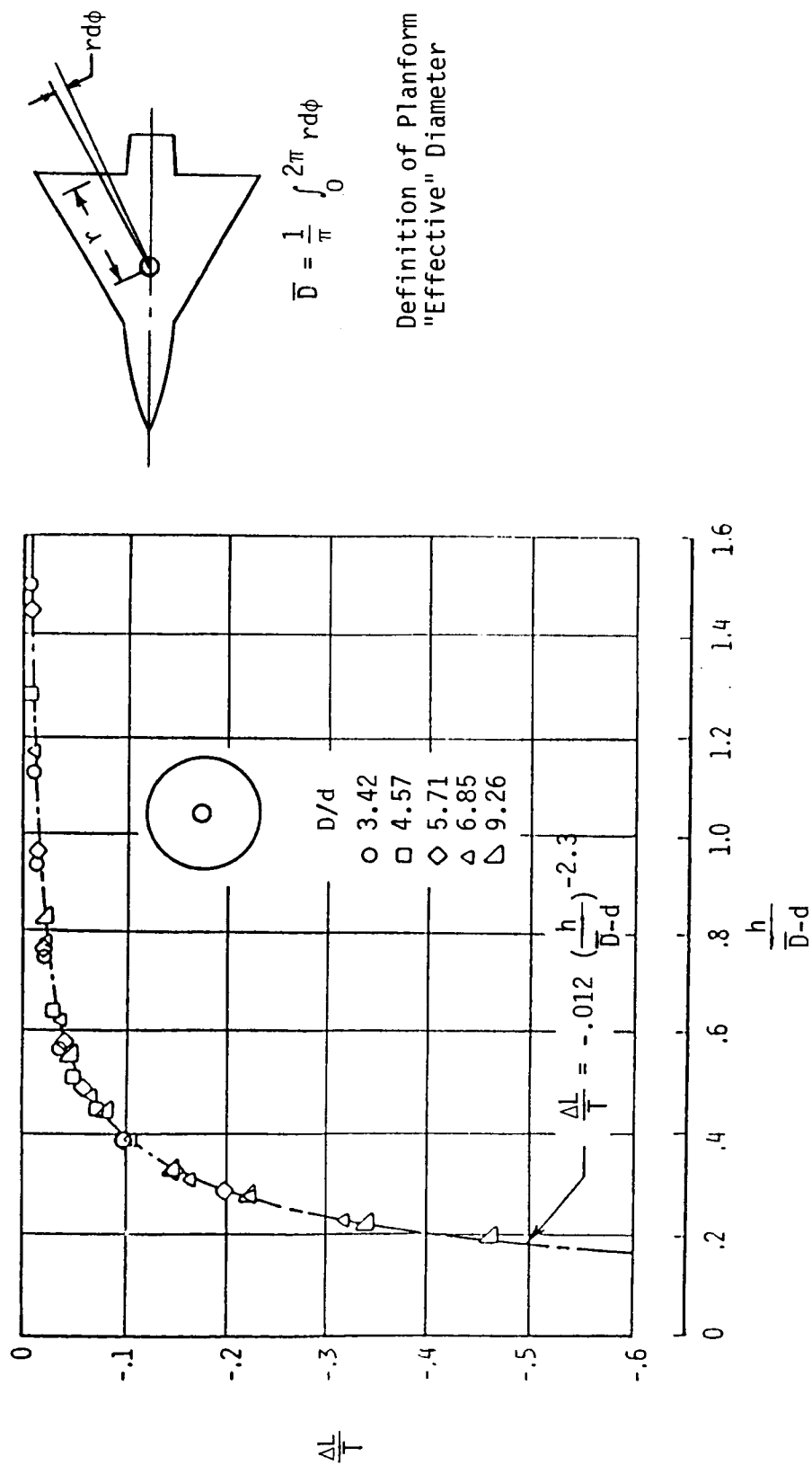
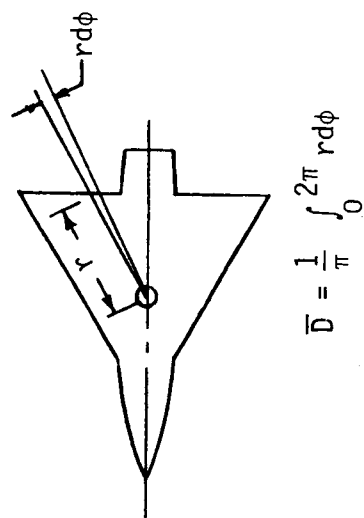


Figure 2.- Data of Reference 2 (Wyatt) NPR = 1.5



Definition of Planform  
"Effective" Diameter

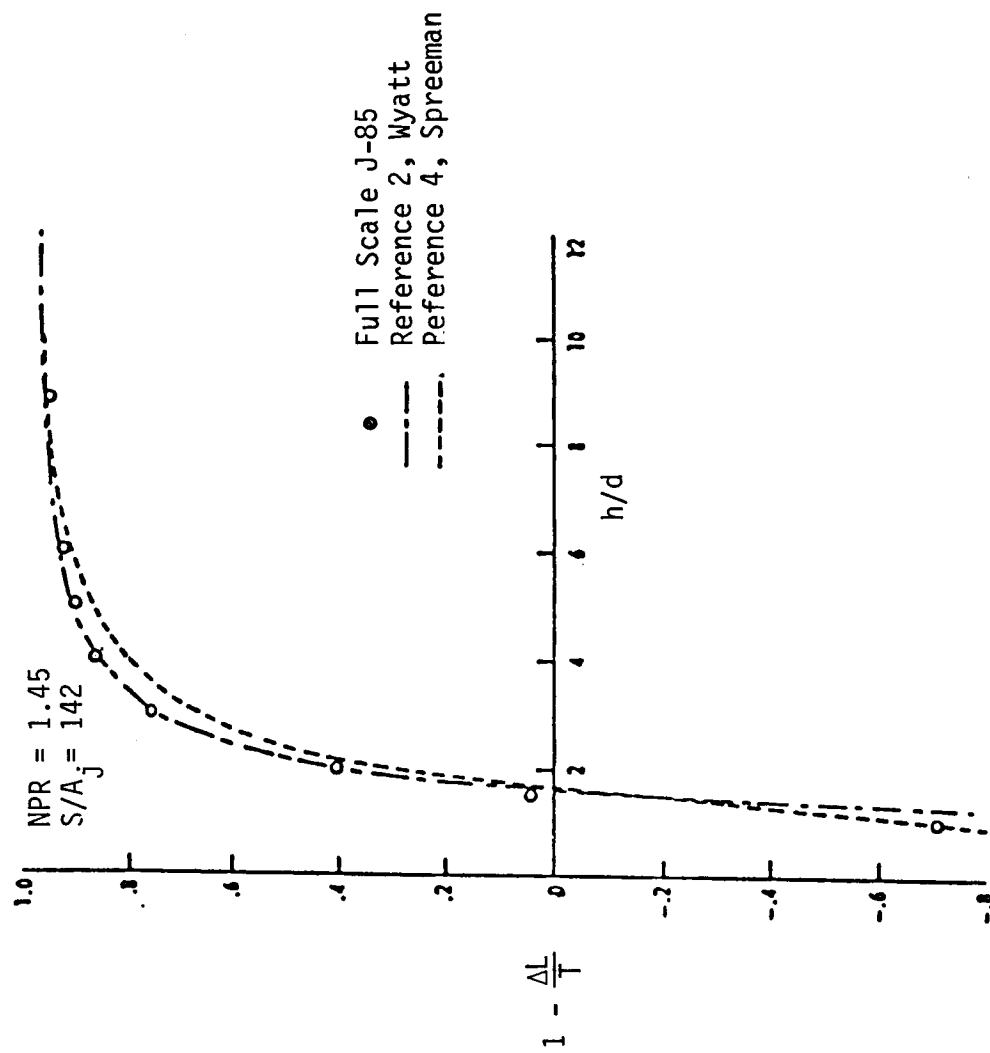


Figure 3.- Comparison of suckdown measured at large scale (Ref. 3) with results from two small scale tests.

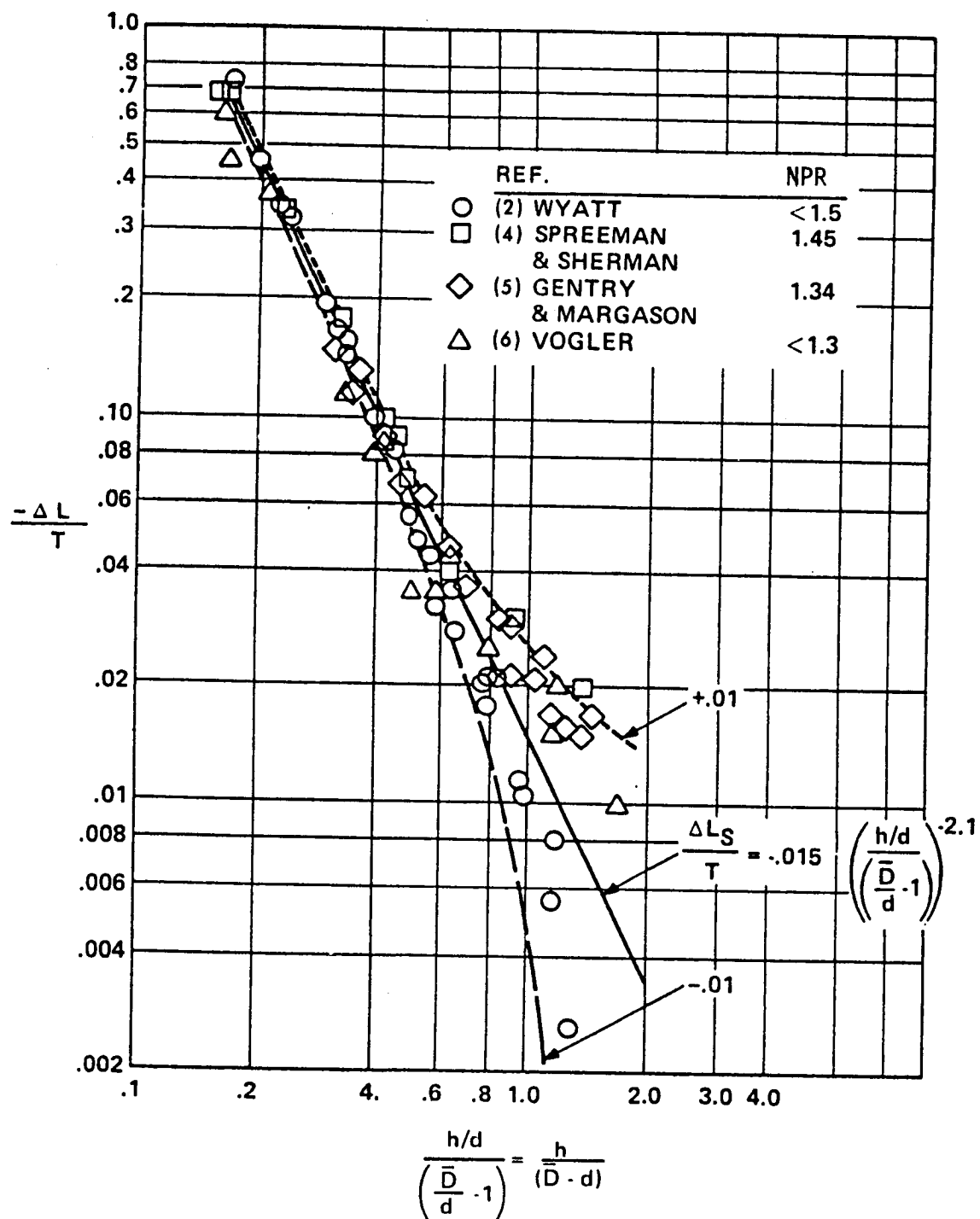


Figure 4.- Ground-induced lift loss on single jet configuration at low pressure ratios. (Ref. 1)

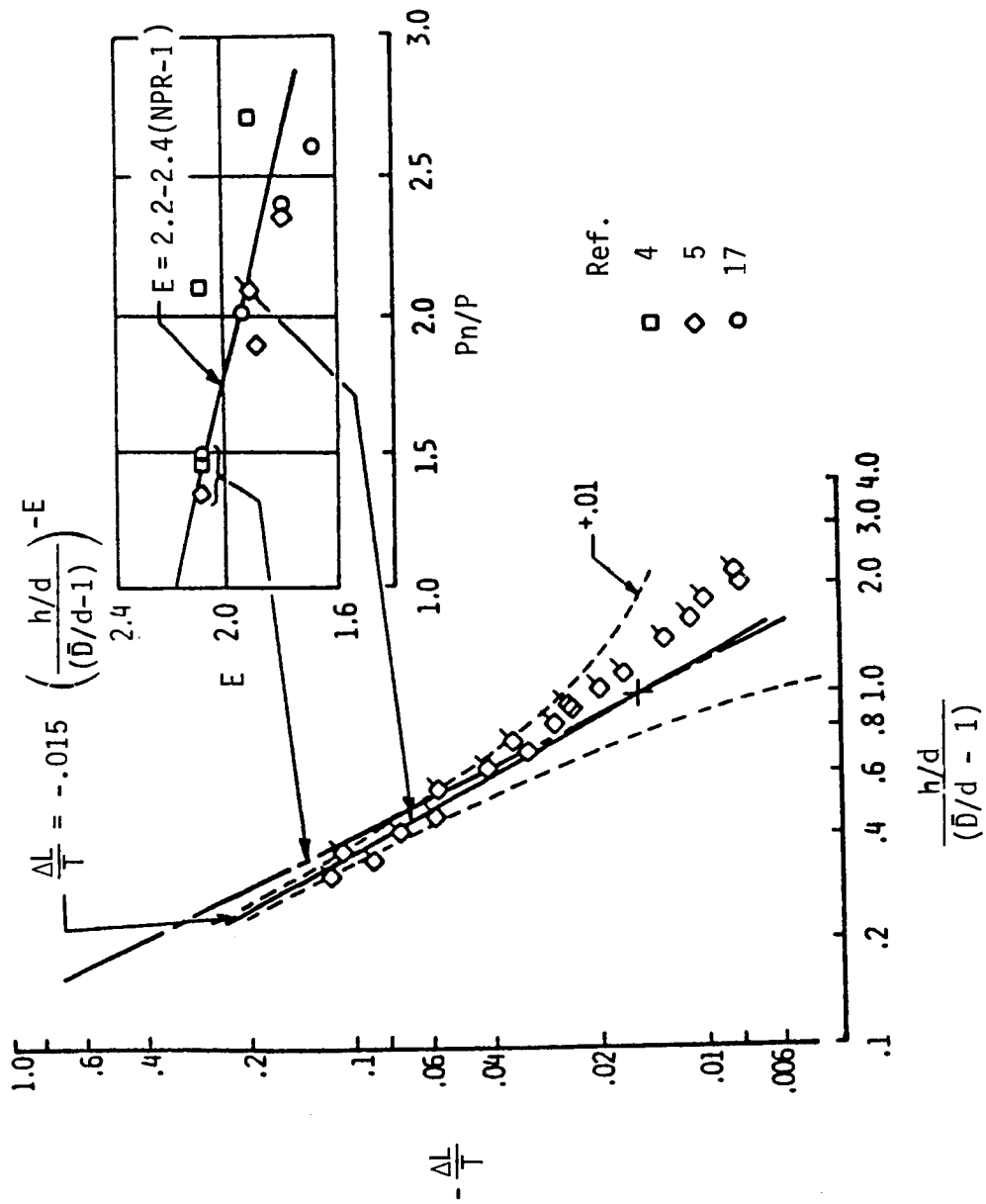


Figure 5.- Effect of pressure ratio on single-jet configuration lift loss in ground effect. (Ref. 1)



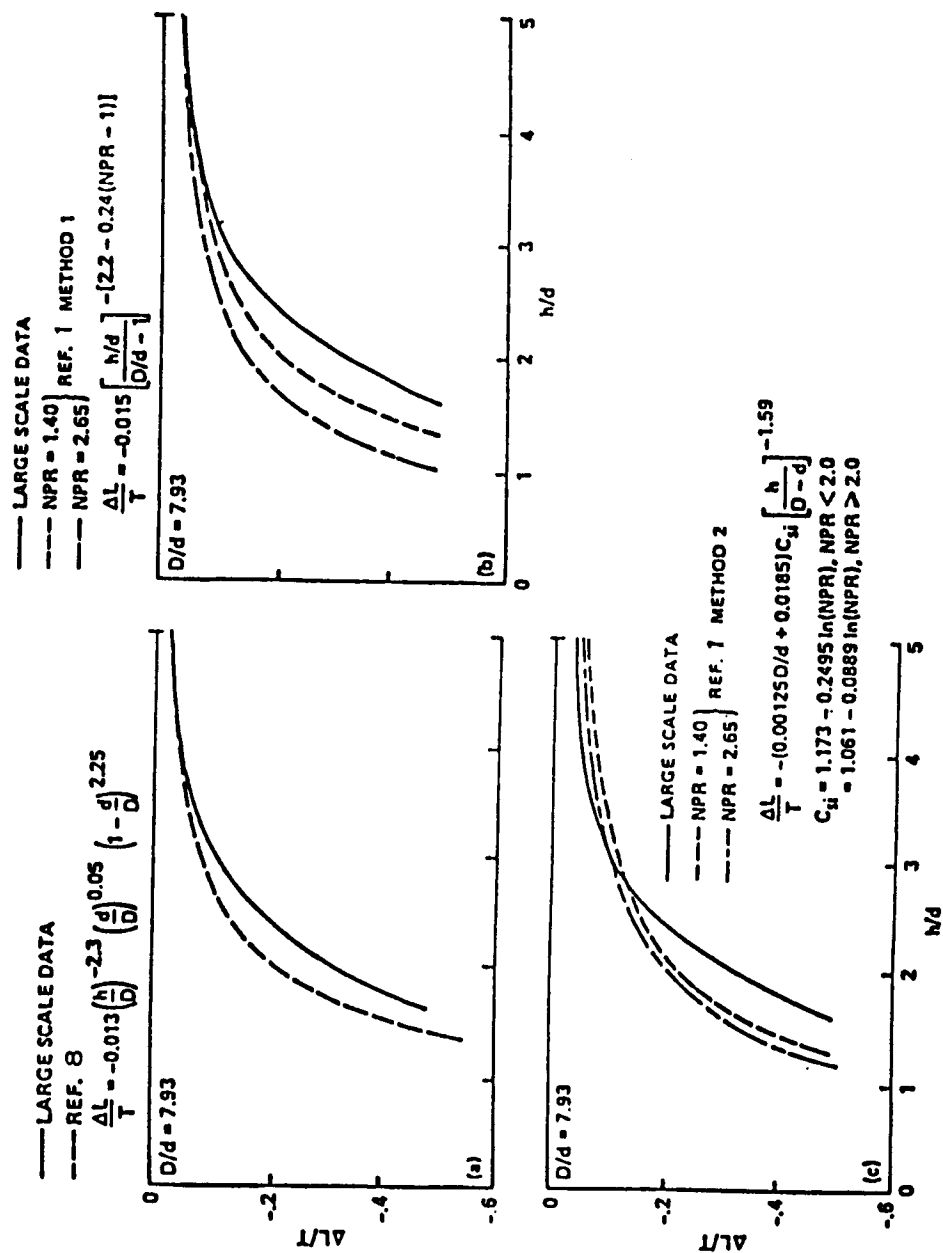


Figure 6.- Comparison of large-scale data with predicted lift losses. (a) Analytical solution; (b) empirical solution I; (c) empirical solution II. (Ref. 7)

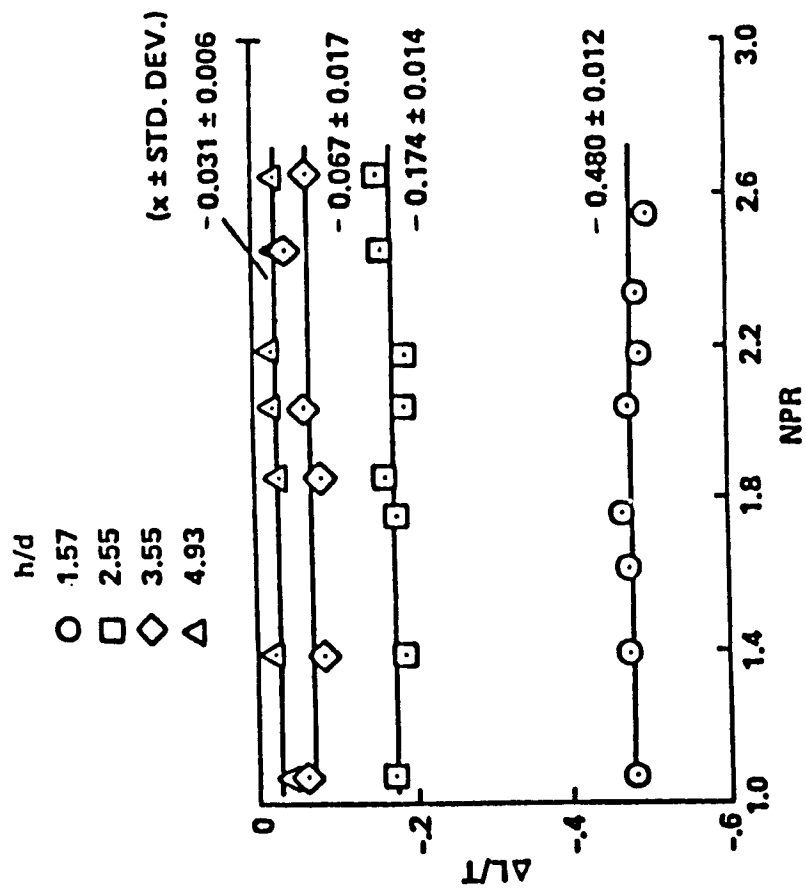


Figure 7.- Effects of pressure ratio on lift loss. (Ref. 7)

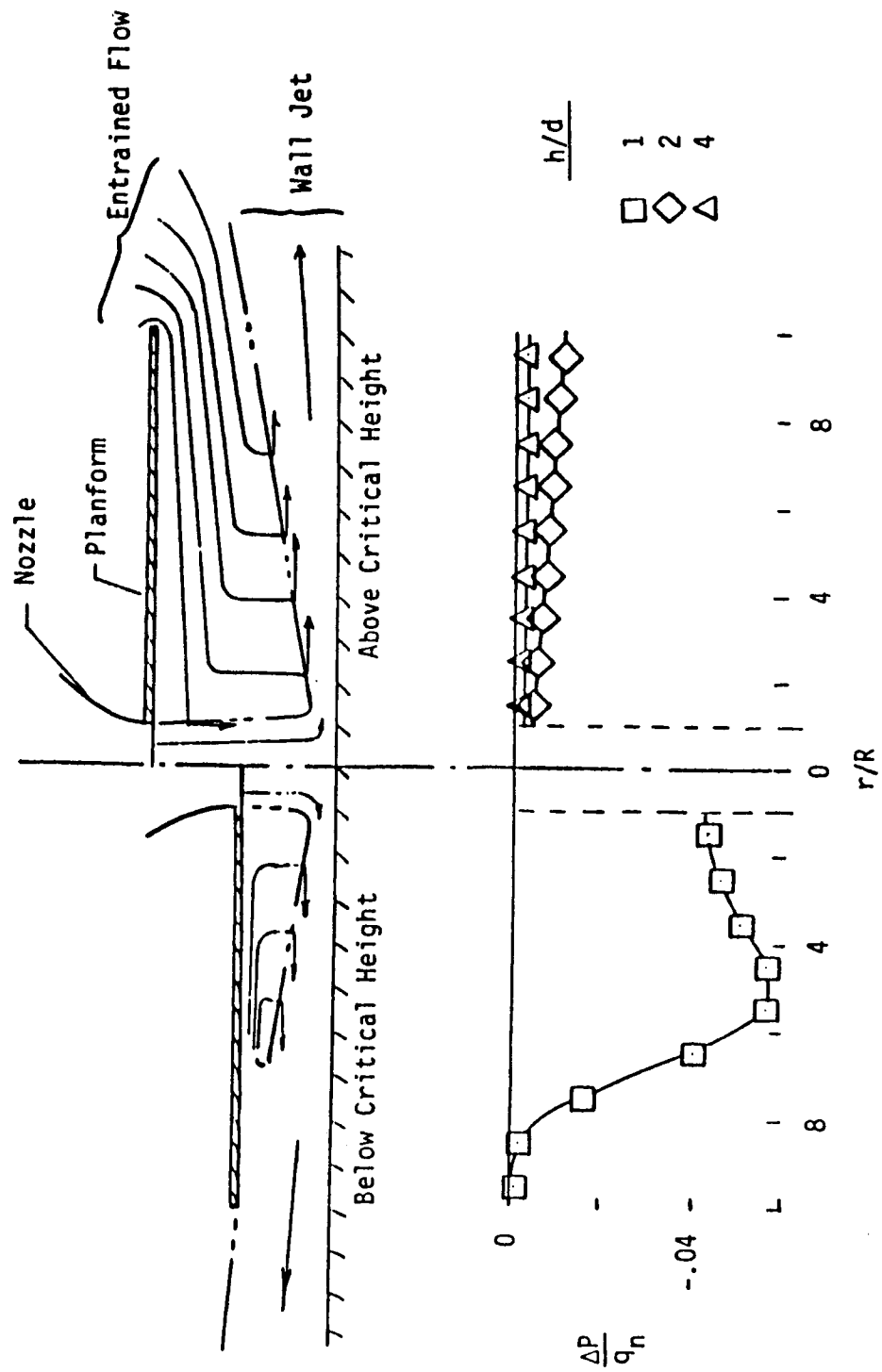


Figure 8.- Pressure on Plate in Hover, (Ref. 4).

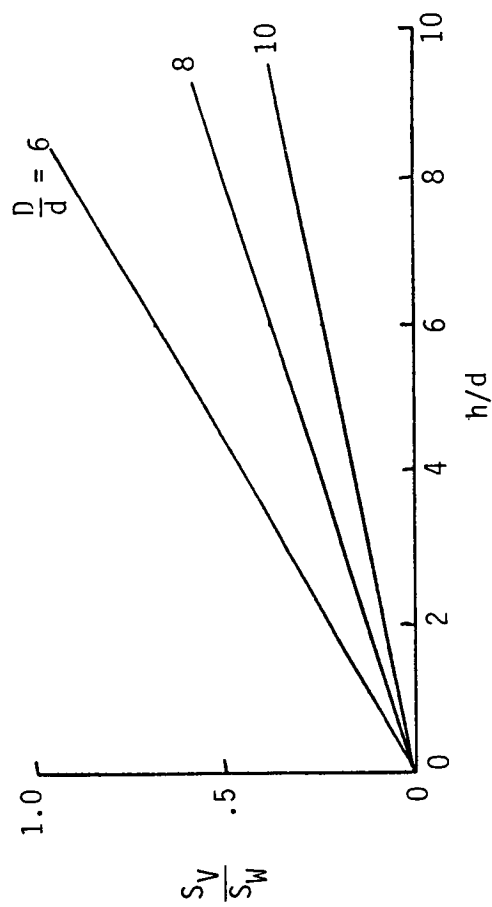
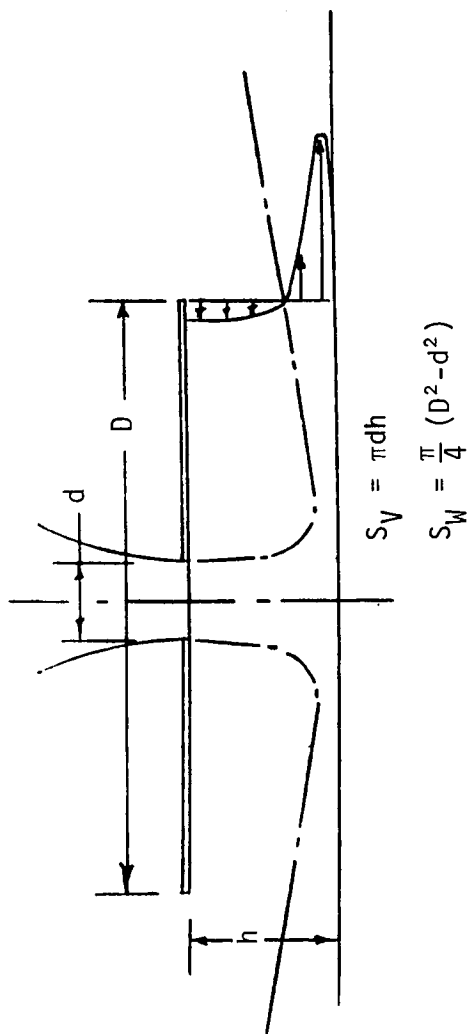


Figure 9.- At Low Operating Heights the Wall Jet is the Primary Entrainment Surface.

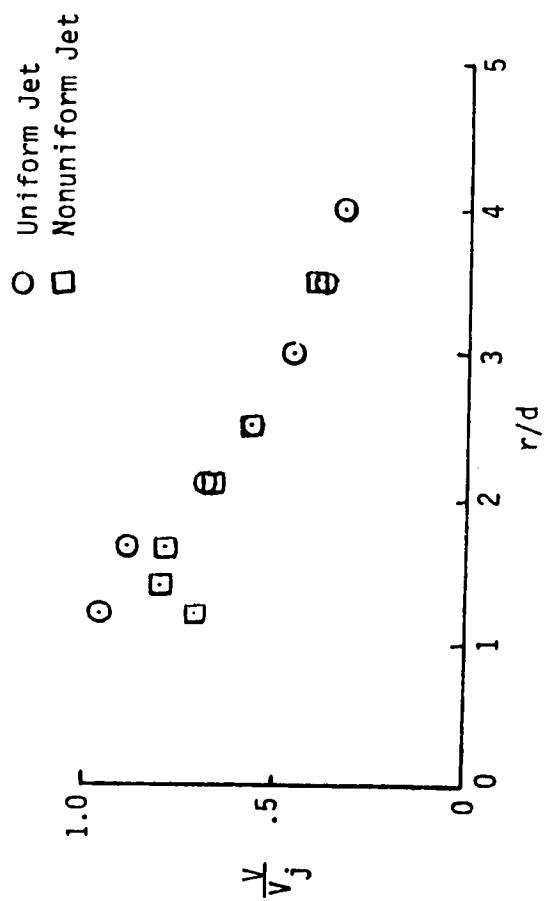
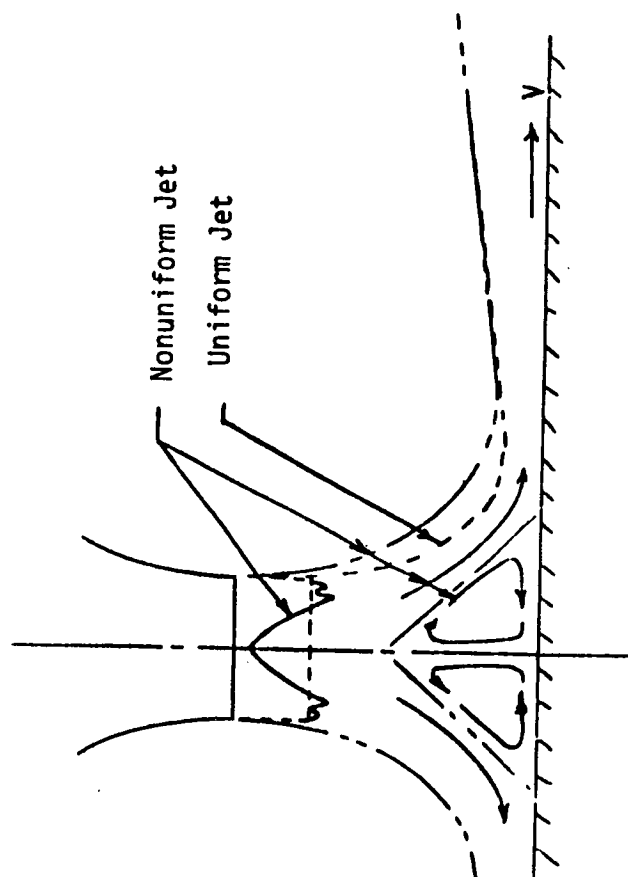


Figure 10.- Effect of exit velocity distribution on wall jet and flow in impingement region. (Ref. 9)

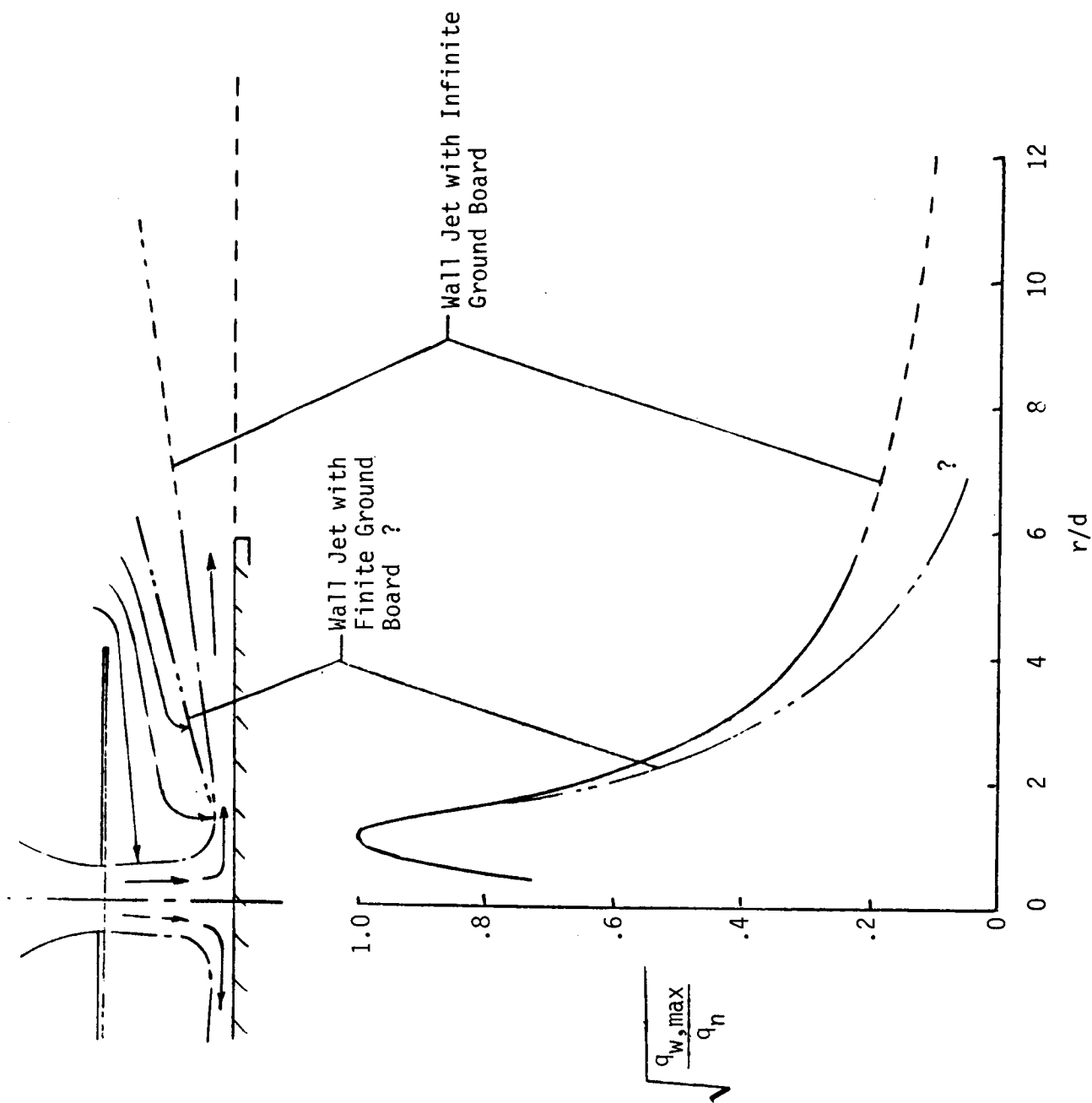


Figure 11.- Is there a significant effect of finite ground board size?

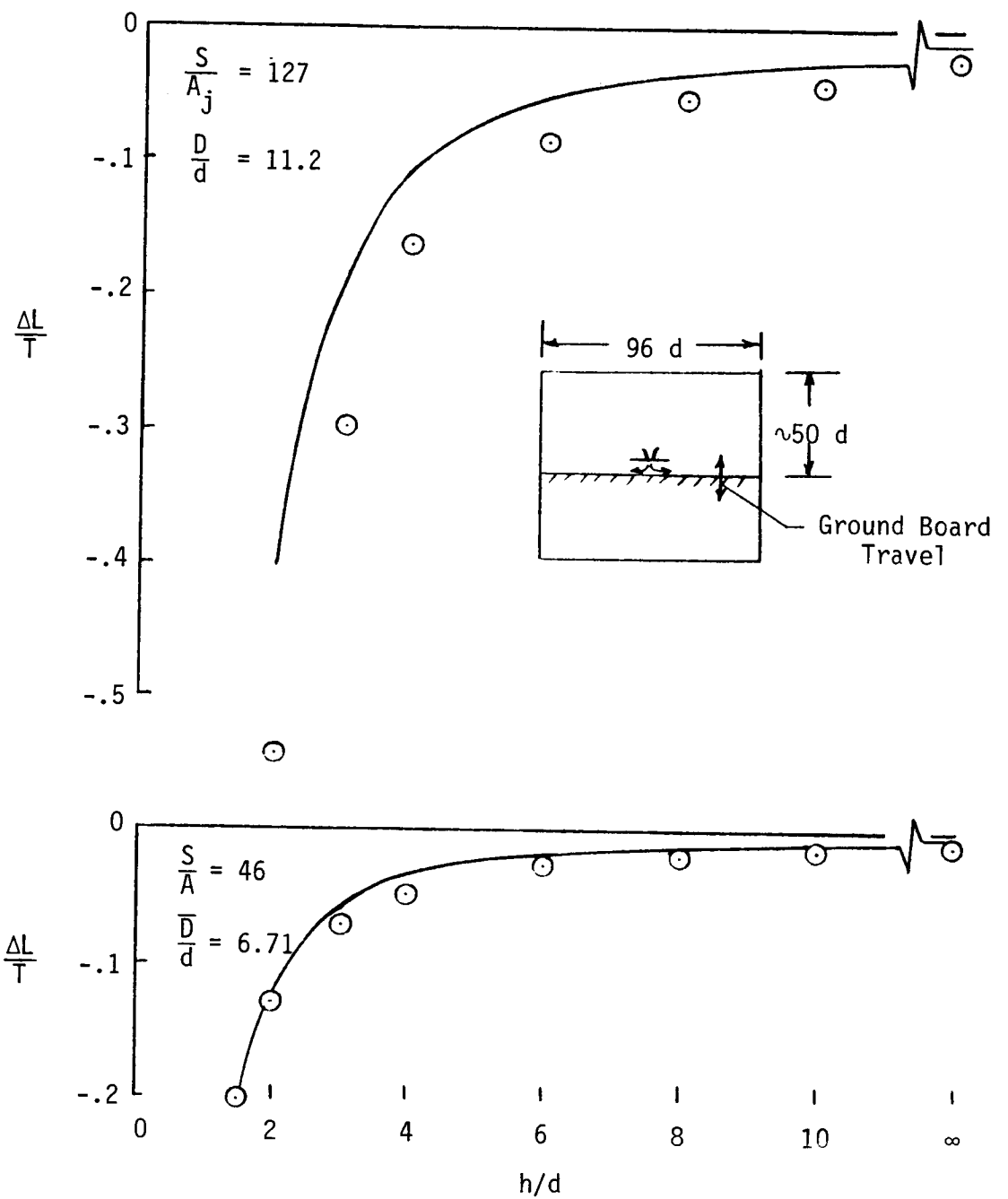


Figure 12.- Data taken in inadequate size test chamber. (Ref. 10)

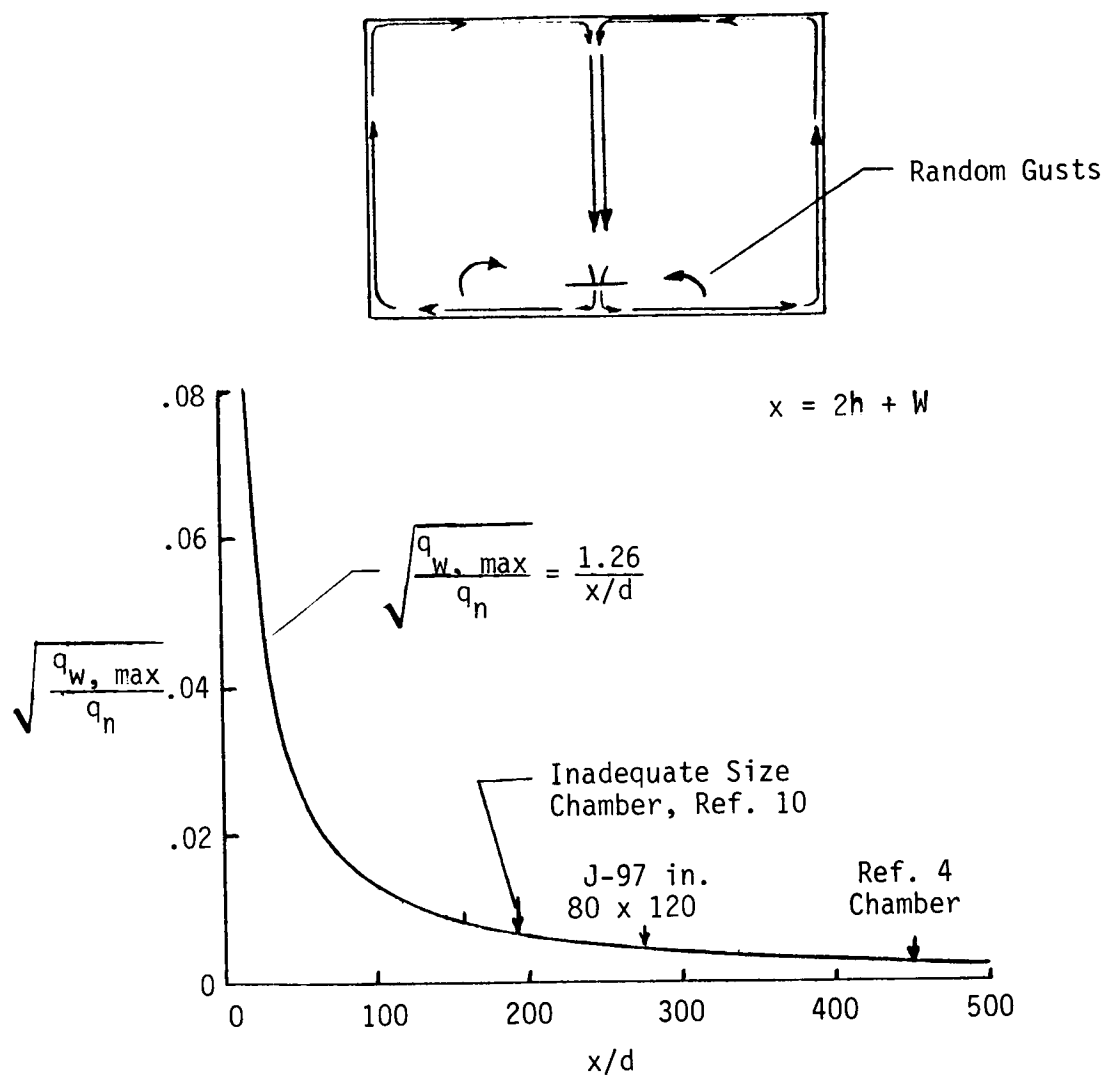


Figure 13.- Decay of velocity with distance from impingement point.



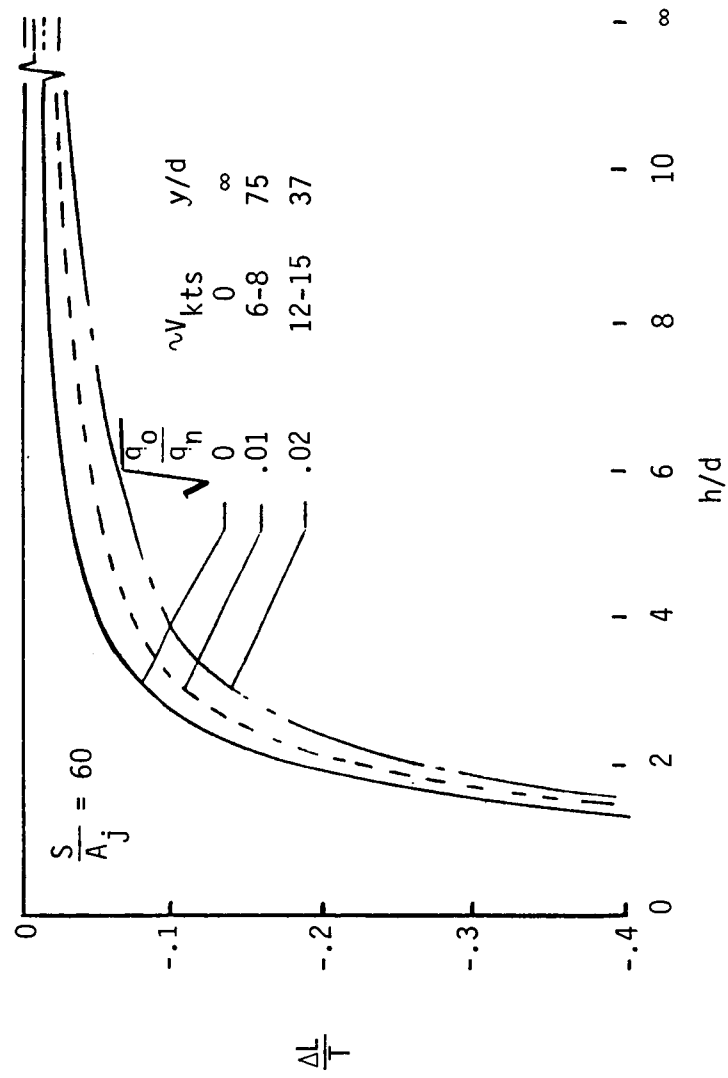
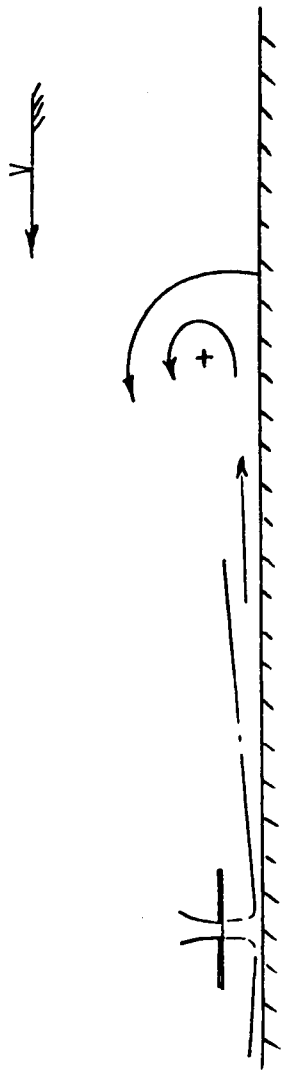


Figure 14.- Effect of Crossflow. (Ref. 10)

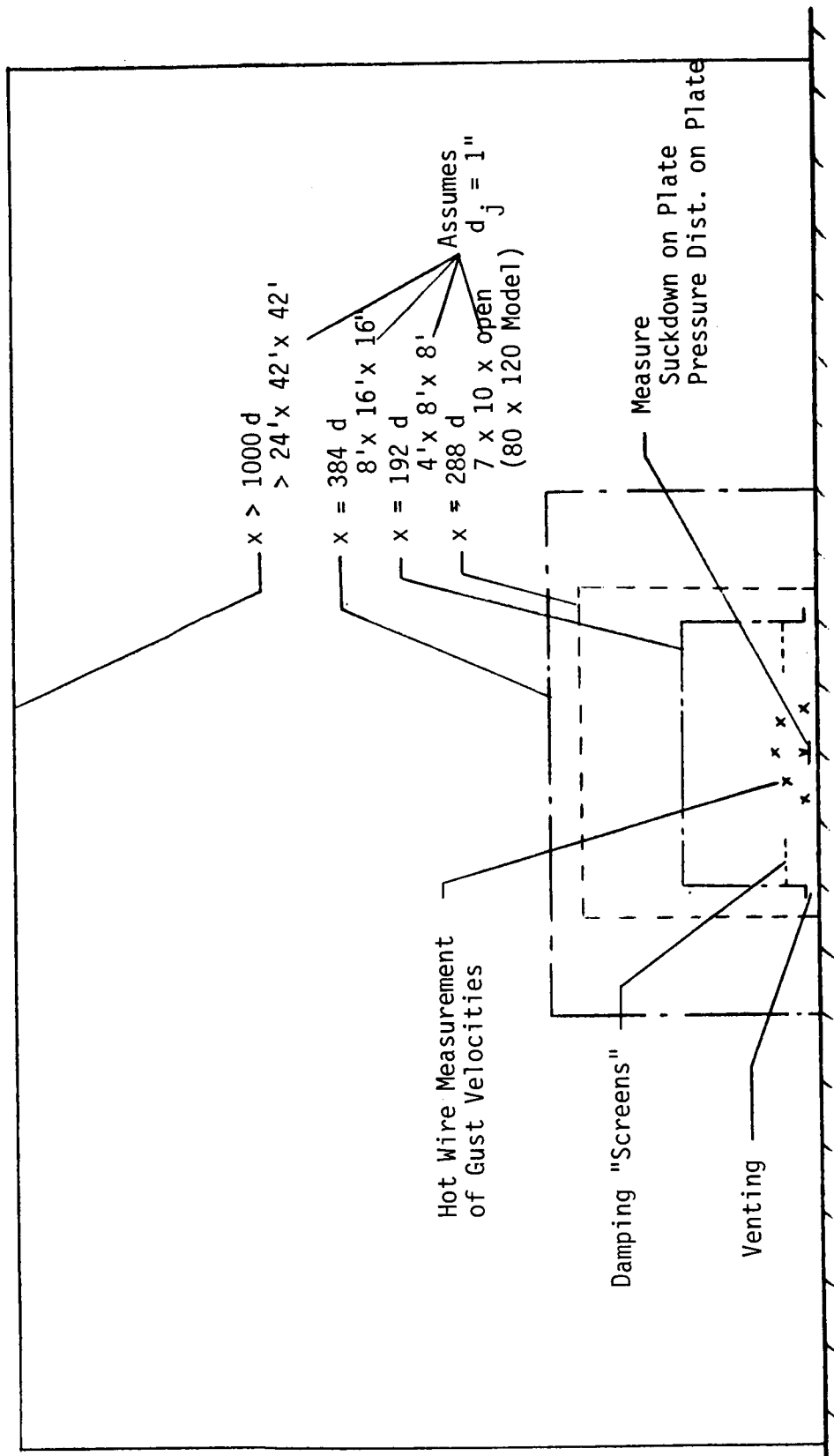


Figure 15.- Test Chamber Size Investigation.

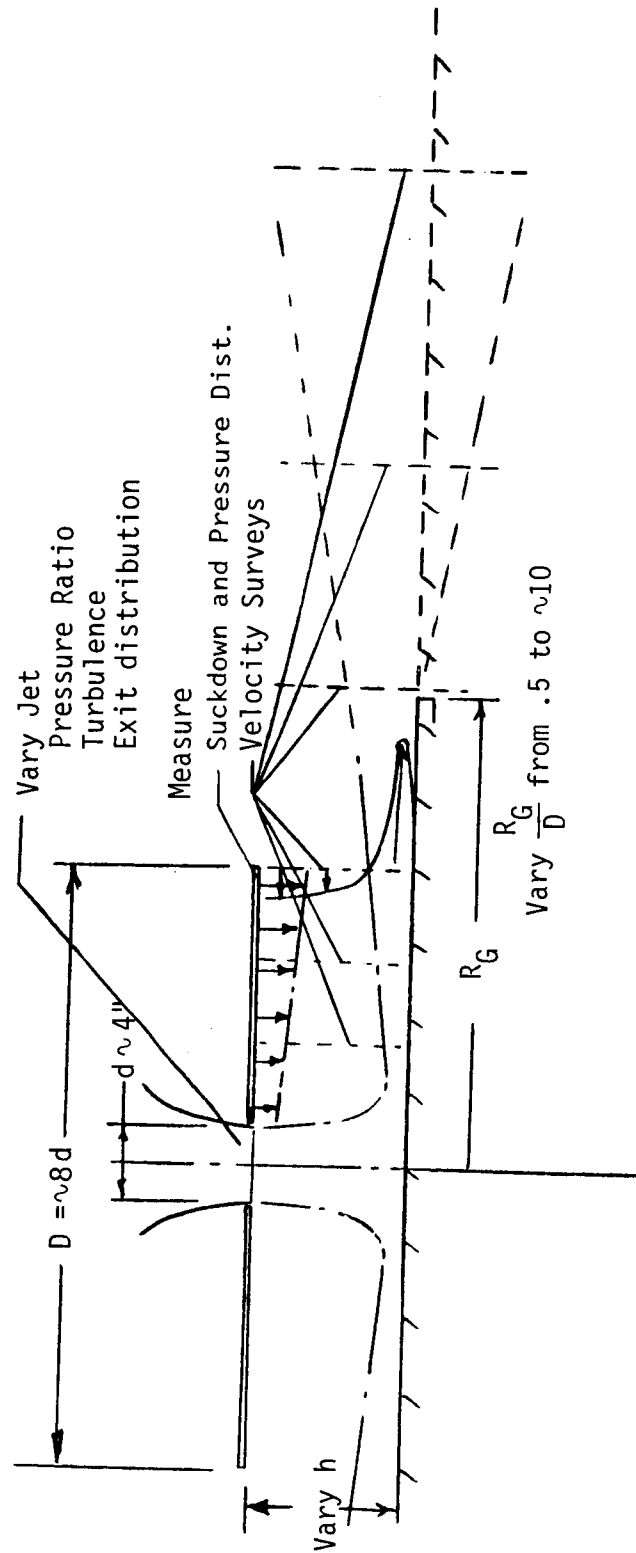


Figure 16.- Investigate Effects on and of Wall Jet Characteristics.

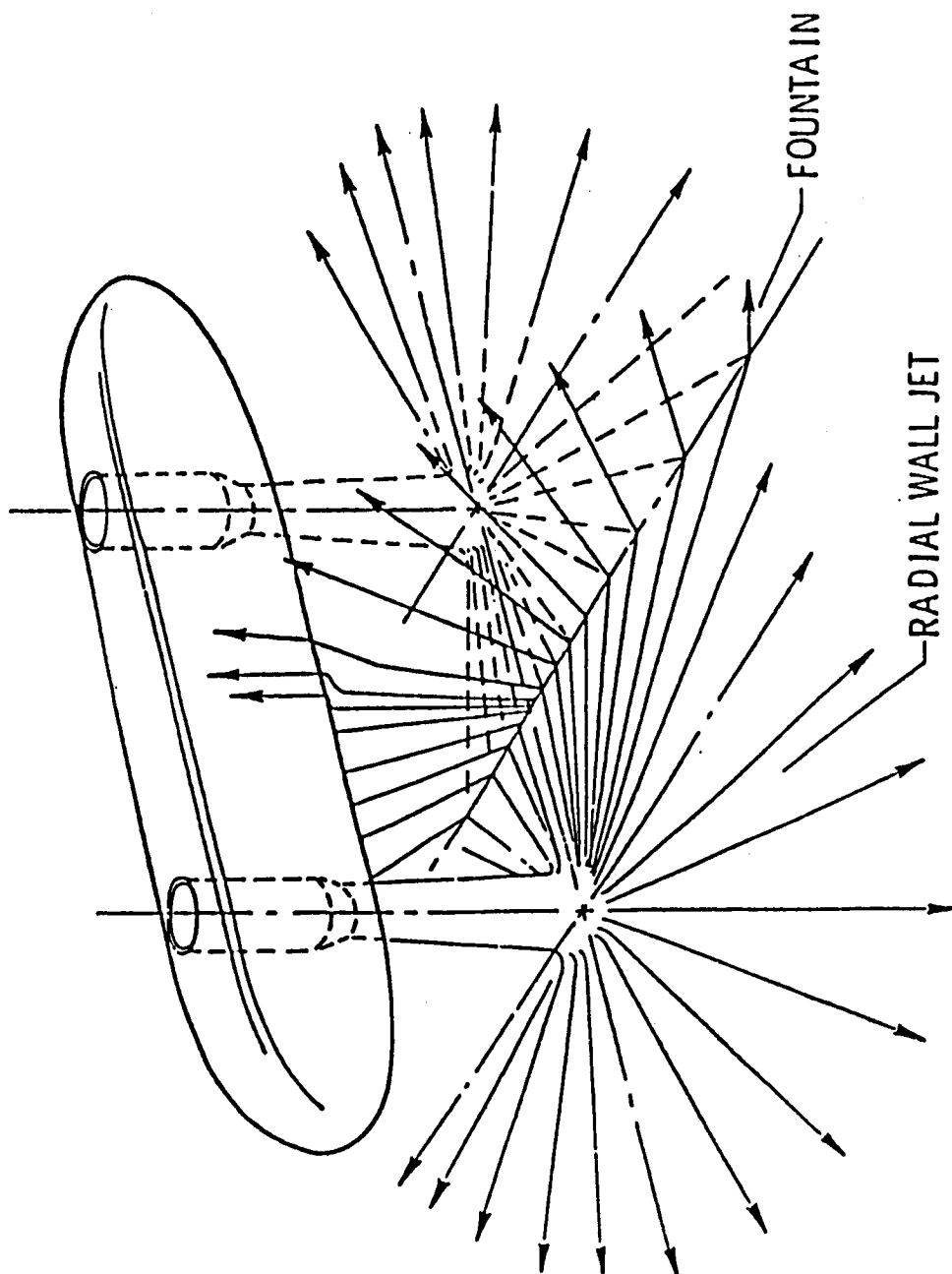


Figure 17.- Fountain flow generated between a pair of jets.

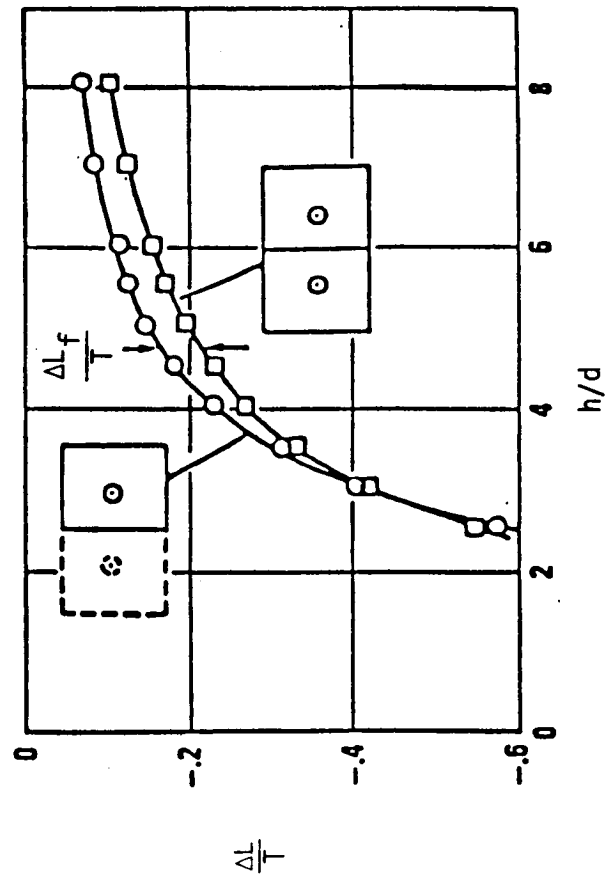


Figure 18.- Isolation of the incremental fountain effect for two nozzles. (Ref. 11)

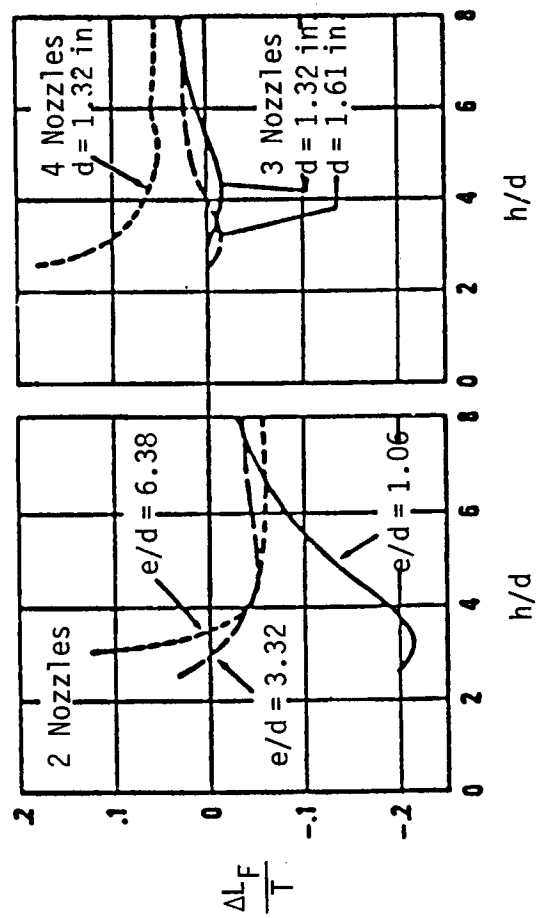


Figure 19.- Incremental fountain lift for two, three and four nozzles.  
(Ref. 11)

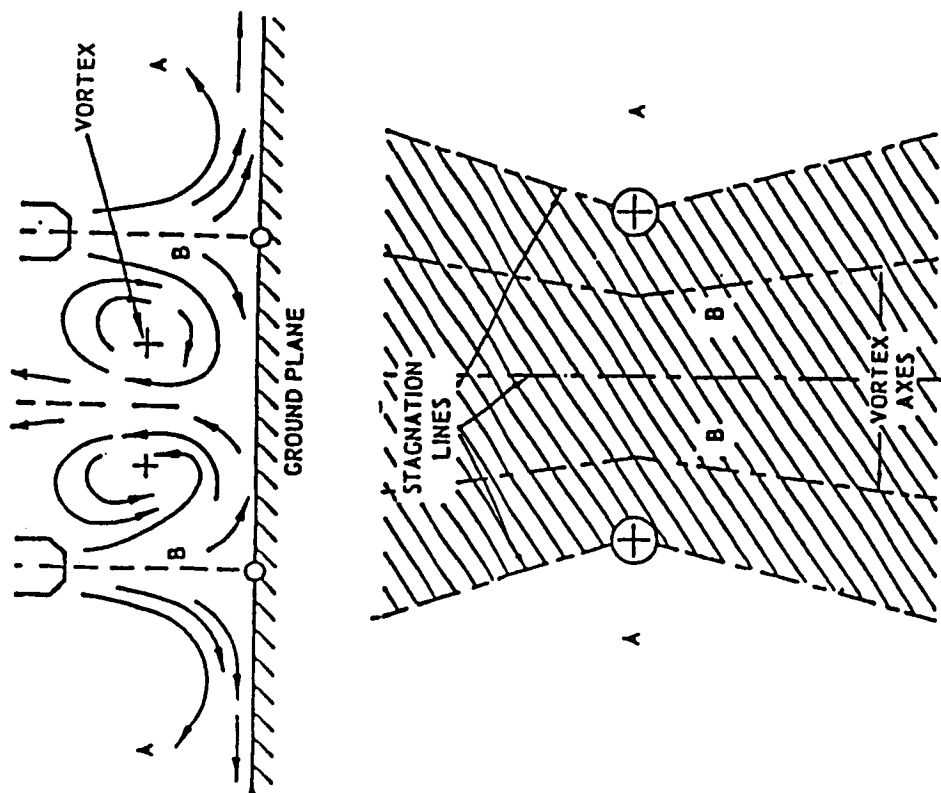


Figure 20.- Flow field between two jets hovering in ground effect. (Ref. 12)

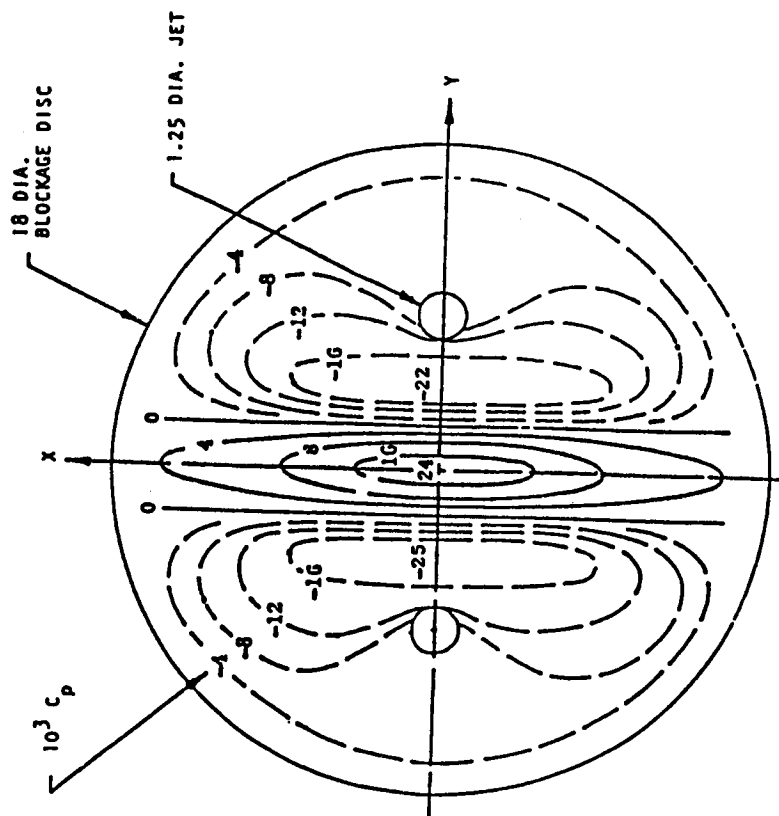


Figure 21.- Pressure distribution due to fountain flow from two jets in ground effect. (Ref. 12)

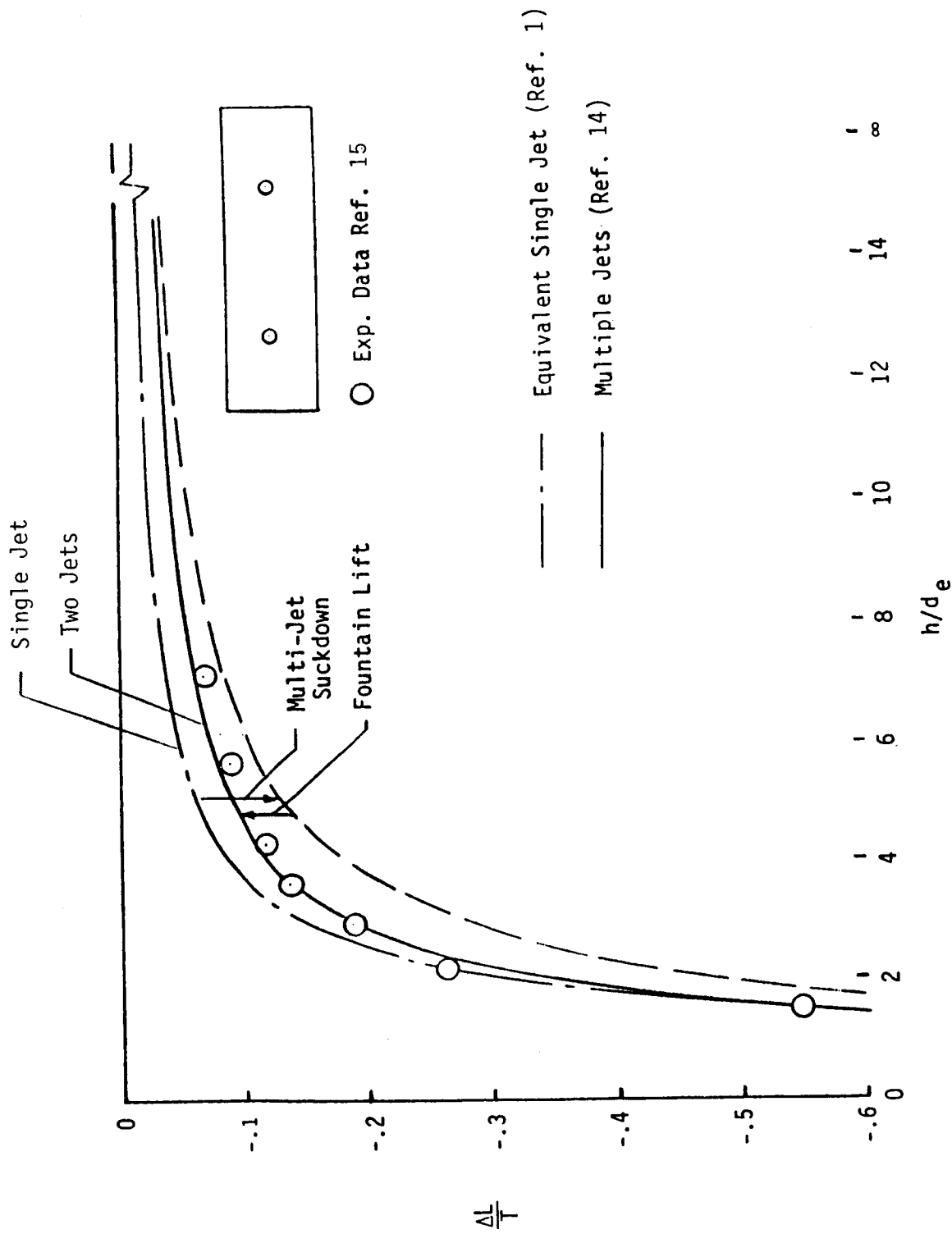


Figure 22.- Fountain lift and the additional multi-jet suckdown generated on a simple two-jet configuration.



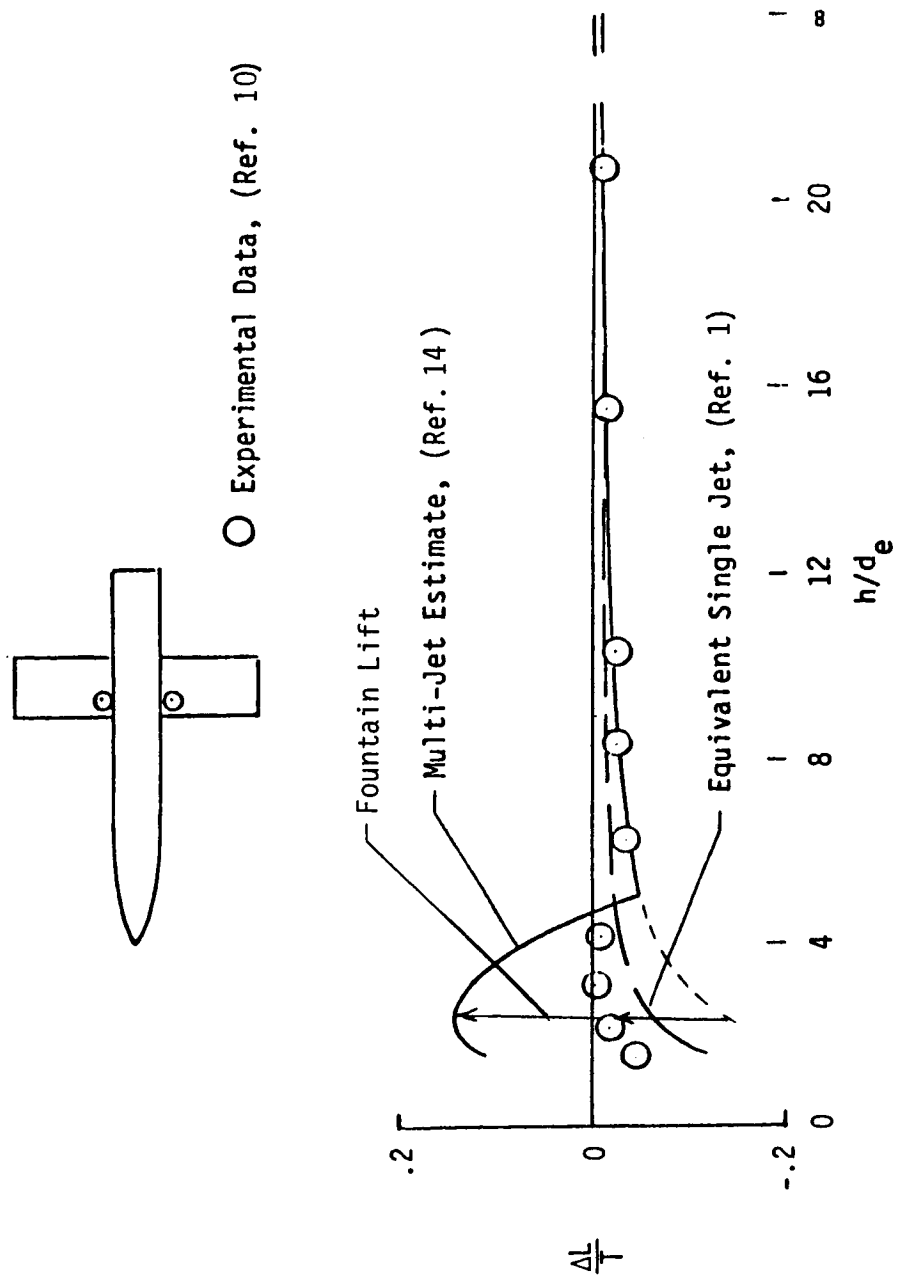


Figure 23.- Lift induced on simple 2-jet high wing configuration hovering in ground effect.

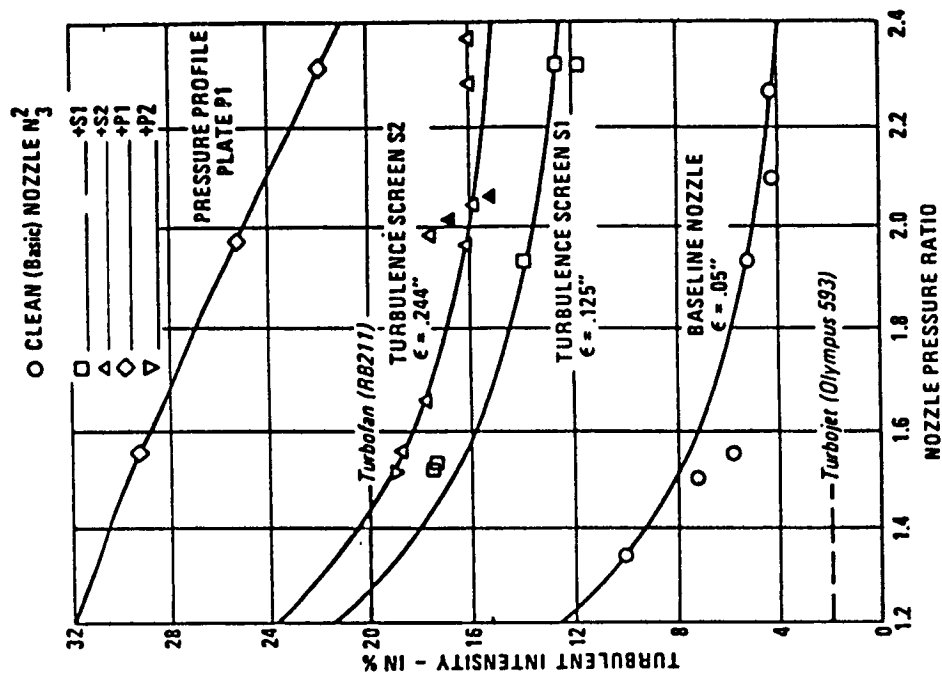


Figure 25.- Turbulent intensity vs. NPR for screens and plates. (Ref. 11)

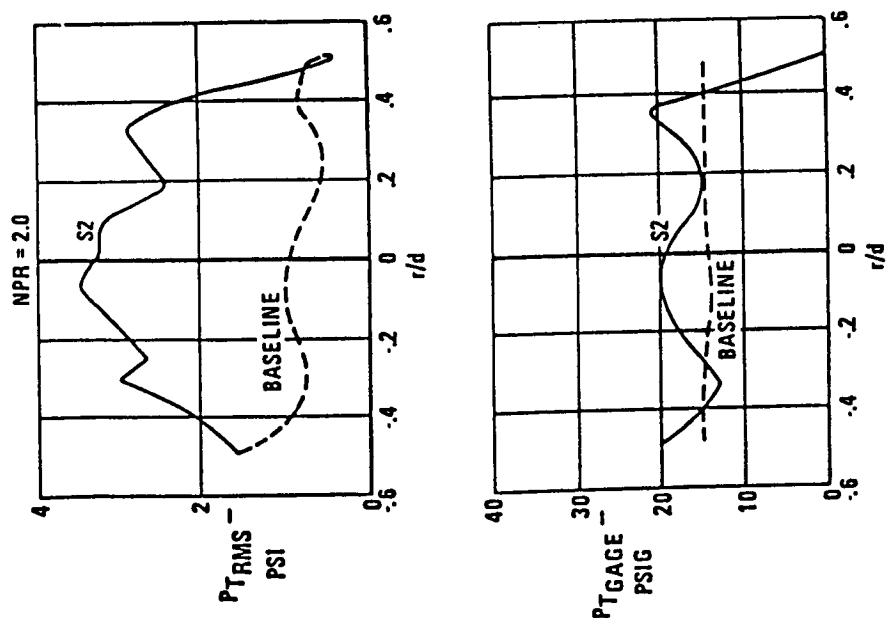


Figure 24.- Typical total pressure and  $P_{T\_RMS}$  surveys of nozzle exit for baseline nozzle and S2. (Ref. 11)

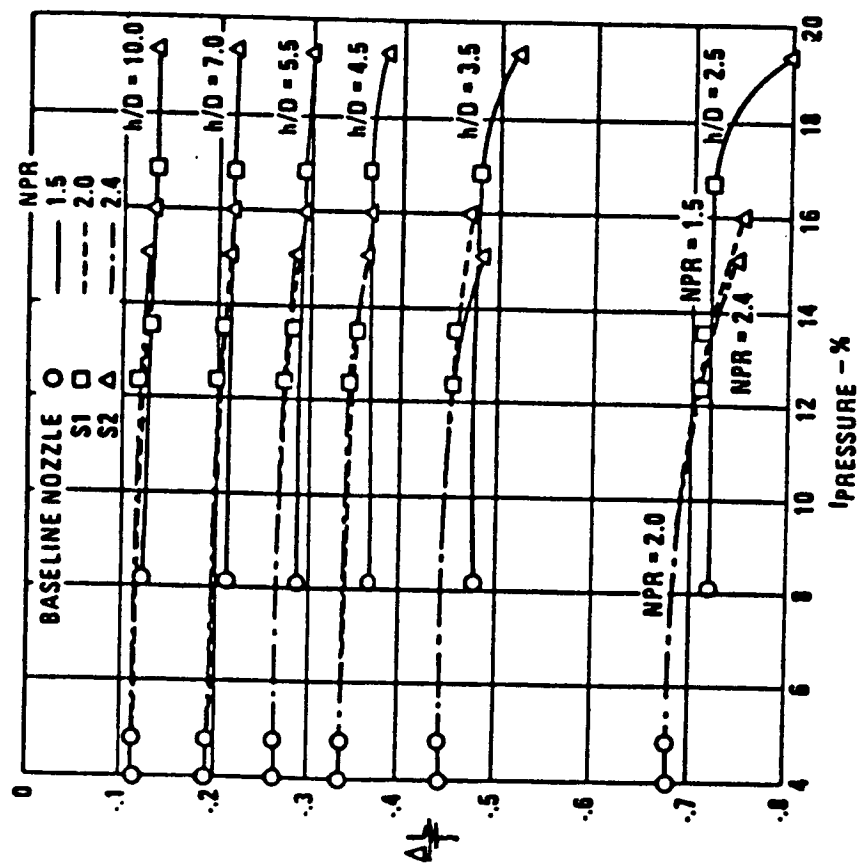


Figure 26.- Turbulence screens and NPR effects on net induced force coefficient for two nozzle configuration. (Ref. 11)

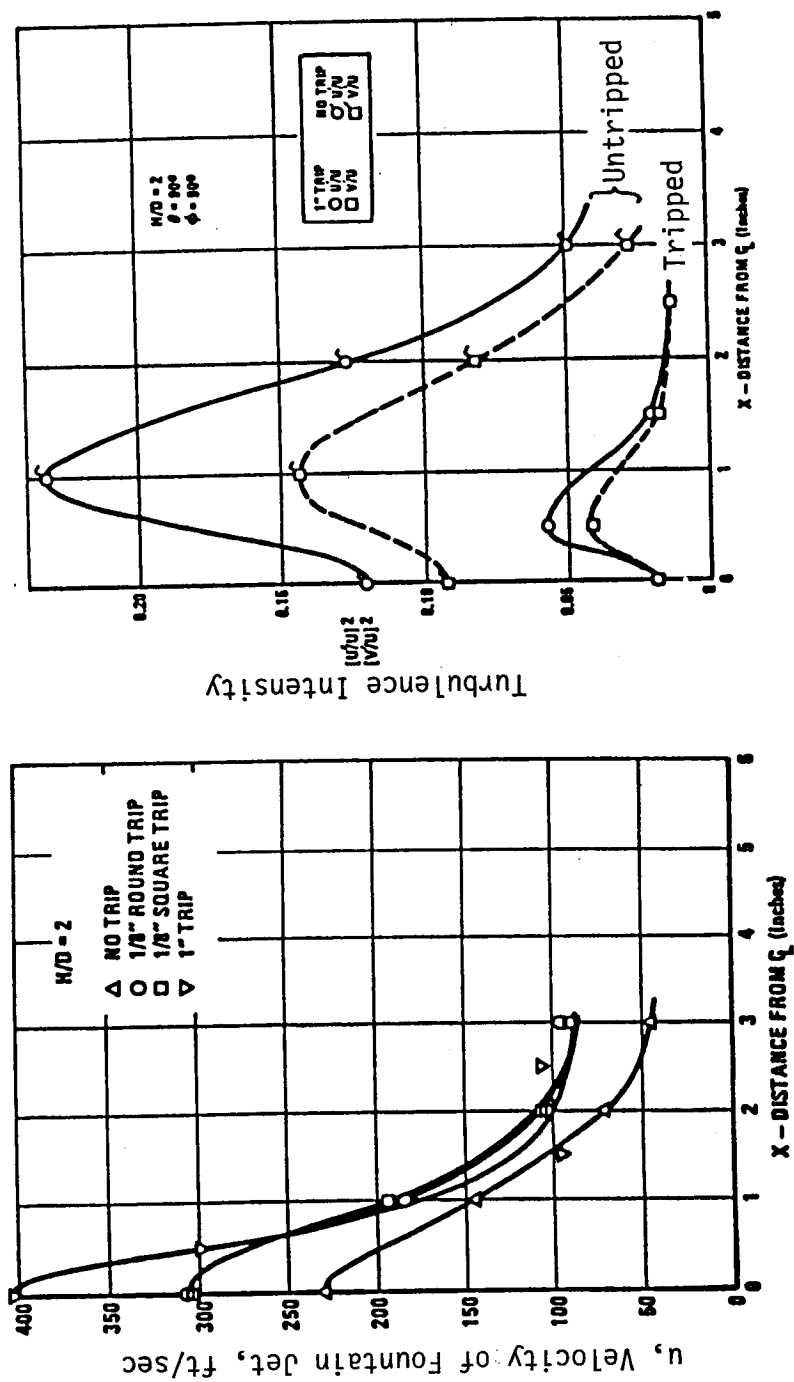
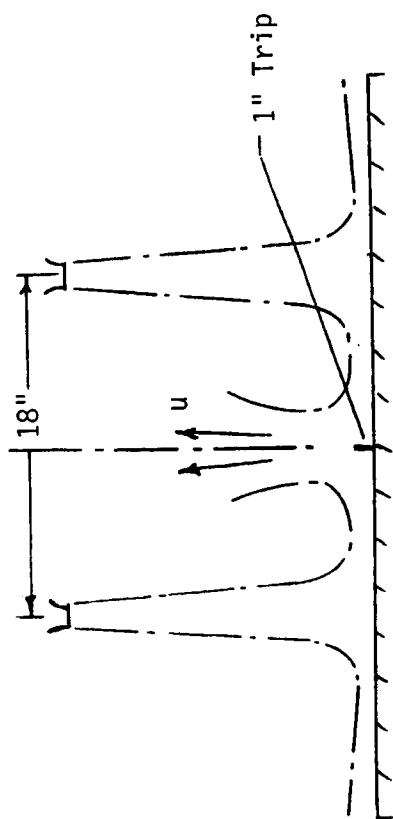


Figure 27.- Fountain turbulence. (Ref. 16)

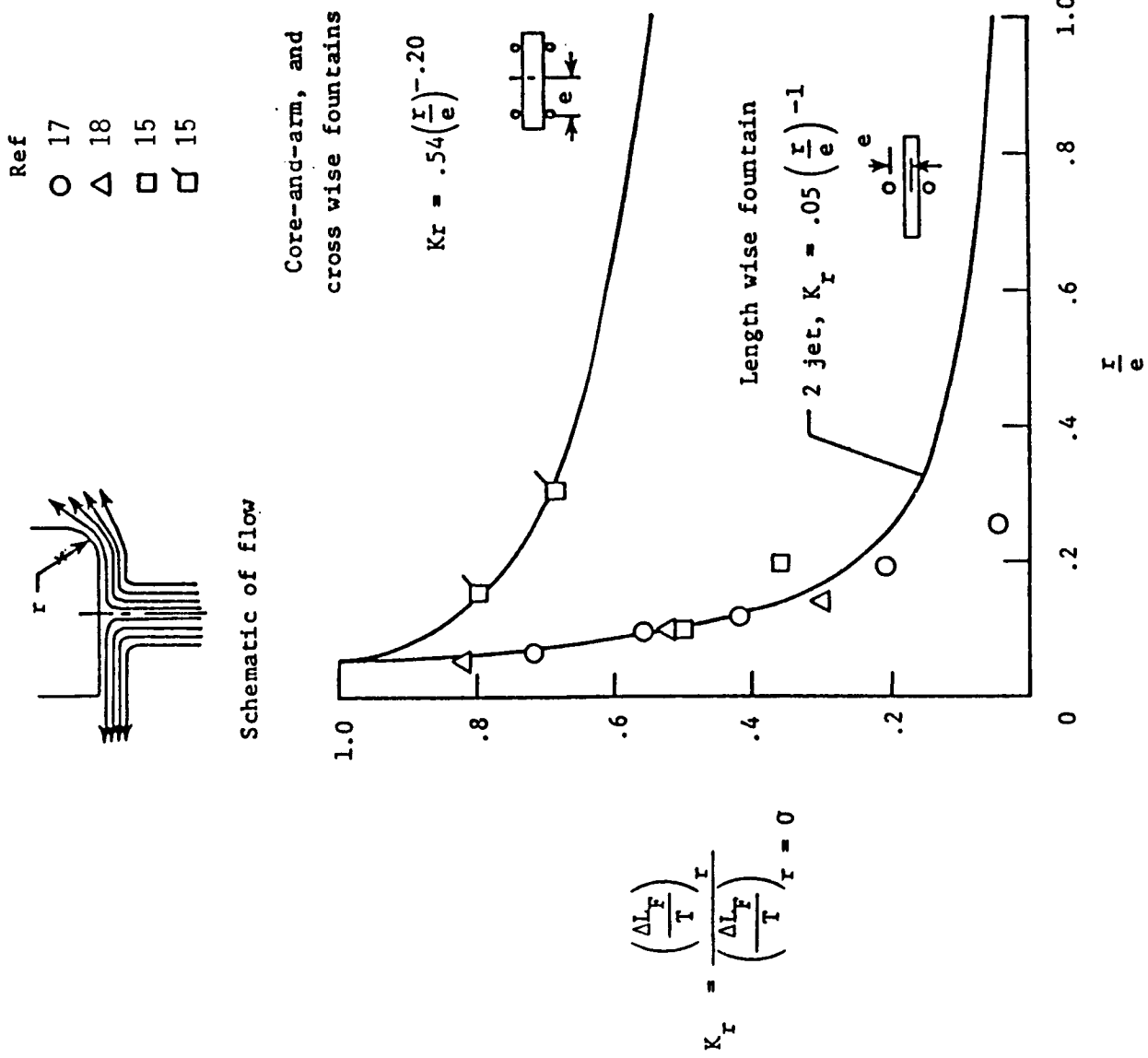


Figure 28.- Effect of lower surface contour. (Ref. 14)

$$\frac{\Delta L_L}{T} = k_L \left( \frac{\Delta L_f}{T} \right)$$

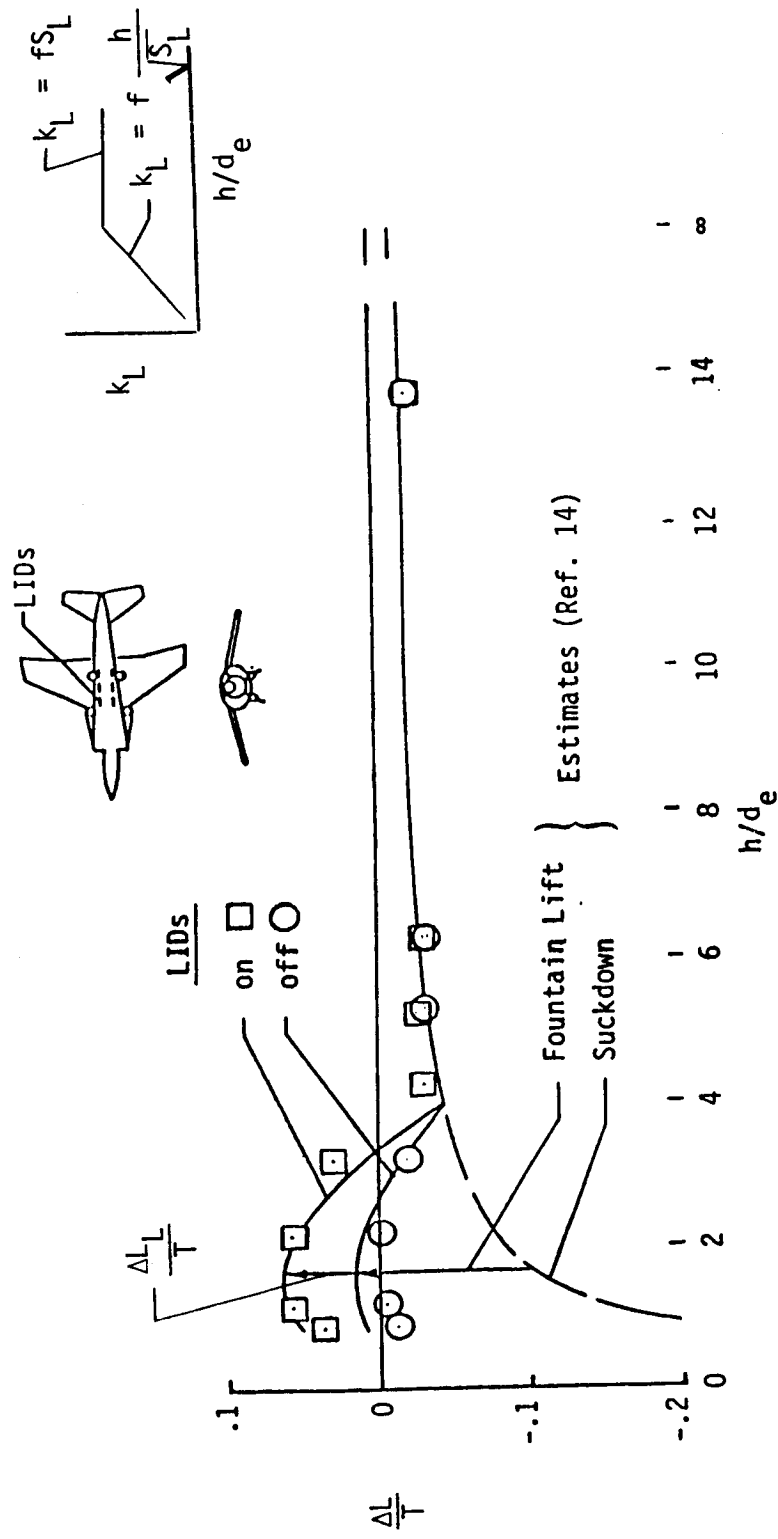


Figure 29.- Lift induced on Harrier configuration hovering in ground effect. (Ref. 19)

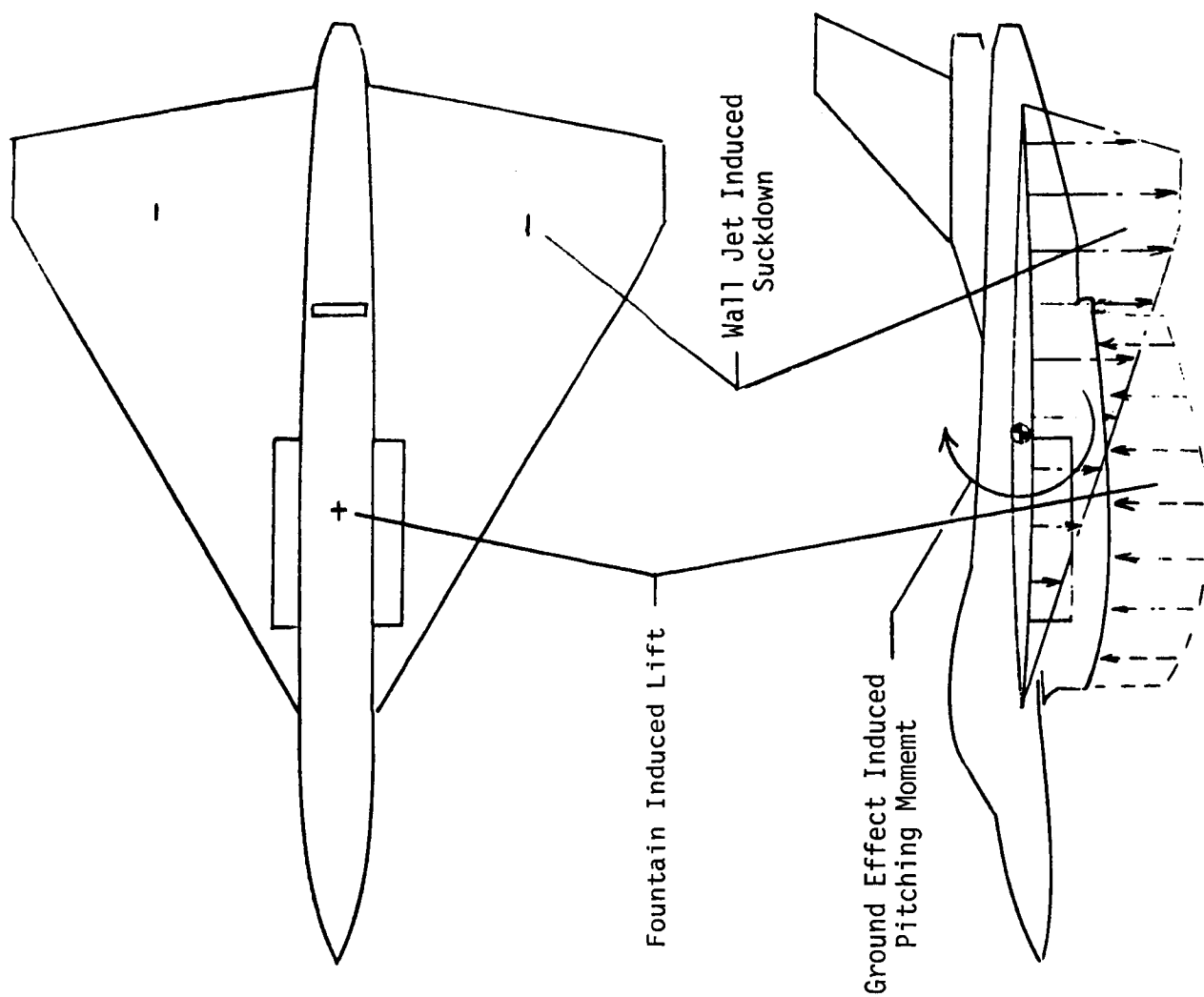


Figure 30.- Ground effect induced pitching moment.

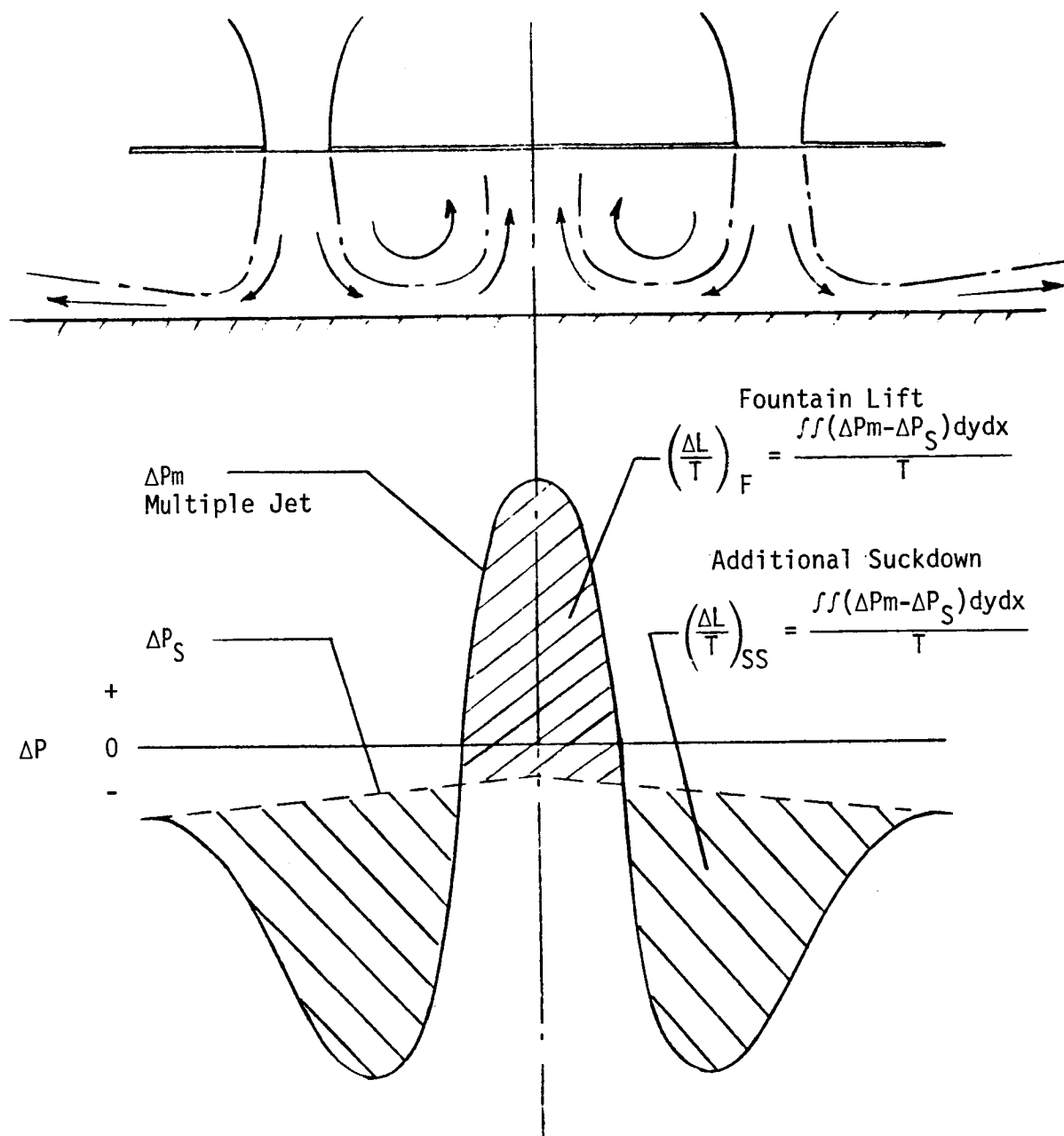


Figure 31.- Proposed method for determining fountain lift and additional suckdown.



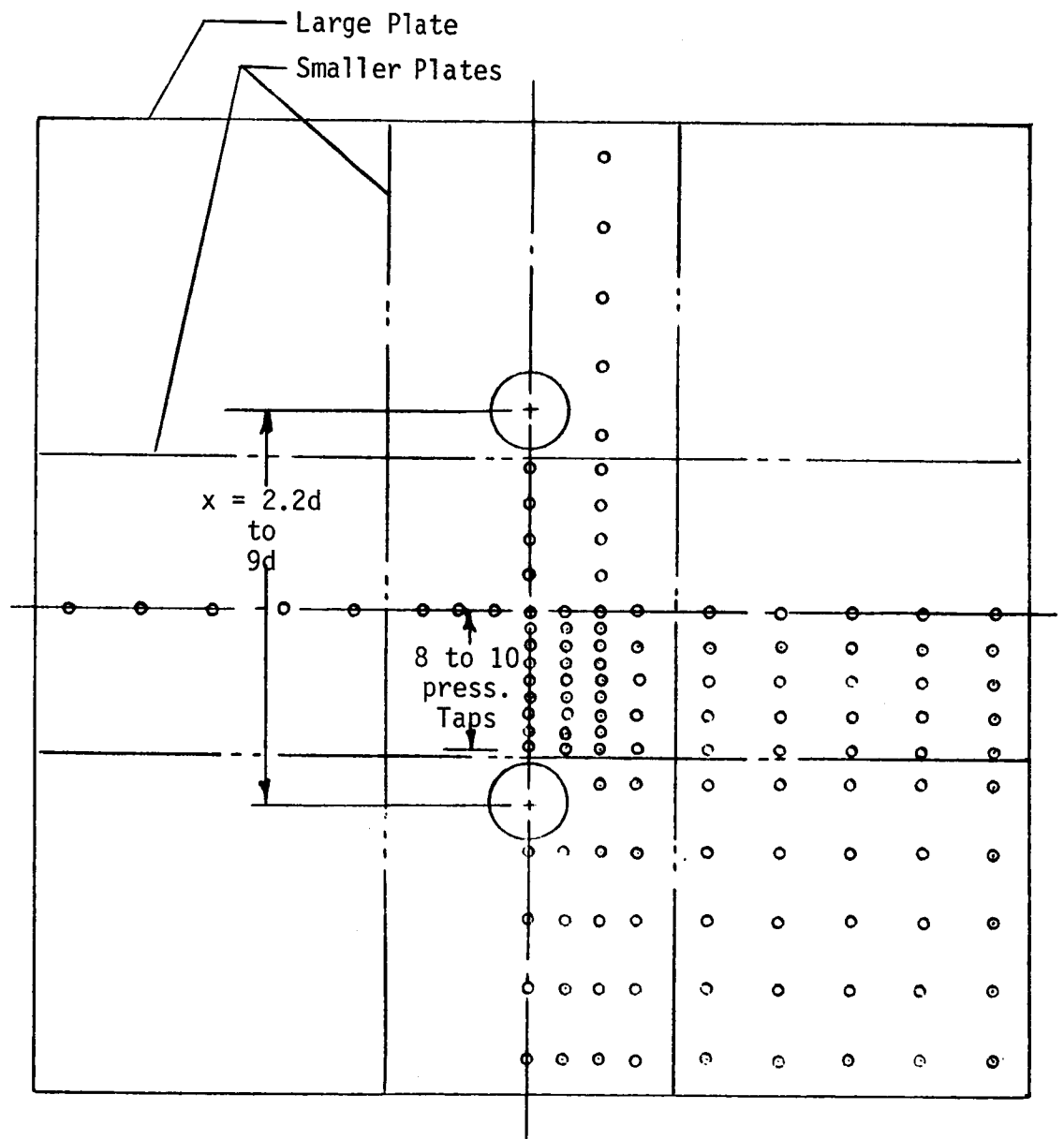


Figure 32.- Typical distribution of pressure taps.

## THE GROUND VORTEX

- Creates and Defines Dust Cloud
- One of Primary Mechanisms in Hot Gas Ingestion
- Causes Lift Loss

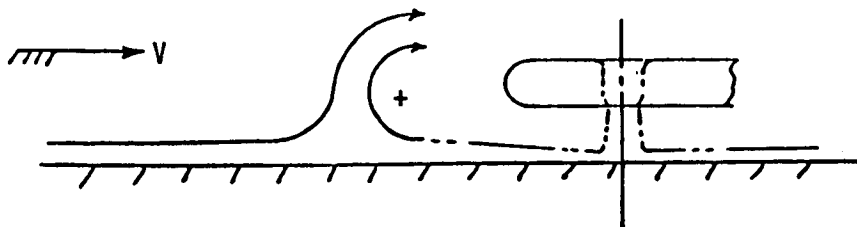
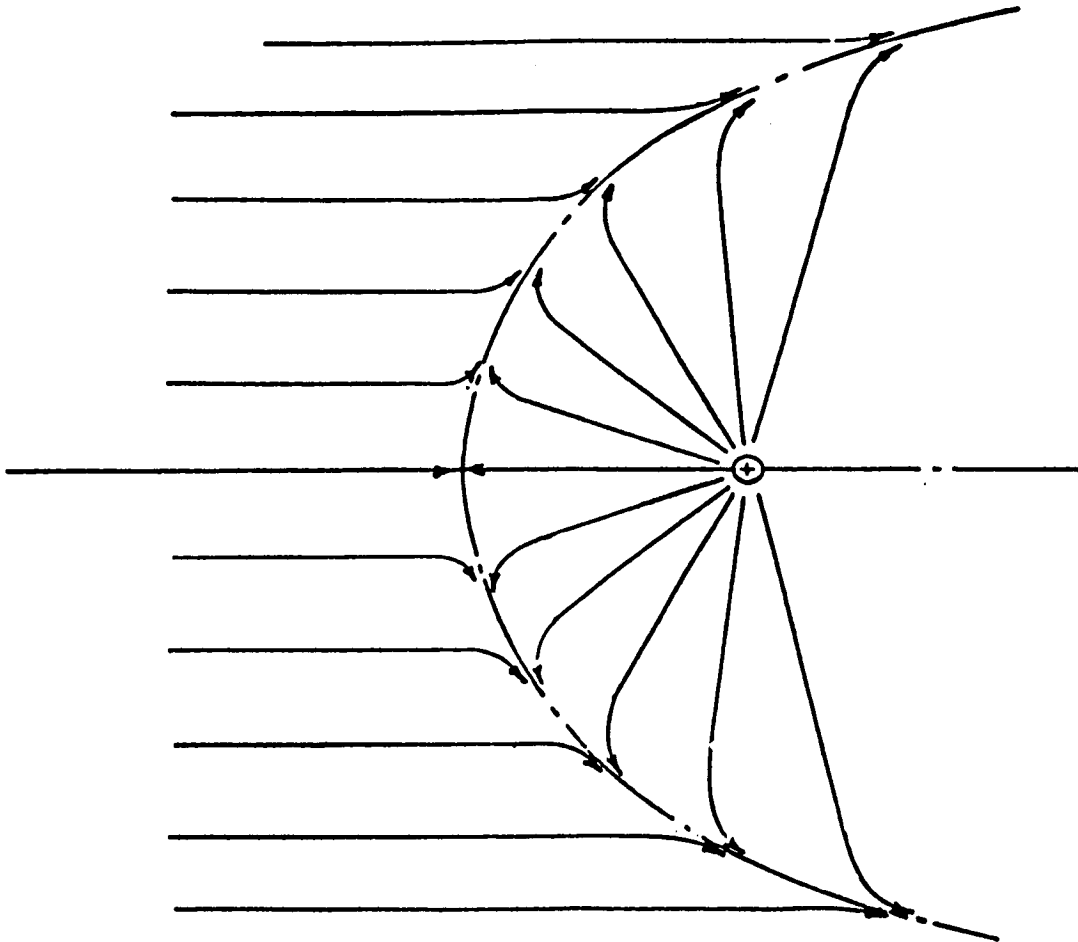


Figure 33.- Formation of ground vortex.

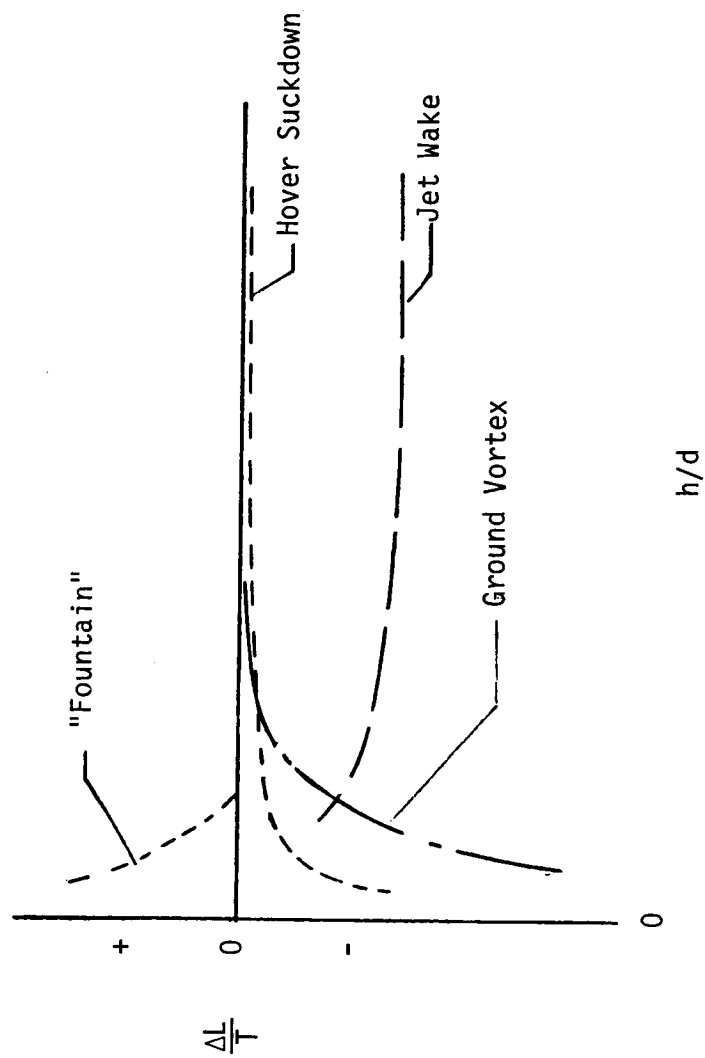


Figure 34.- STOL ground effect induced lift increments.

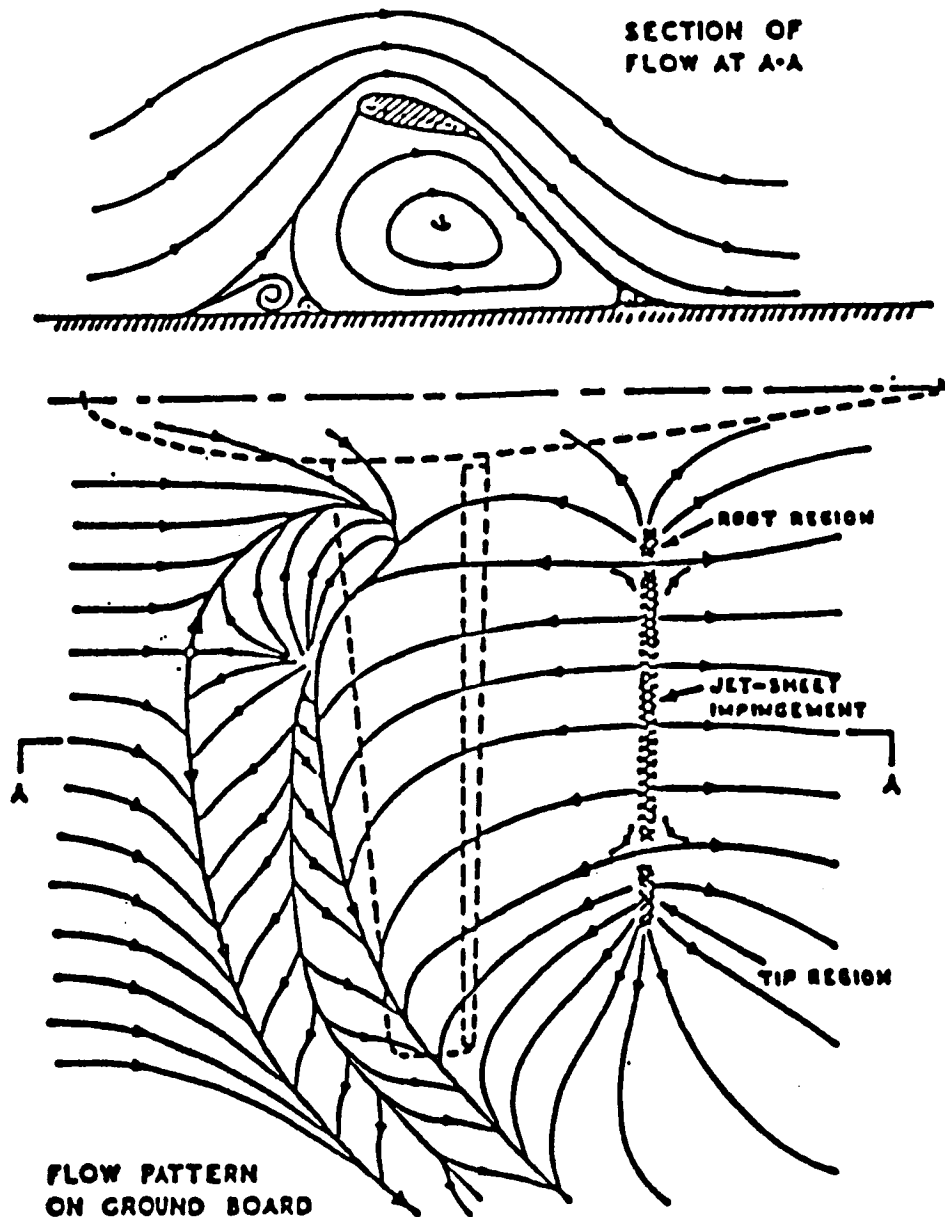


Figure 35.- Flow field under jet flap model with jet impingement on ground. (Ref. 20)

$$\alpha = 15^\circ, C_\mu = 2.1, H/\bar{c} = 1.5, \delta \sim 50^\circ.$$

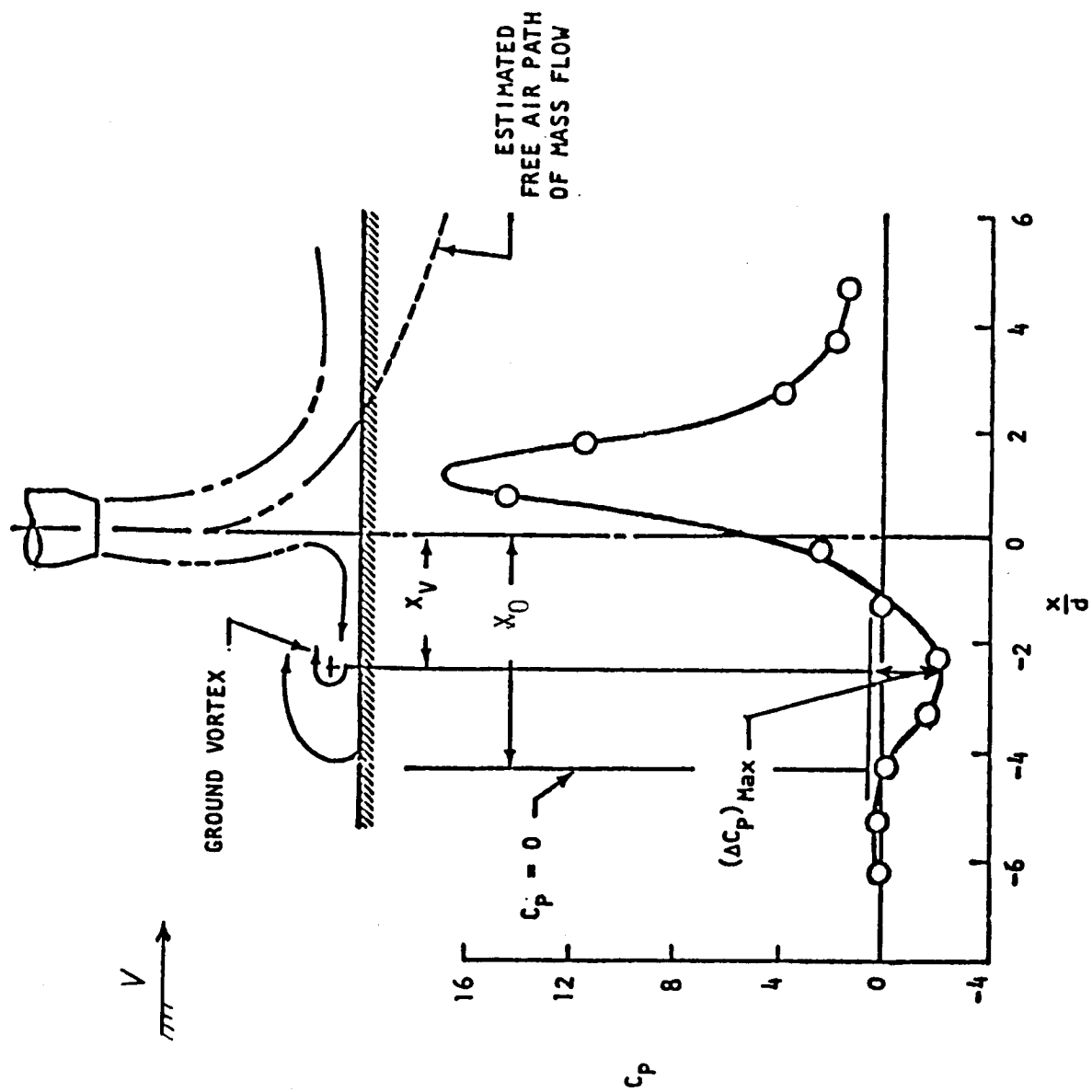


Figure 36.- Typical pressure distribution on ground board with definition of terms.

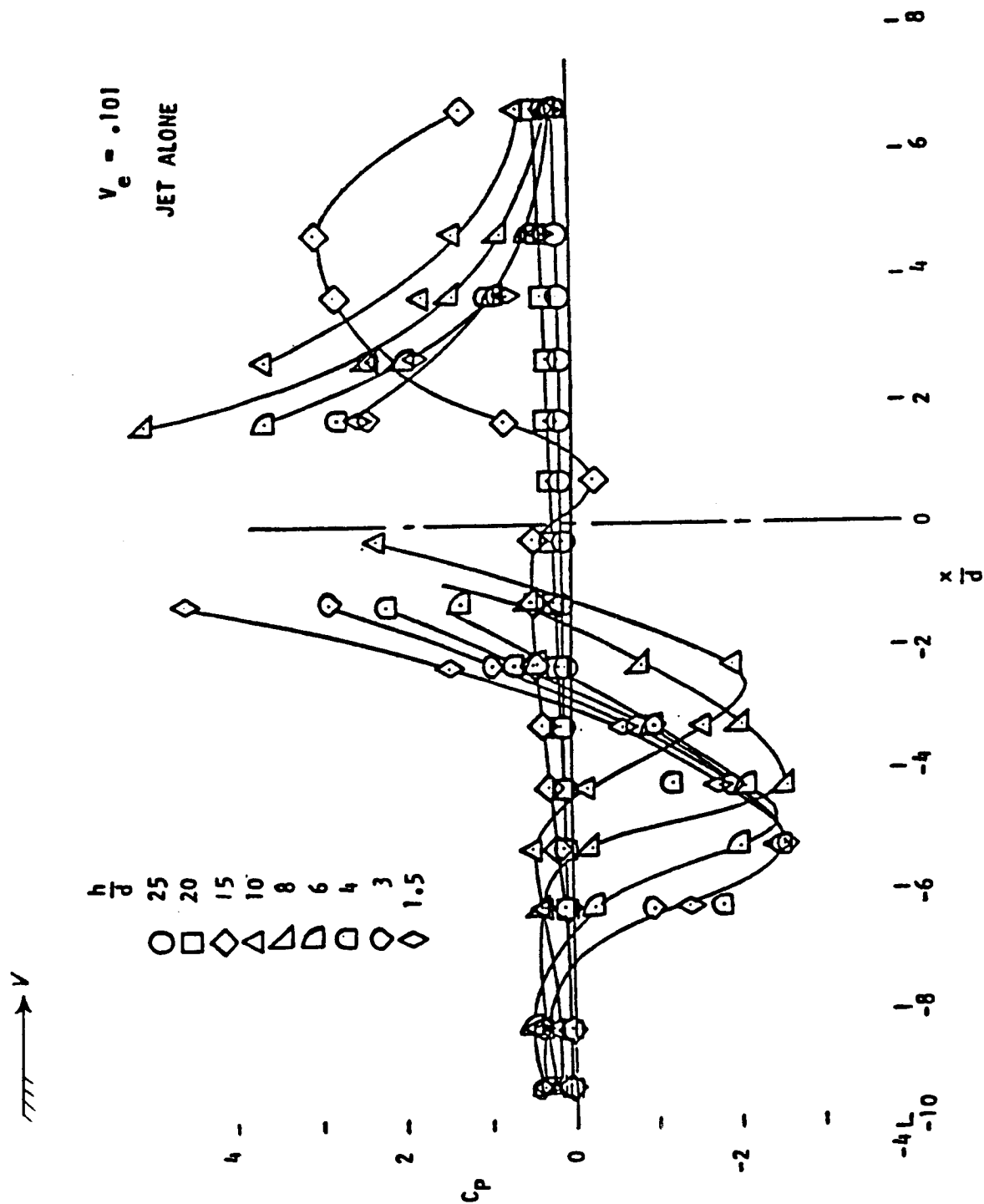


Figure 37.- Effect of height on pressure distribution measured on ground board jet alone,  $V_e = .101$ . (Ref.10)

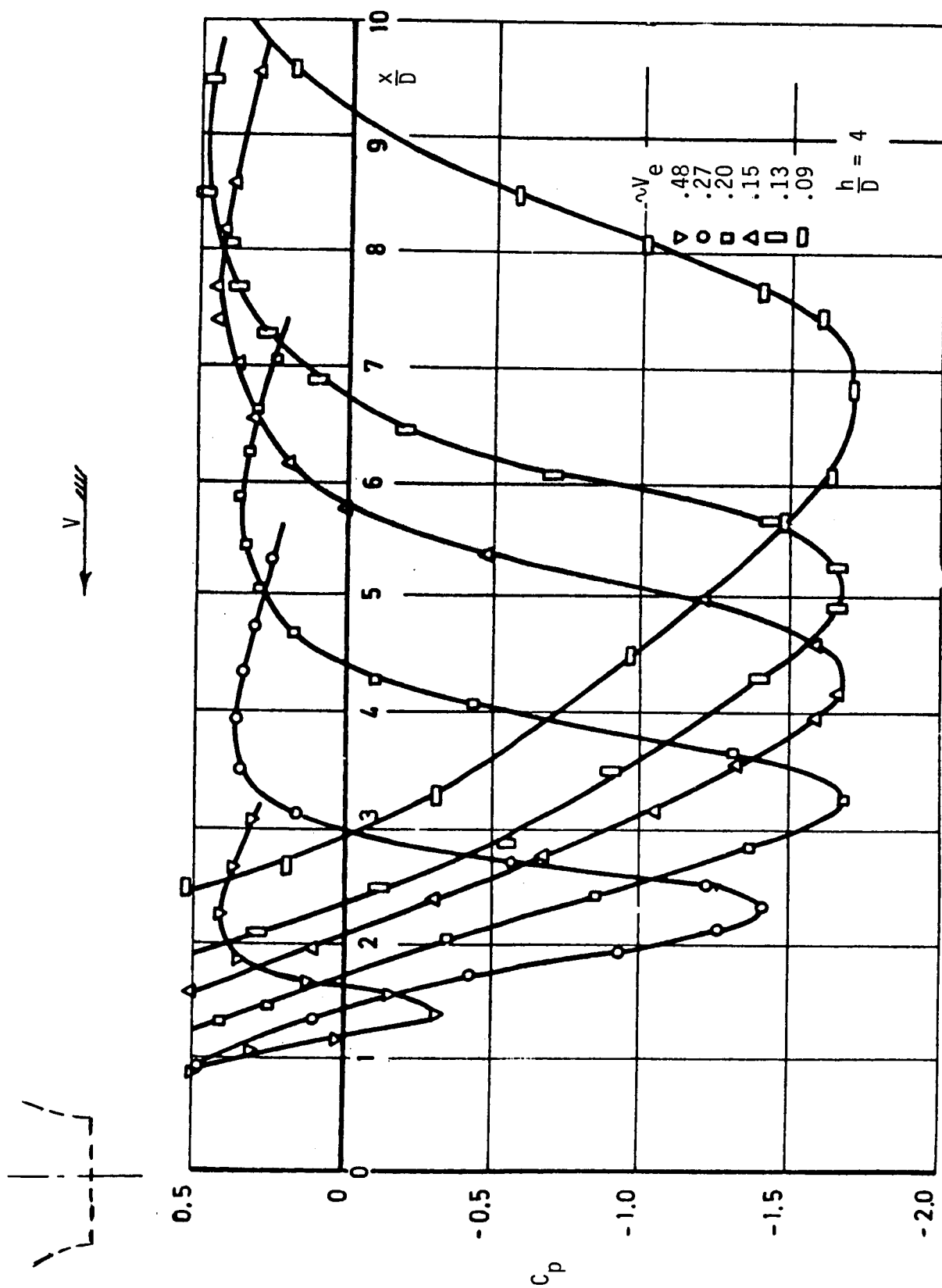


Figure 38.- Wall static pressure distribution under ground vortex. (Ref. 24)

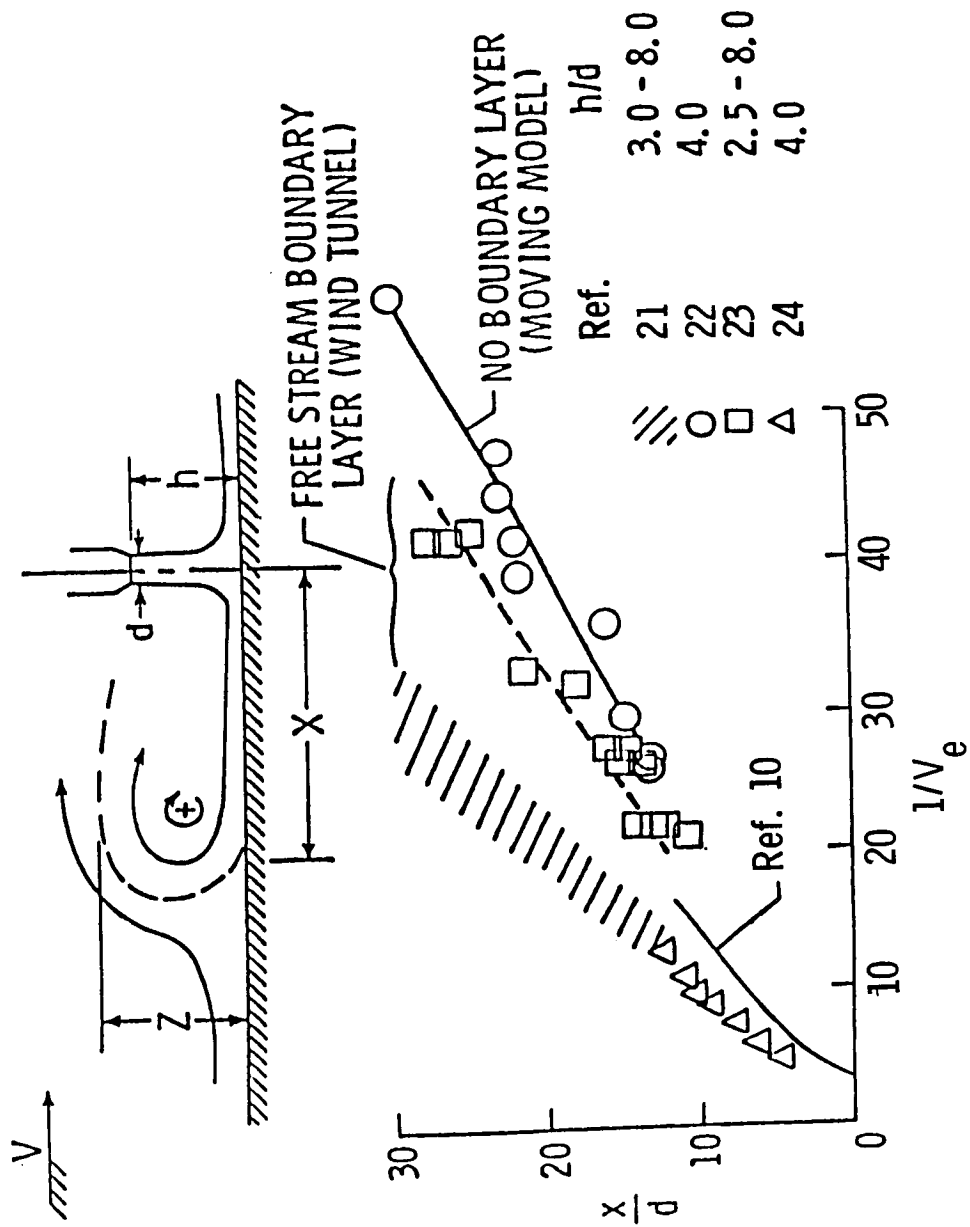


Figure 39.- Effect of ground boundary layer on forward extent of ground vortex.



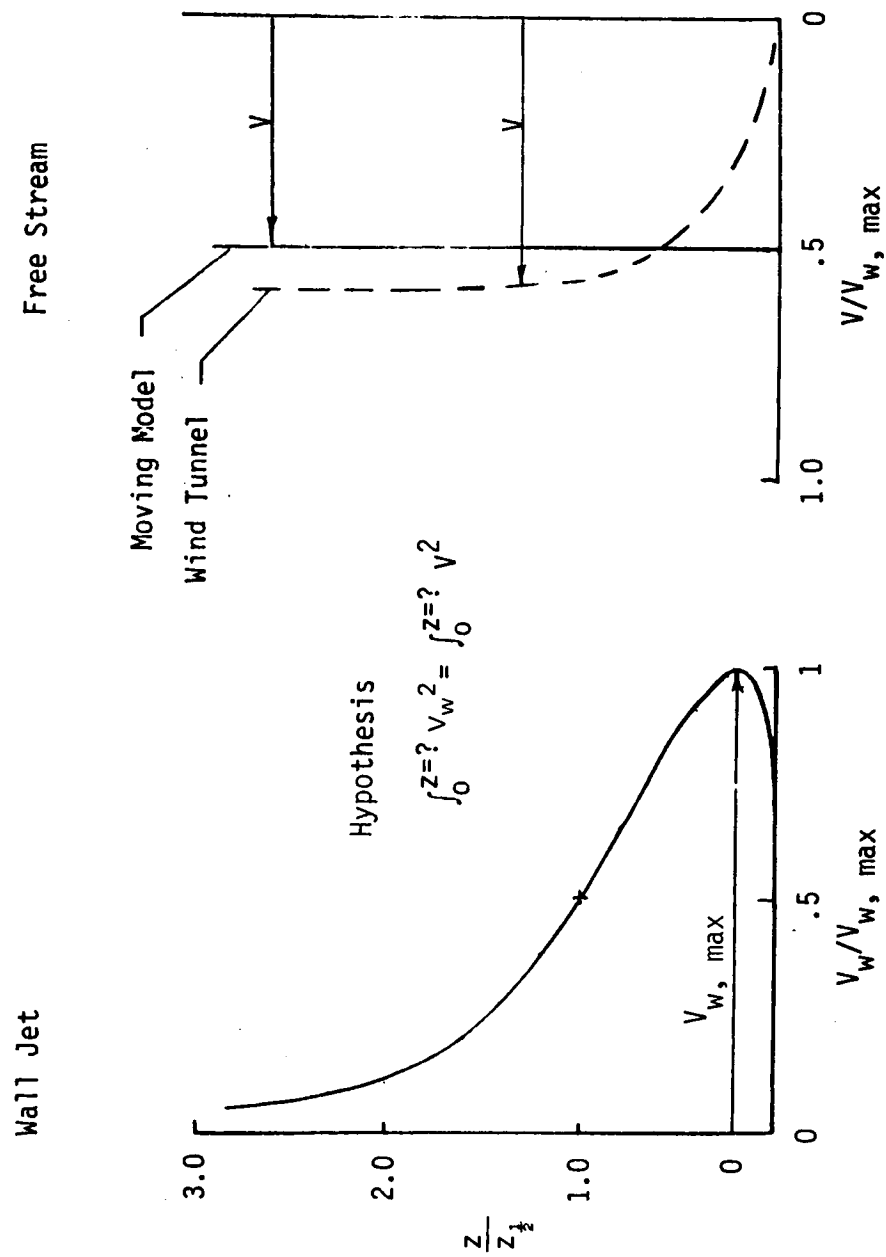


Figure 40.- At the point of maximum forward penetration the maximum velocity in the wall jet is twice the free stream velocity (without boundary layer). (Ref. 22)

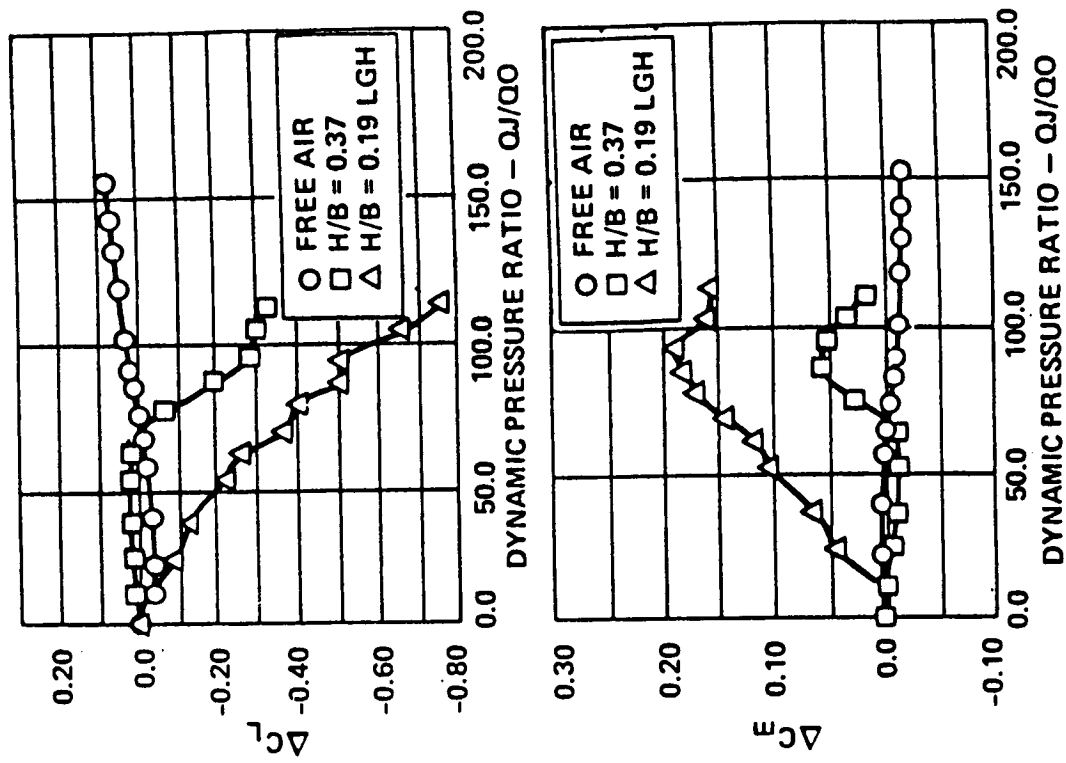
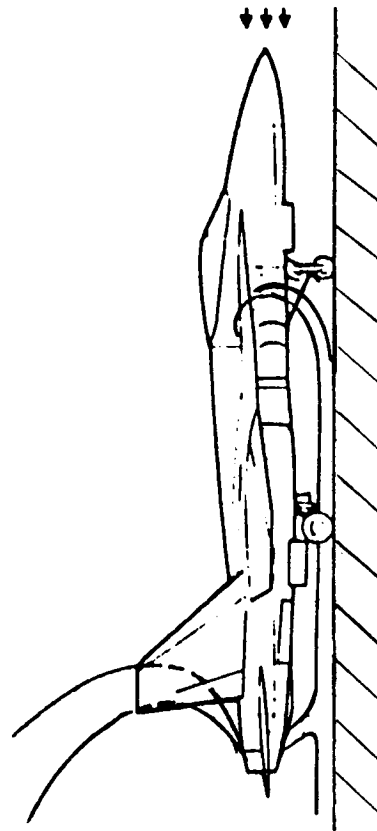


Figure 41.- Lift and moment induced by thrust reverser generated wall jet and ground vortex. (Ref. 25)

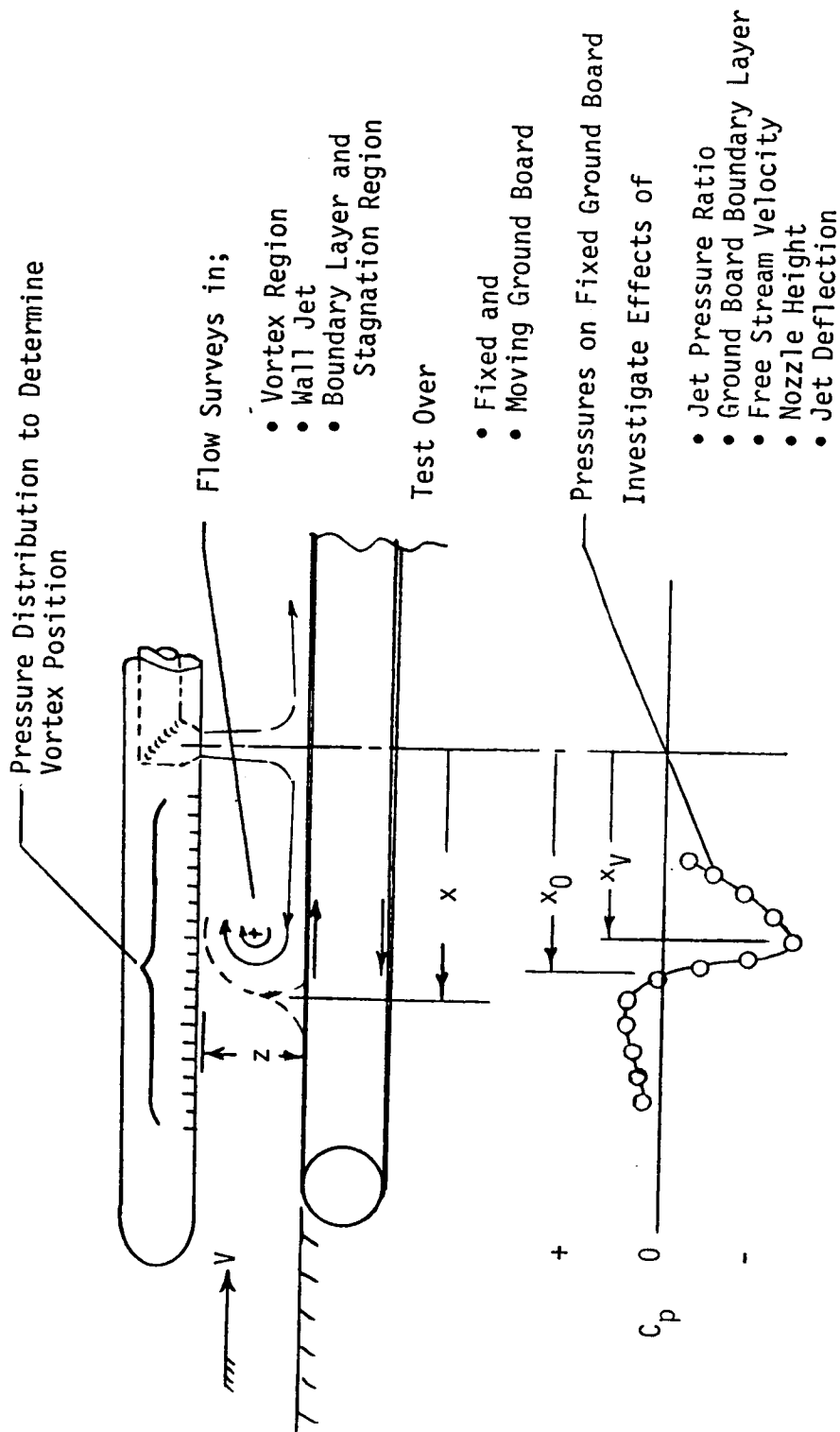


Figure 42.- Recommended ground vortex investigation.

# FLOW STUDIES OVER FIXED AND MOVING GROUND PLANES

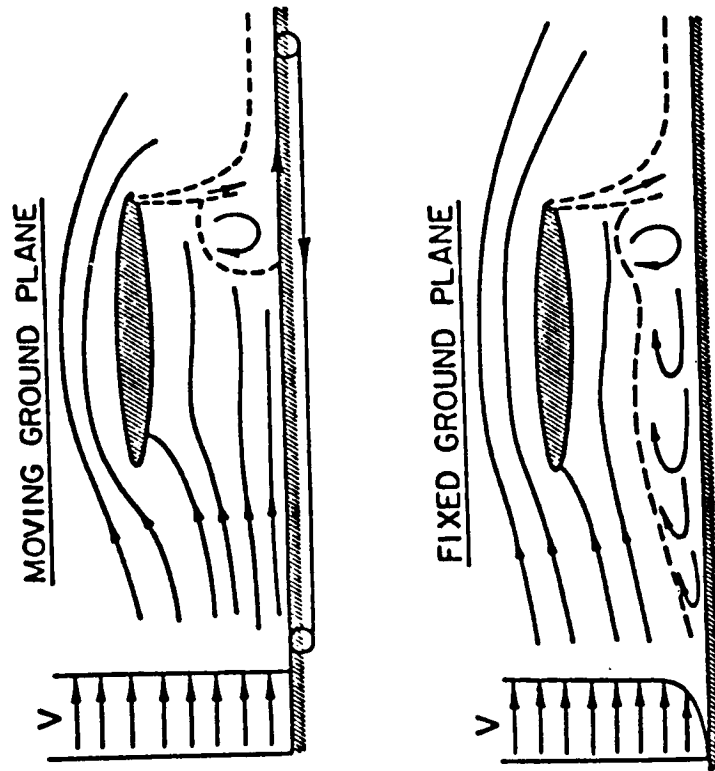


Figure 43.- Jet induced flow over fixed and moving ground planes. (Ref. 27)

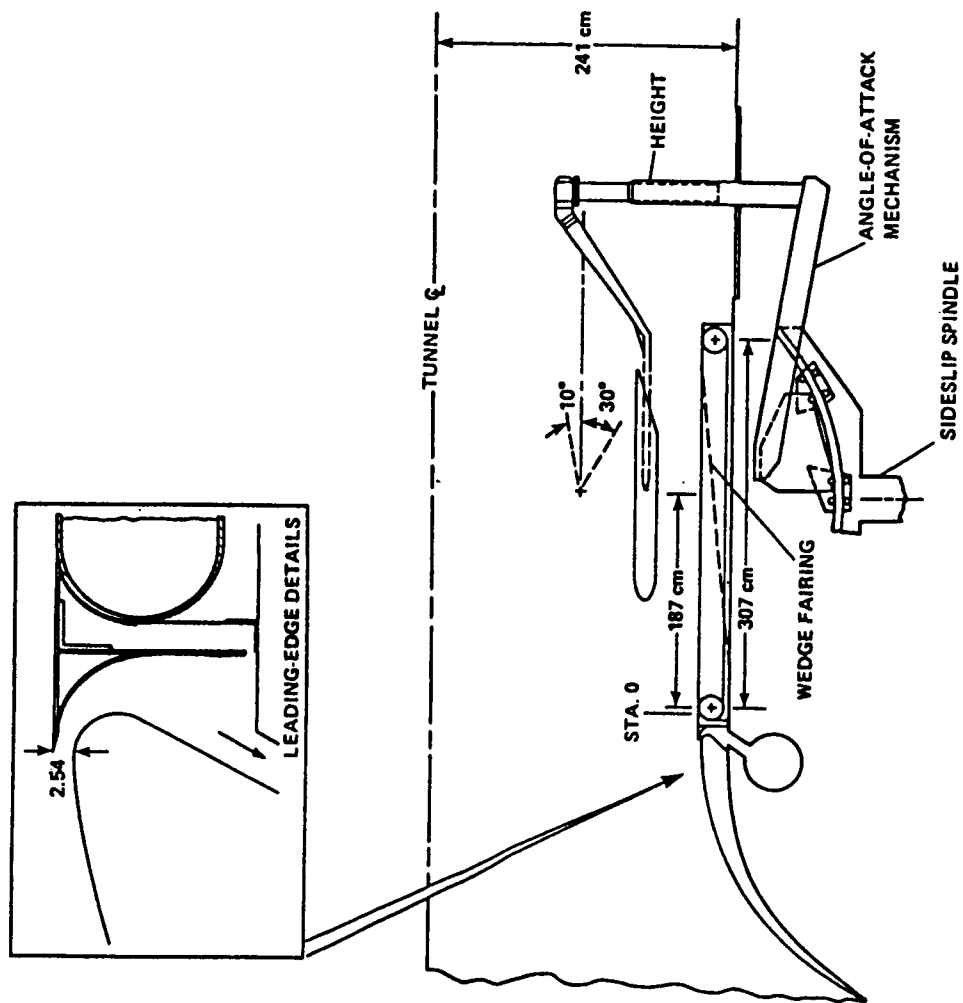


Figure 44.- Turner's moving-belt installation. (Ref. 28)

# LIFT LOSS FOR MOVING MODEL AND ENDLESS-BELT GROUND PLANE

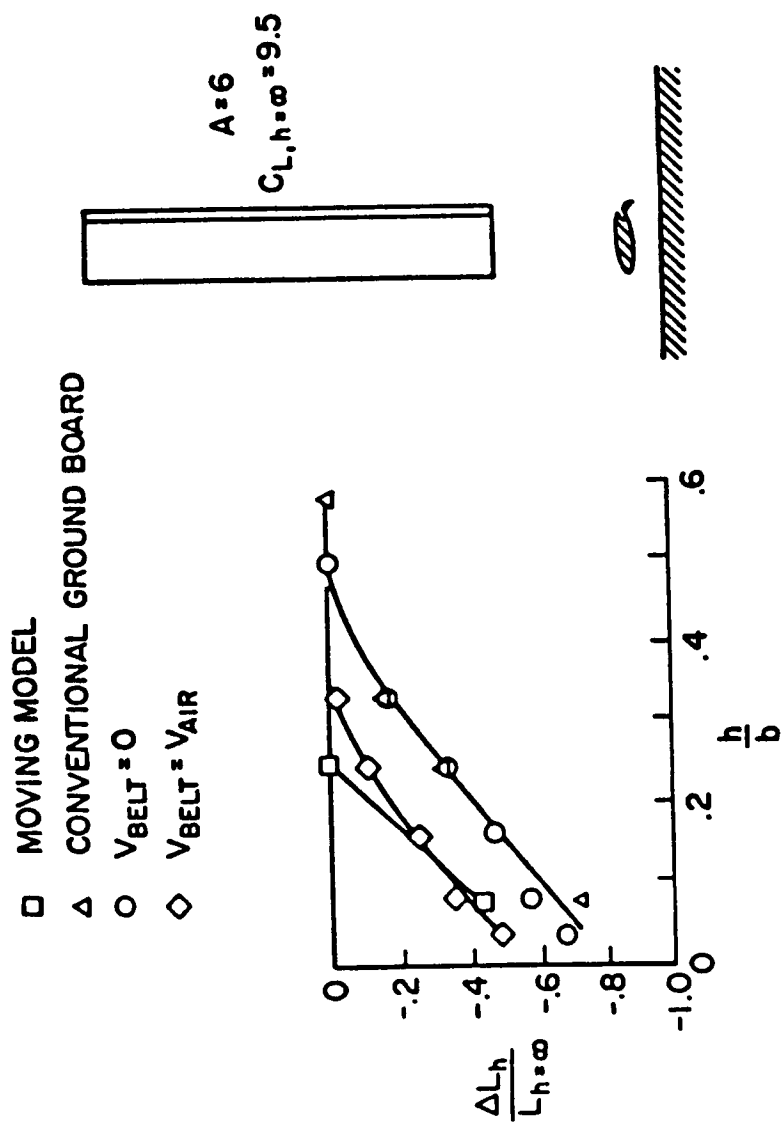


Figure 45.- Lift loss for jet flap model as determined by several testing techniques. (Refs. 28 and 29)

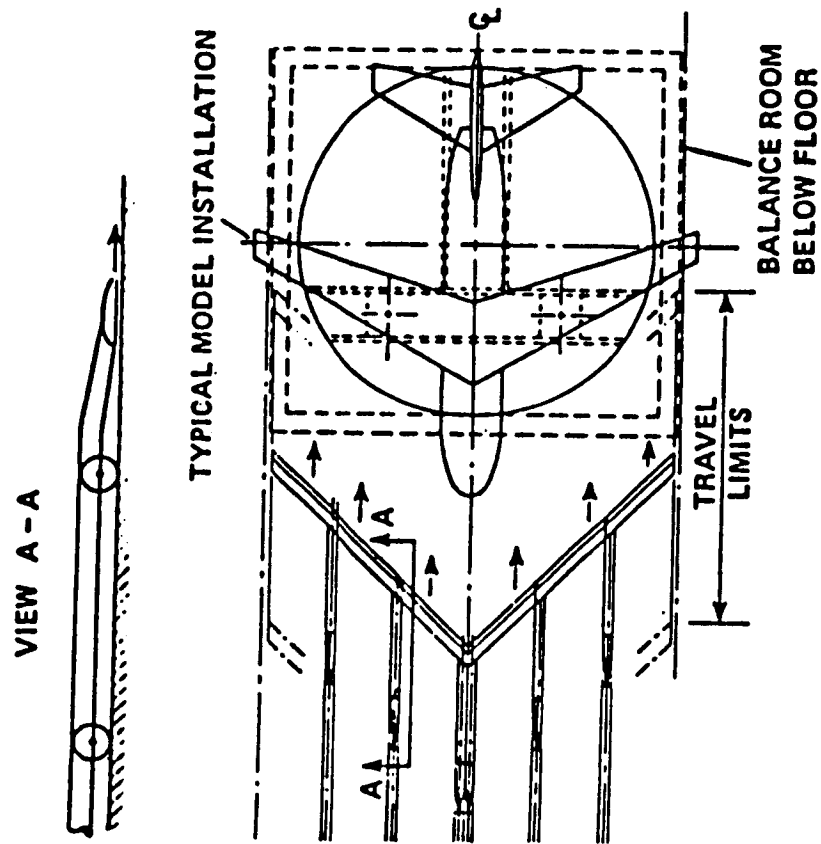


Figure 46.- Ames 40 by 80 proposed floor BLC design. (Ref. 30)

# EFFECT OF BELT VELOCITY

$A = 7.0$ ;  $\frac{h}{b} = 0.166$ ;  $C_{L,h=\infty} = 7.4$

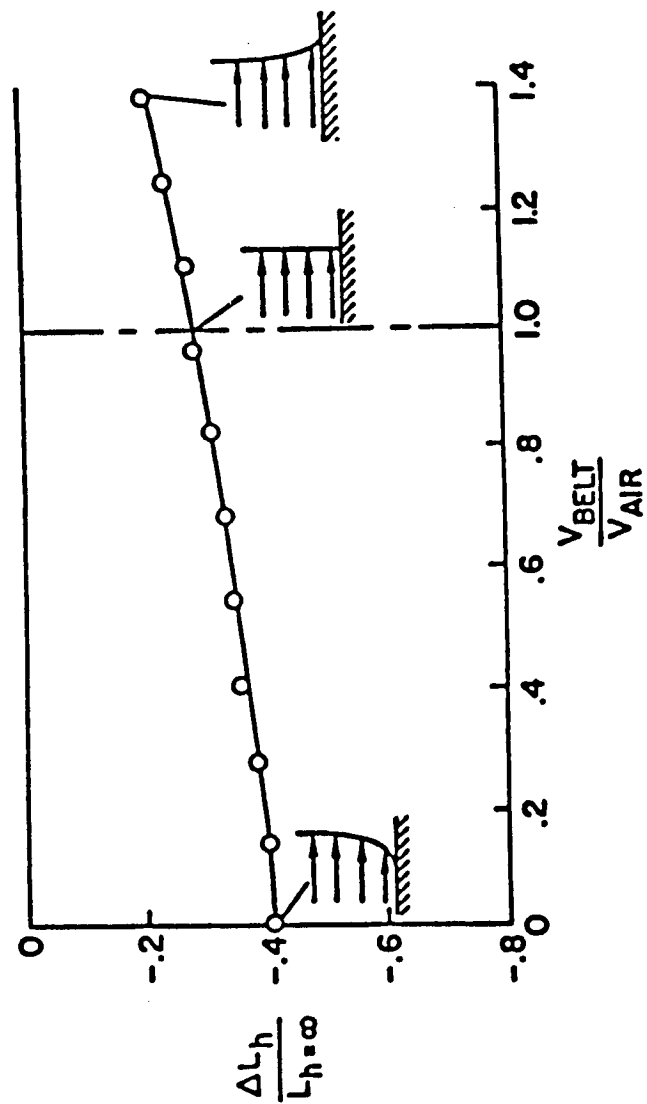


Figure 47.- A "negative" boundary layer may artificially increase lift. (Ref. 29)



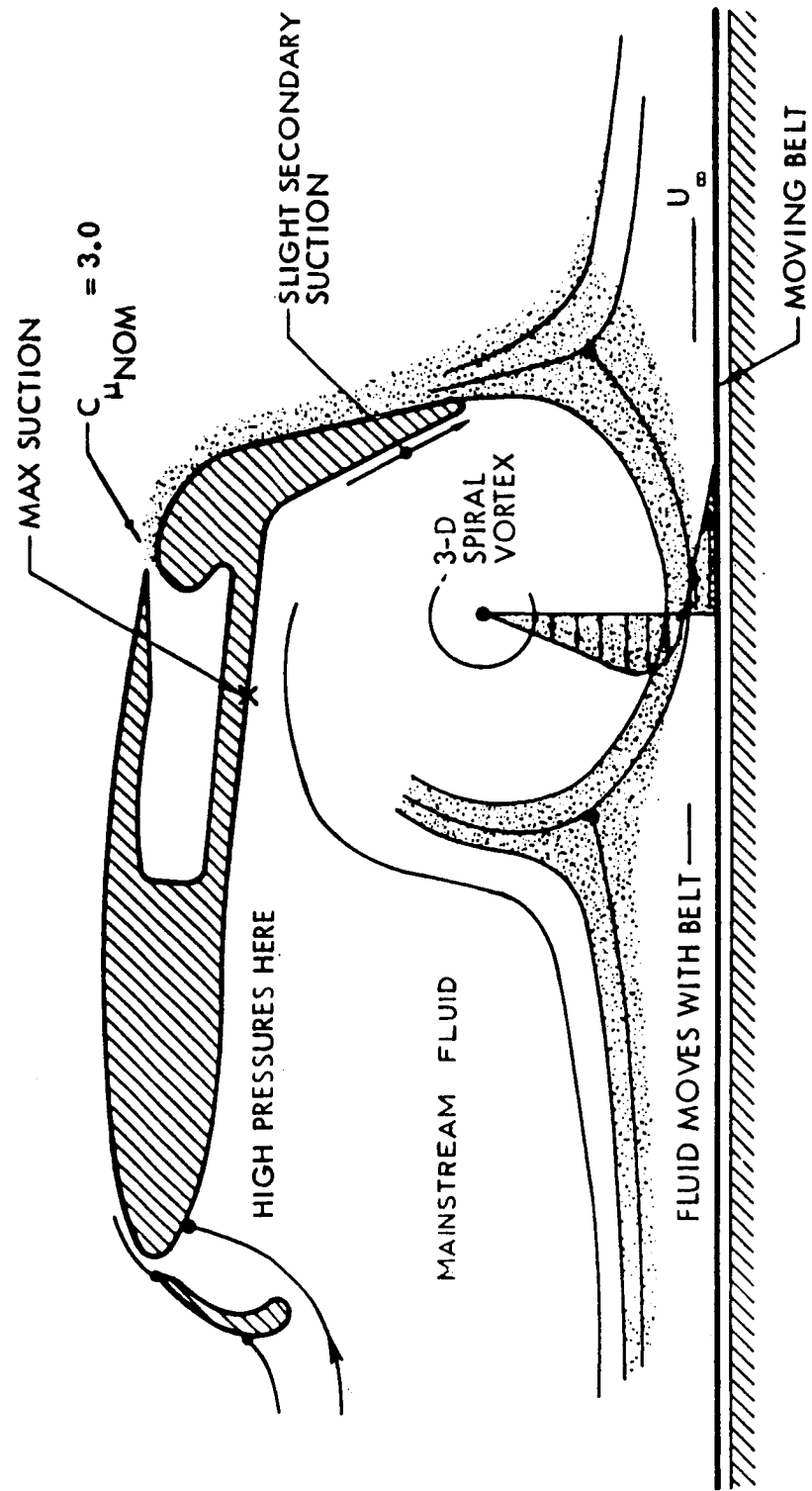


Figure 48.- Formation of trapped, underwing vortex at low altitude and high jet momentum. (Ref. 31)

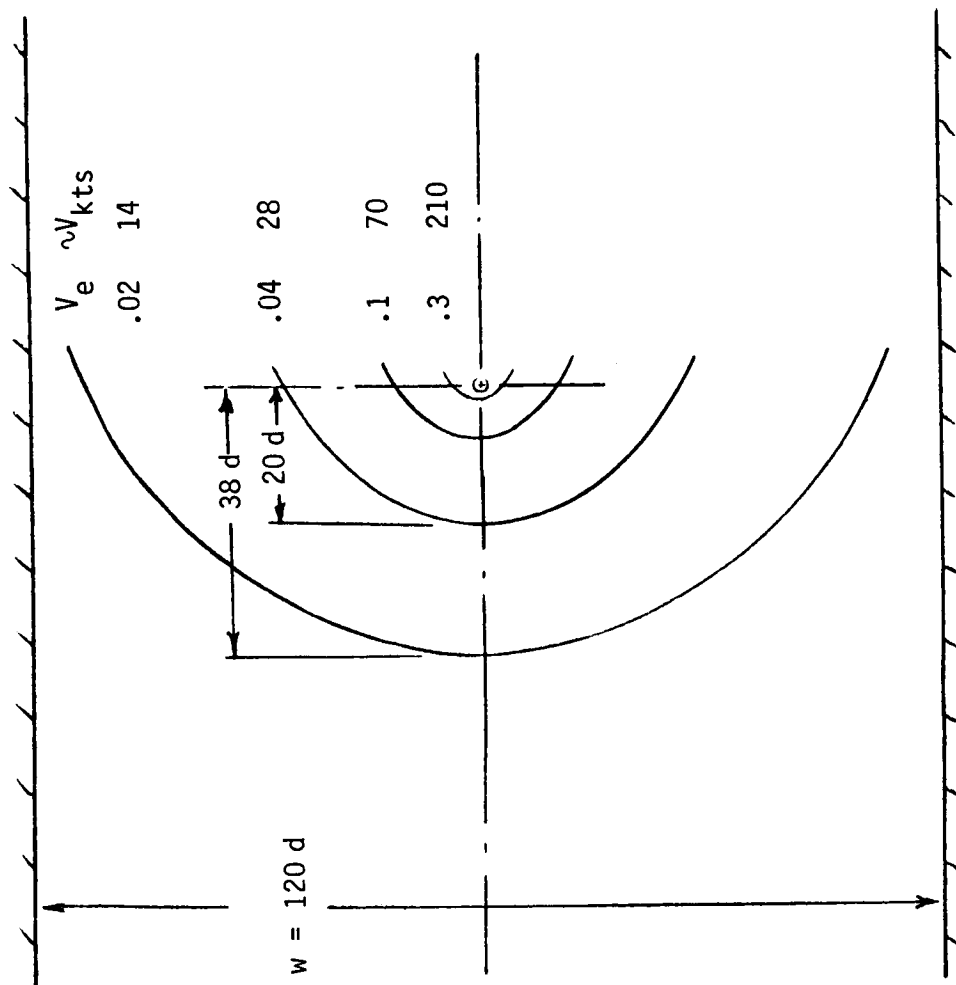


Figure 49.- Approximate leading edge of ground vortex flow,  $h/d = 1.0$  without boundary layer removal.

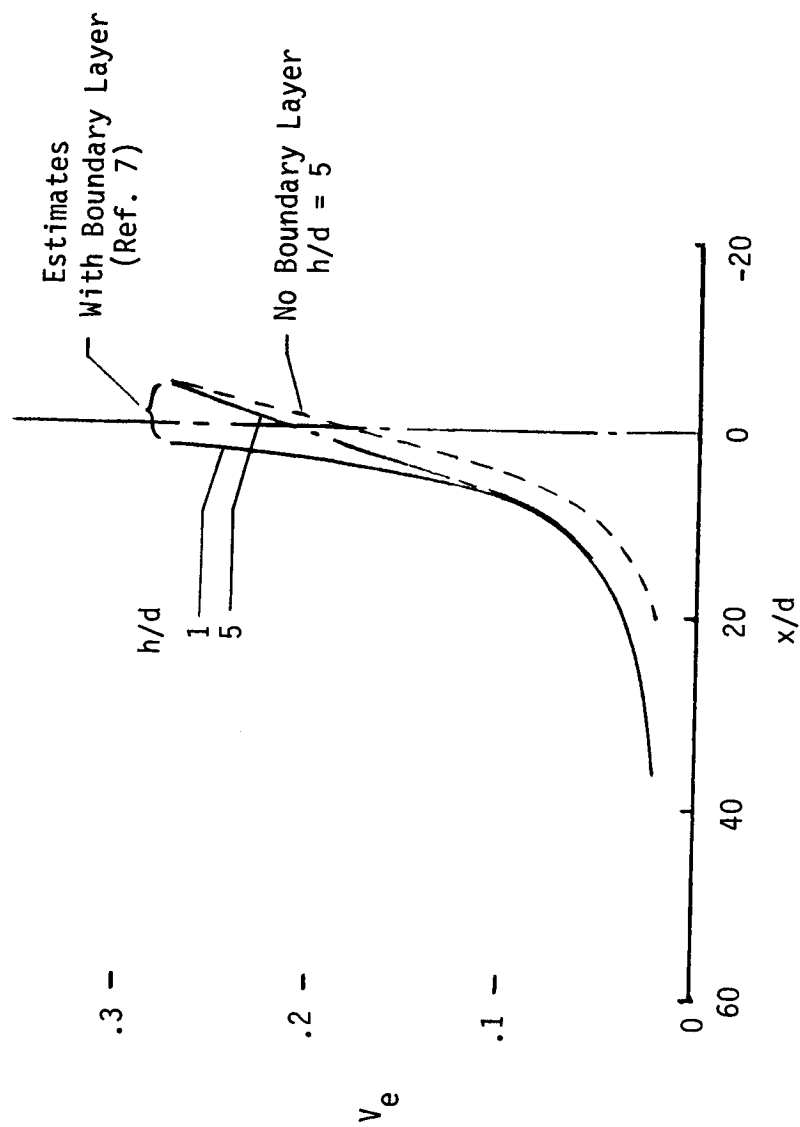


Figure 50.- Estimated position of leading edge of ground vortex flow at centerline.

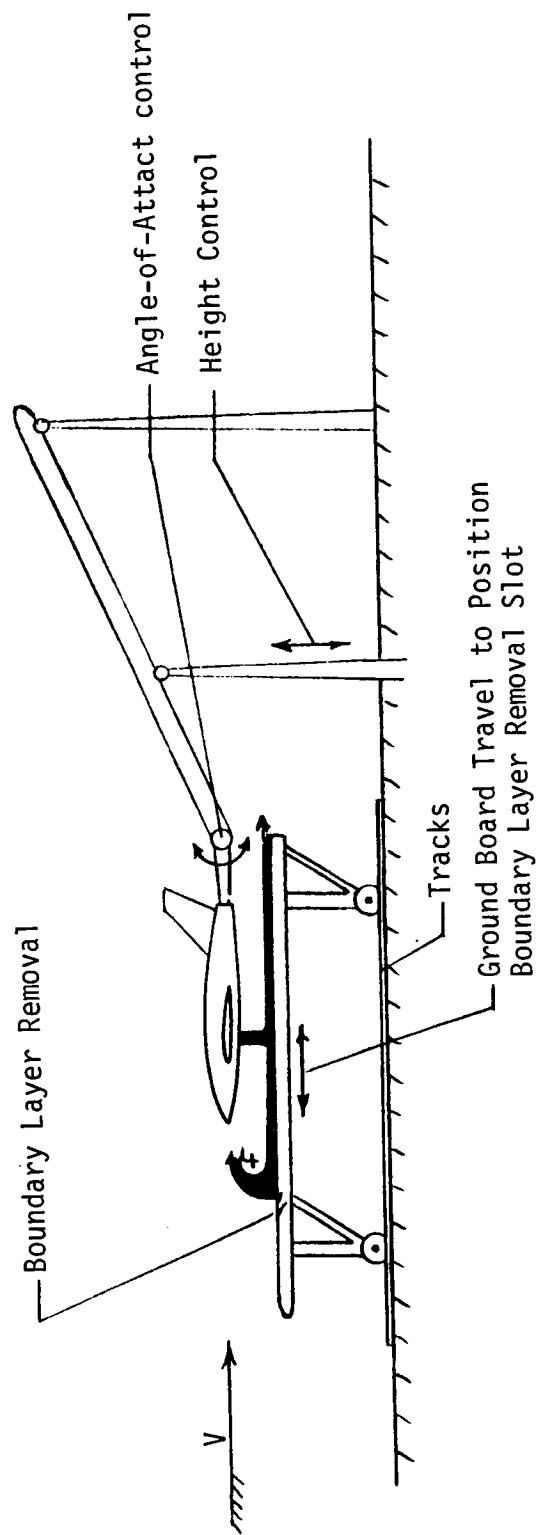


Figure 51.- Schematic of Proposed Ground Board Arrangement.

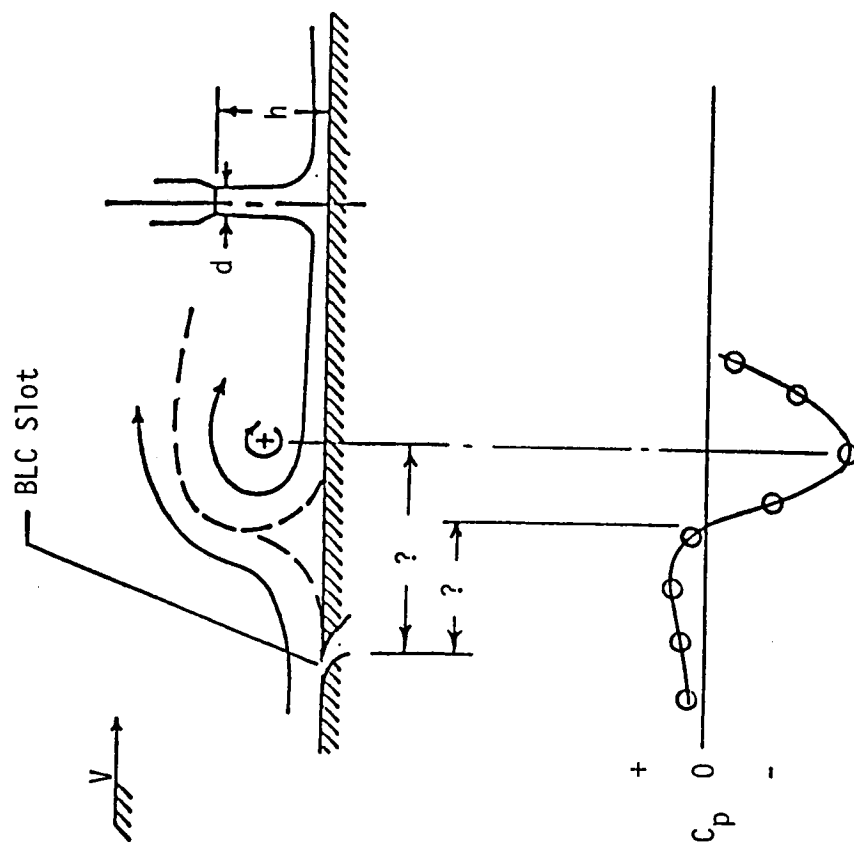


Figure 52.- The ground vortex pressure signature could be used to locate the BLC slot.

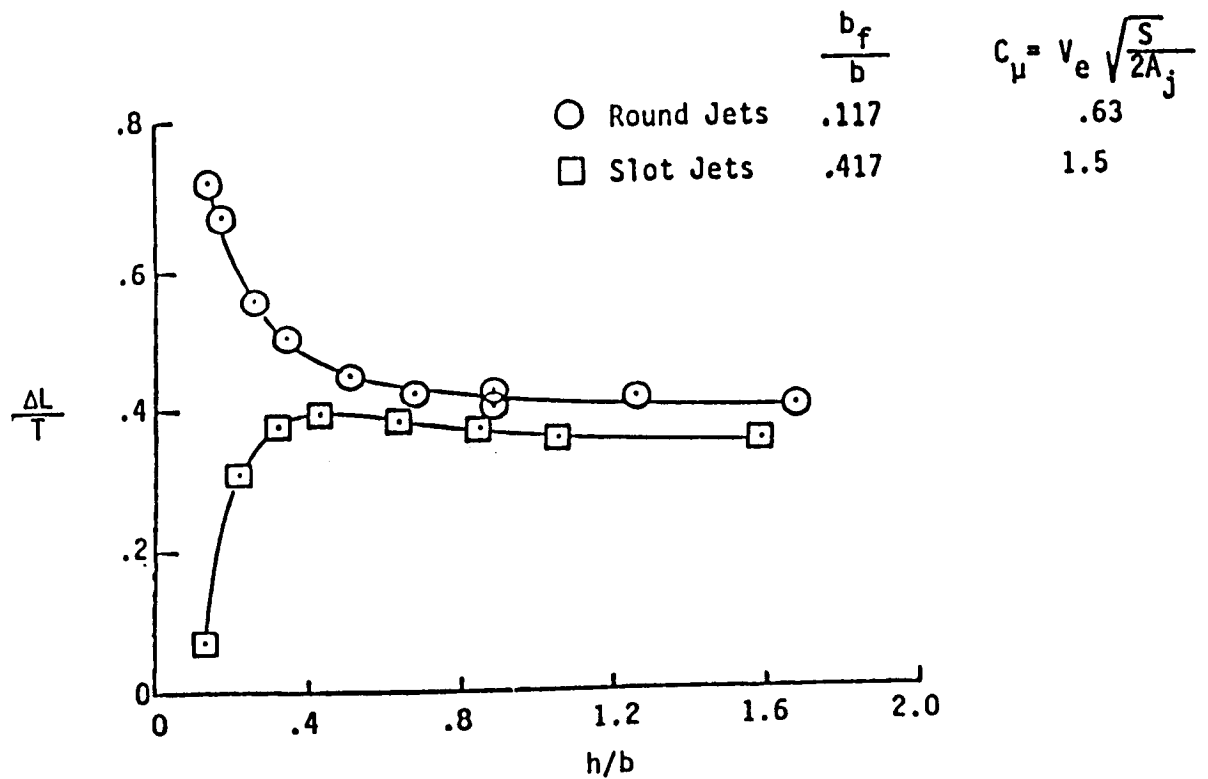
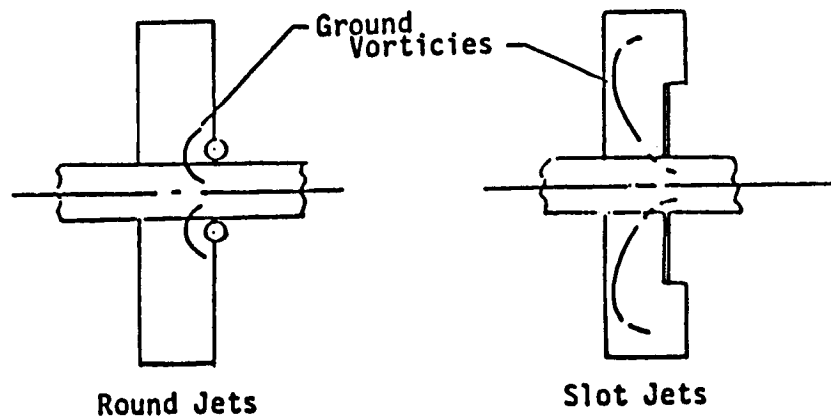


Figure 53.- Comparison of ground effects on circular (direct thrust) and slot jet (jet flap) configuration. (Ref. 10)

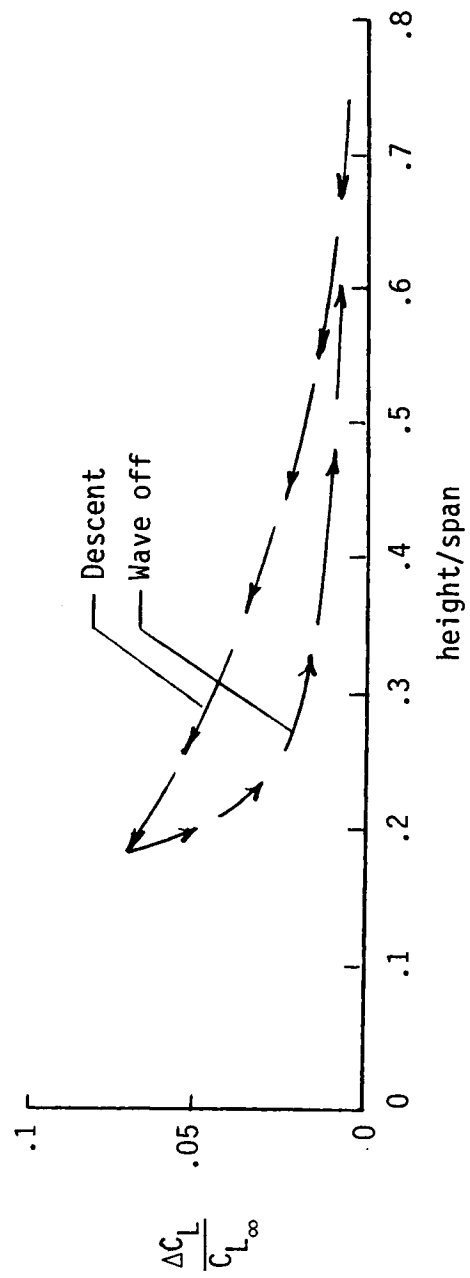


Figure 54.- Touch-and-Go landings show ground effect hysteresis.  $C_{L_\infty} \sim 2.5$ , (Ref. 33)

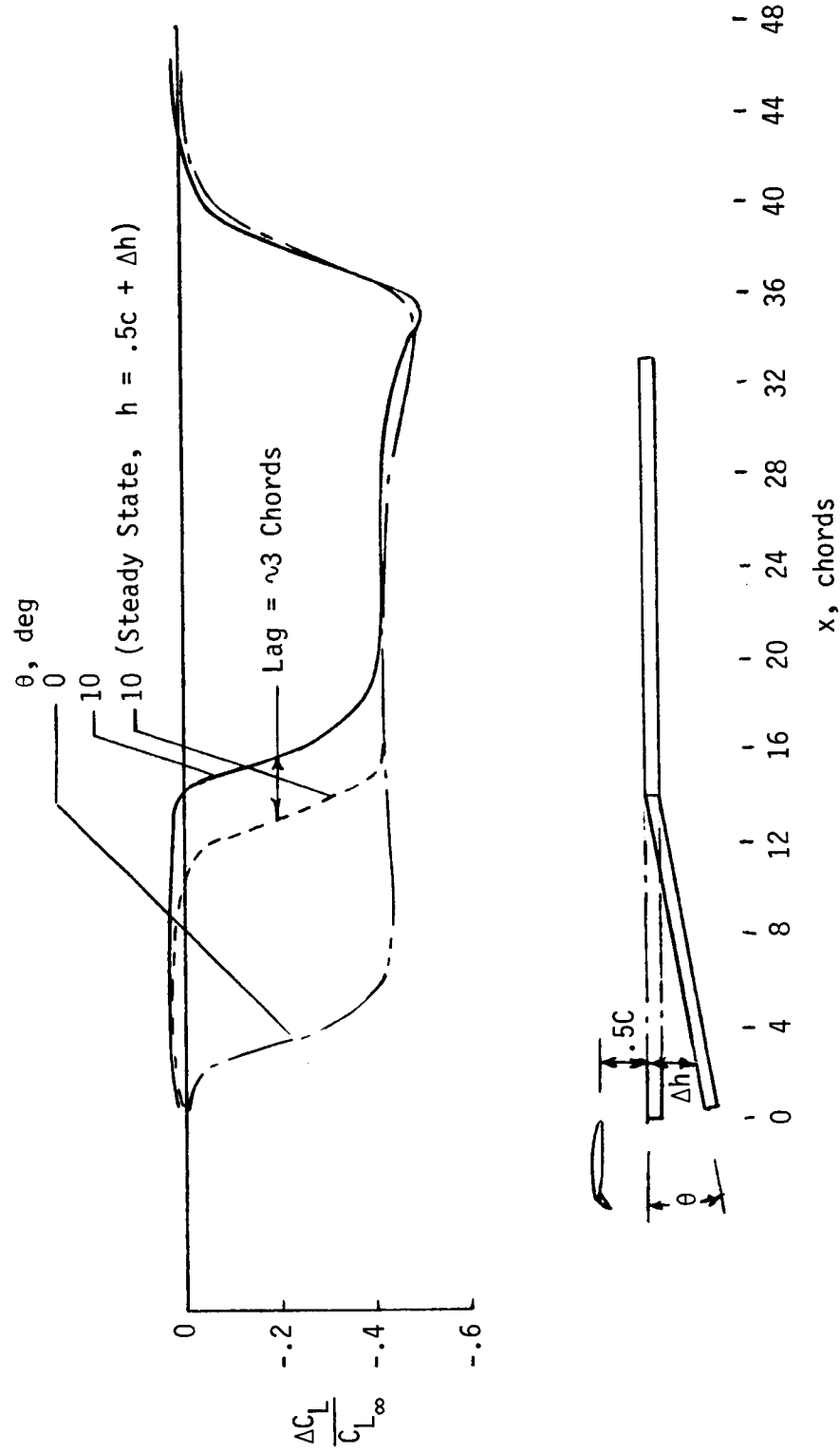


Figure 55.- Moving model tests show lag in development of jet flap ground effects.  $C_{L_\infty} = 9.5$ , (Ref.26)



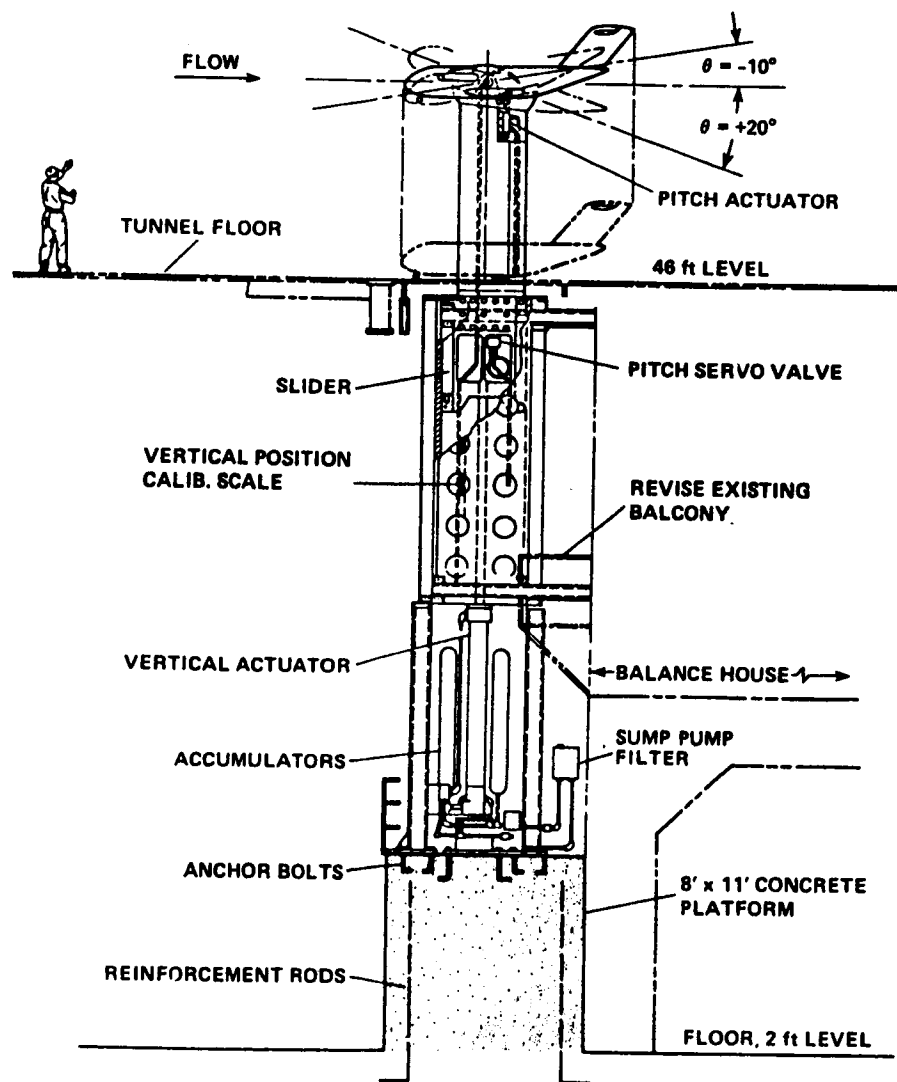


Figure 56.- Transient ground-effect support design for the Ames 40 by 80. (Ref. 34)

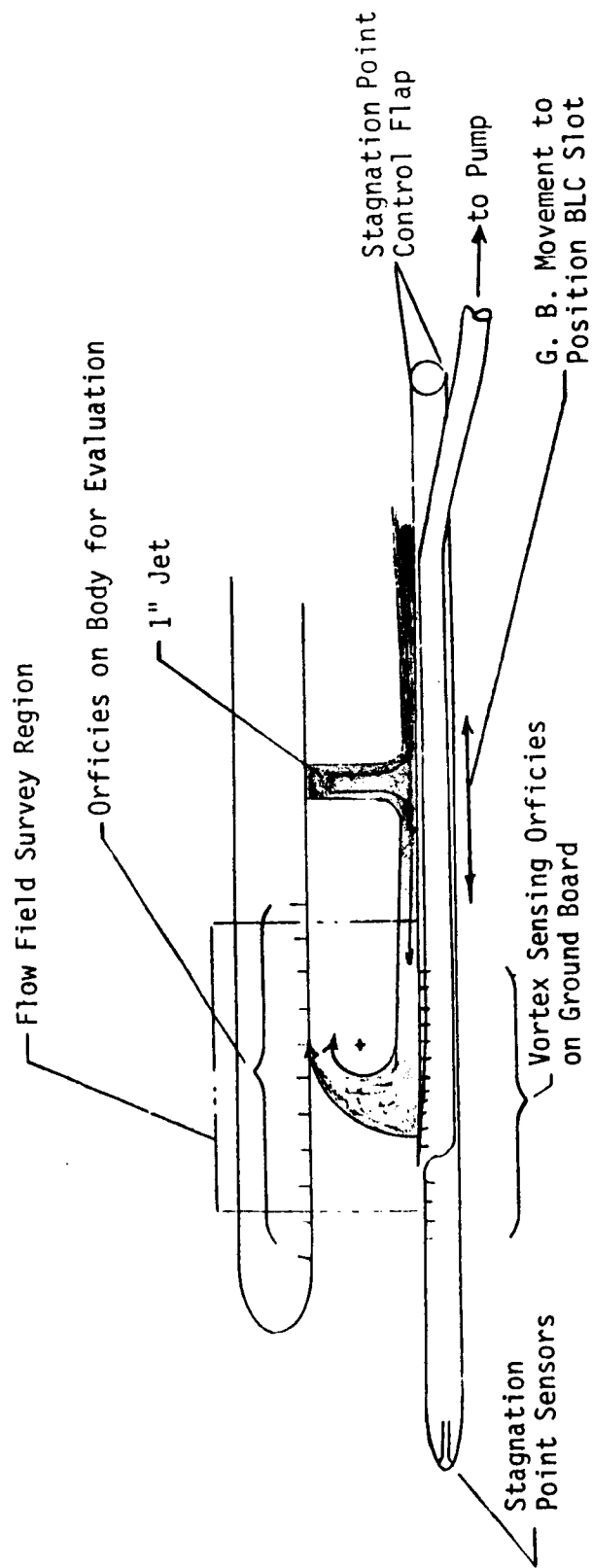


Figure 57.- Ground-vortex-signature controlled translating ground board concept.

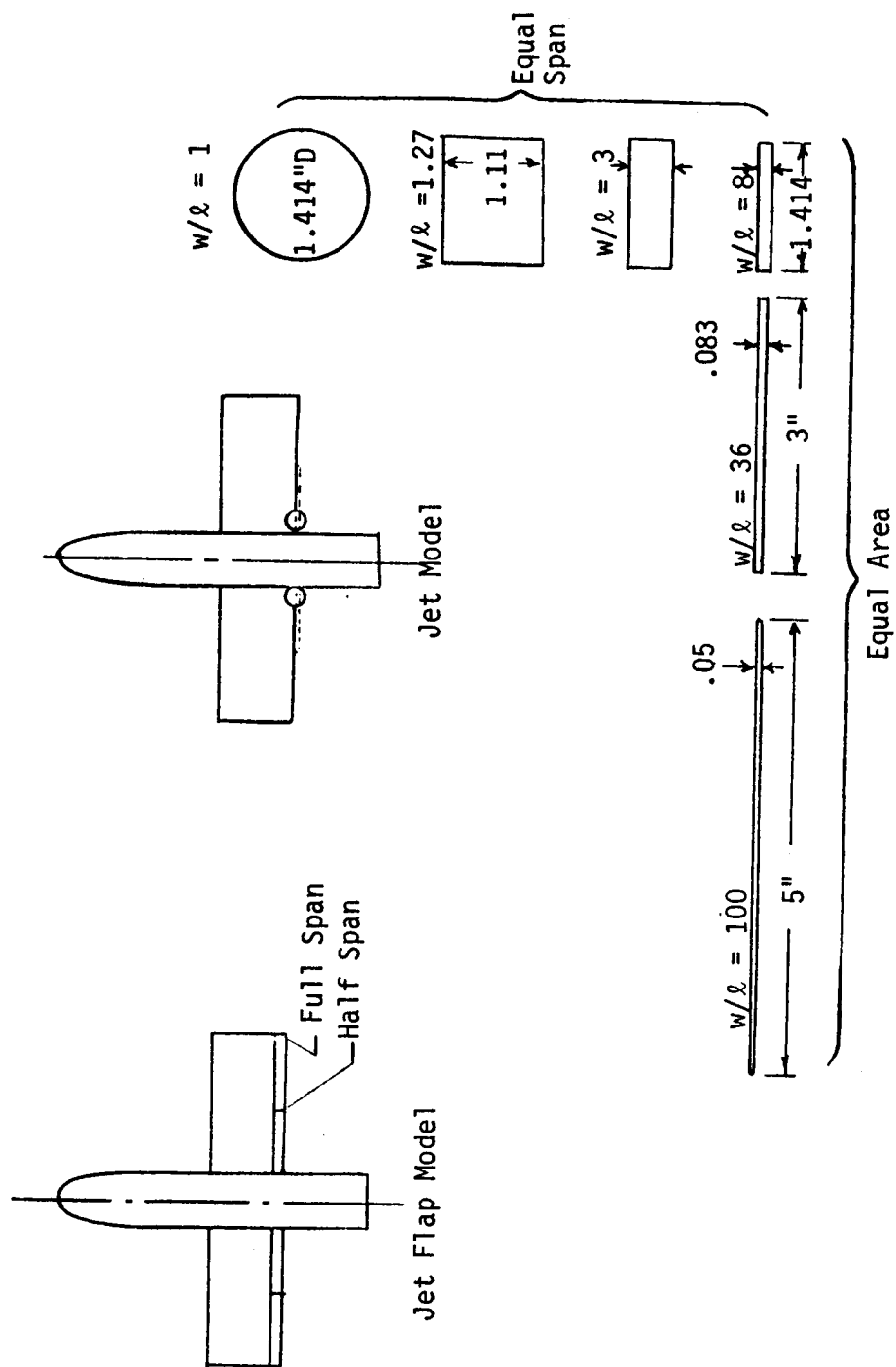


Figure 58.- Suggested model configurations for jet configuration effects investigation.

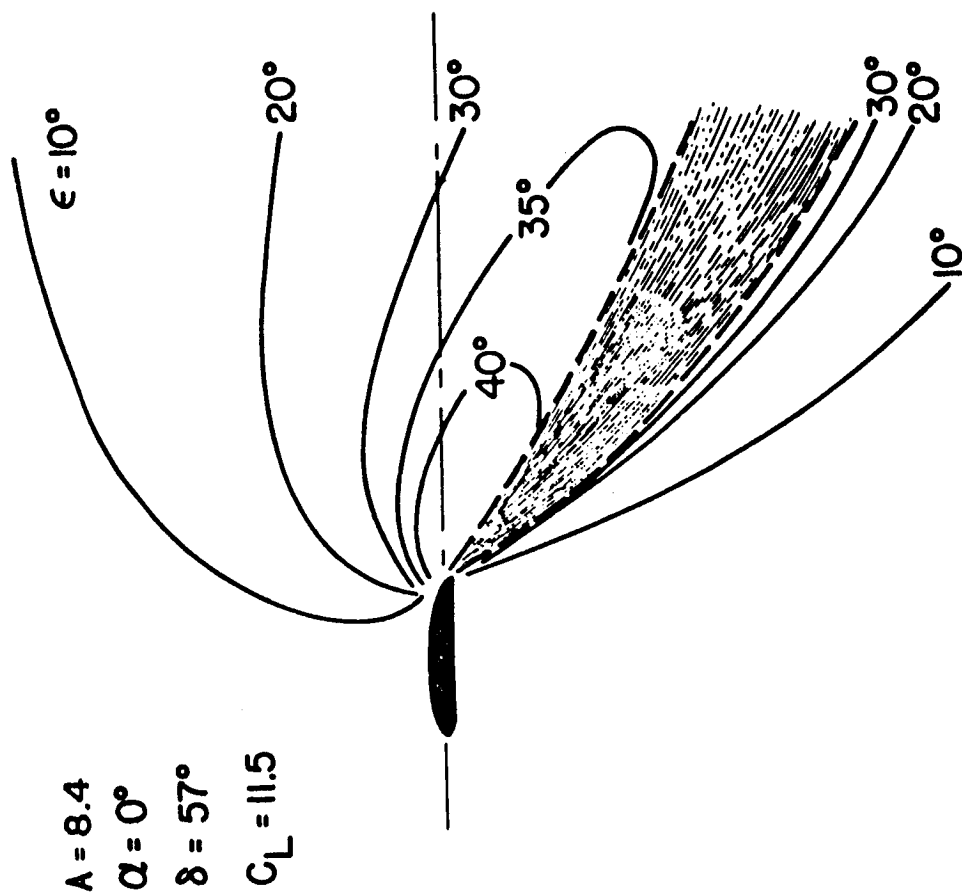


Figure 59.- Downwash field behind a jet-augmented flap at the midsemispan station. (Ref. 35)

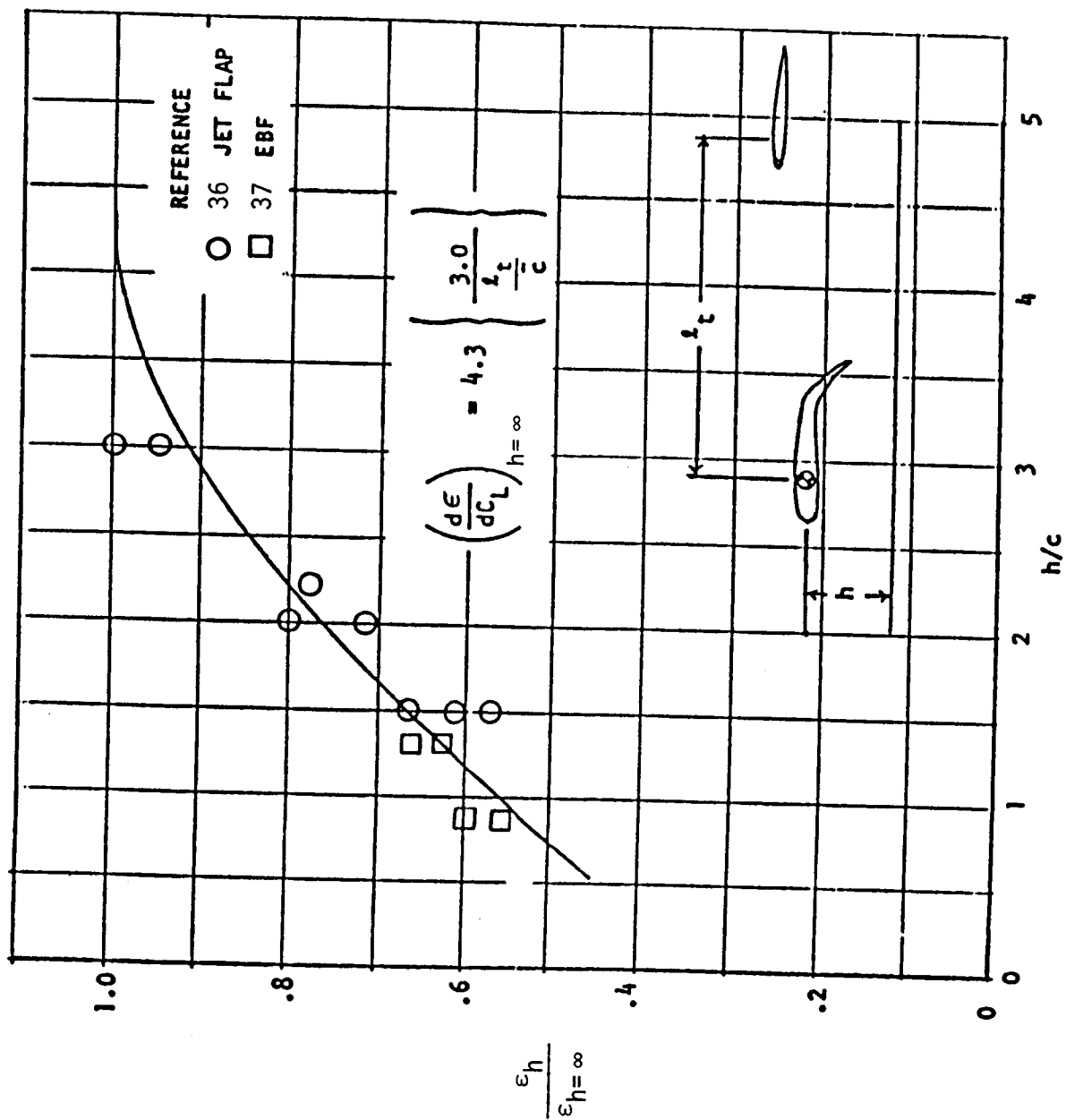


Figure 60.- Effect of ground proximity on downwash. (Ref. 10)

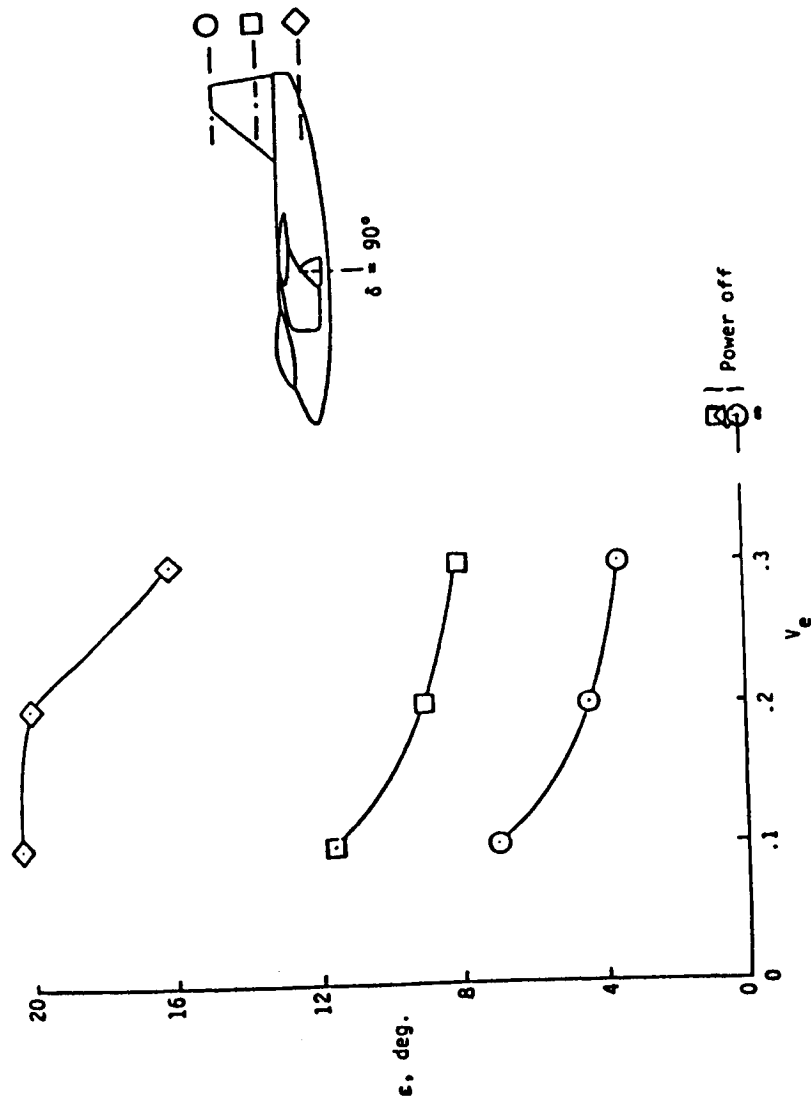


Figure 61.- Jet induced downwash for configuration of Ref. 38 showing effect of tail height.

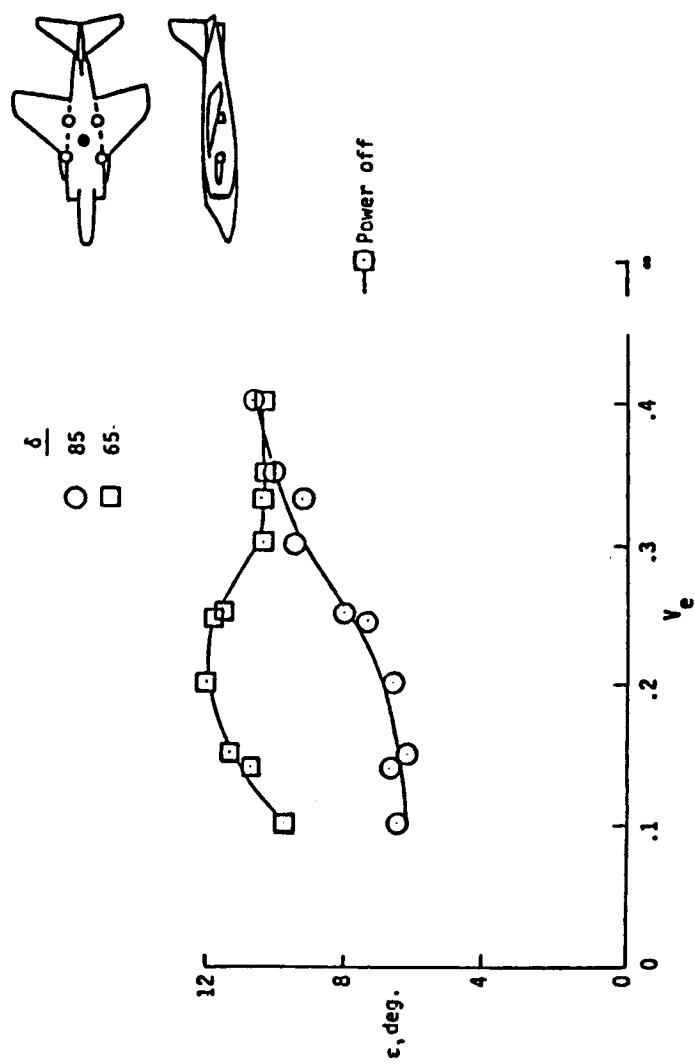


Figure 62.- Jet induced downwash for configuration of Ref. 39.

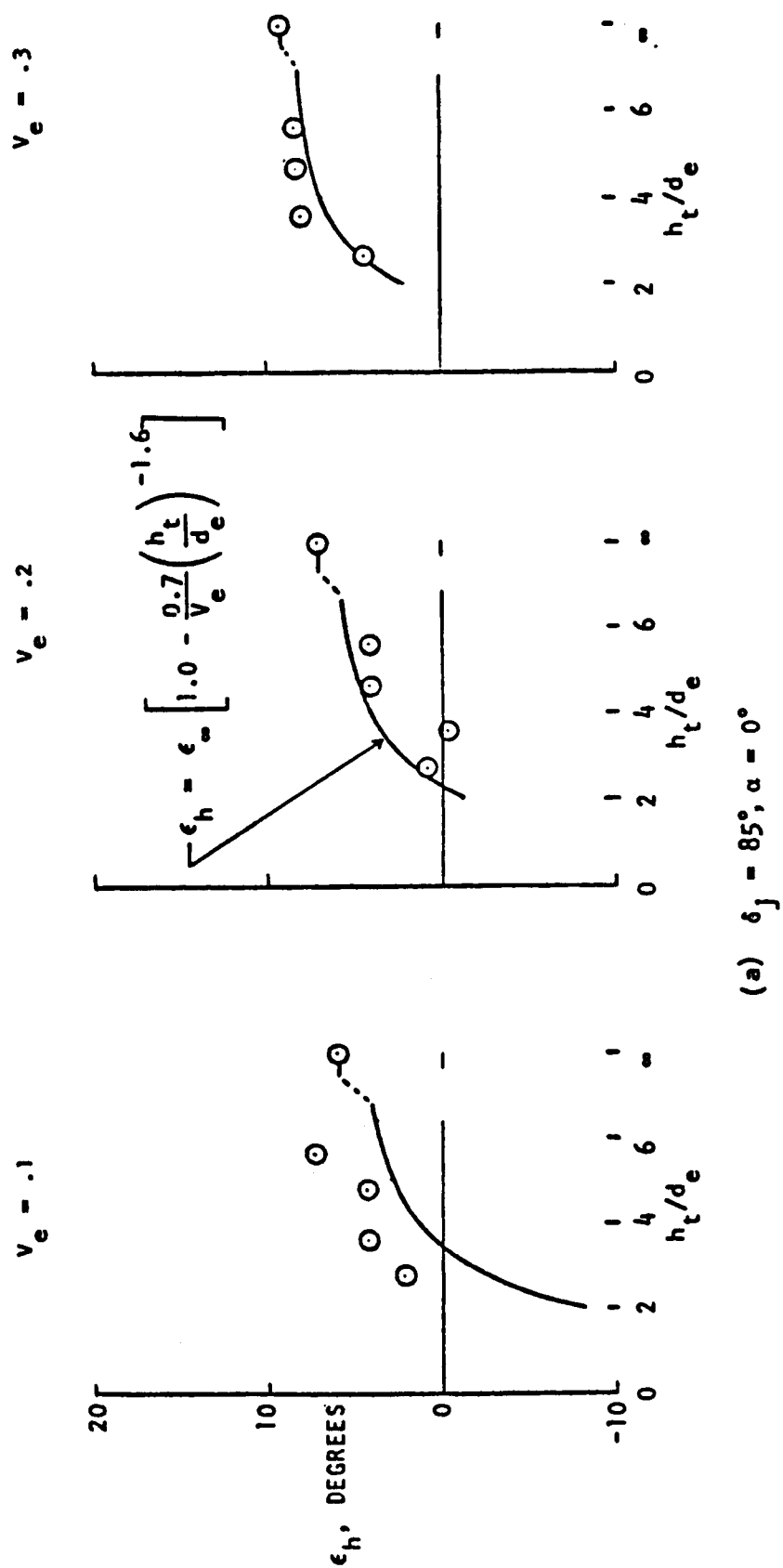
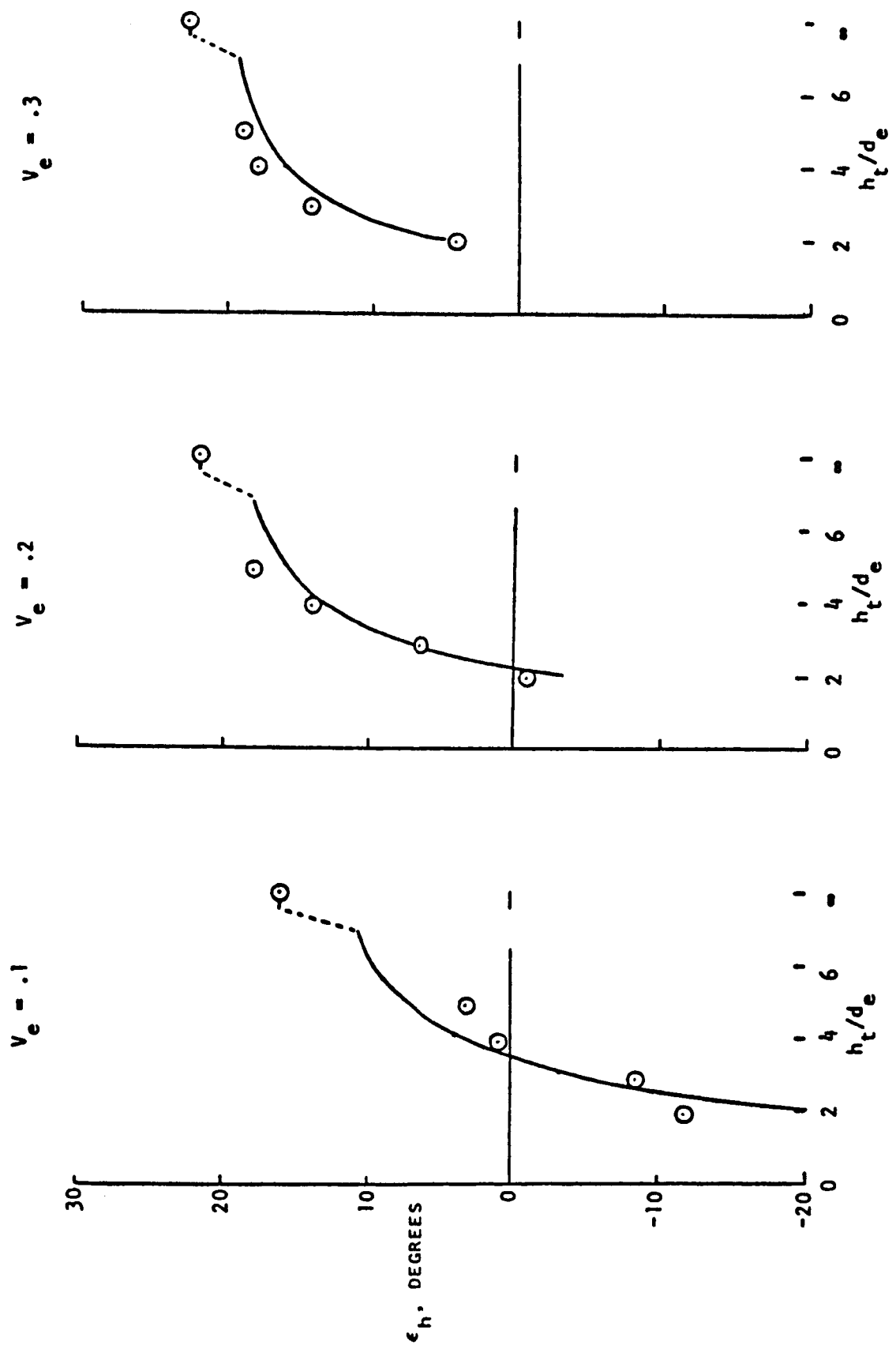


Figure 63.- Effect of ground proximity on downwash at tail of configuration of Ref. 39.





(d)  $\delta_j = 65^\circ$ ,  $\alpha = 9^\circ$

Figure 63.- (Concluded).

# Far Field Flow

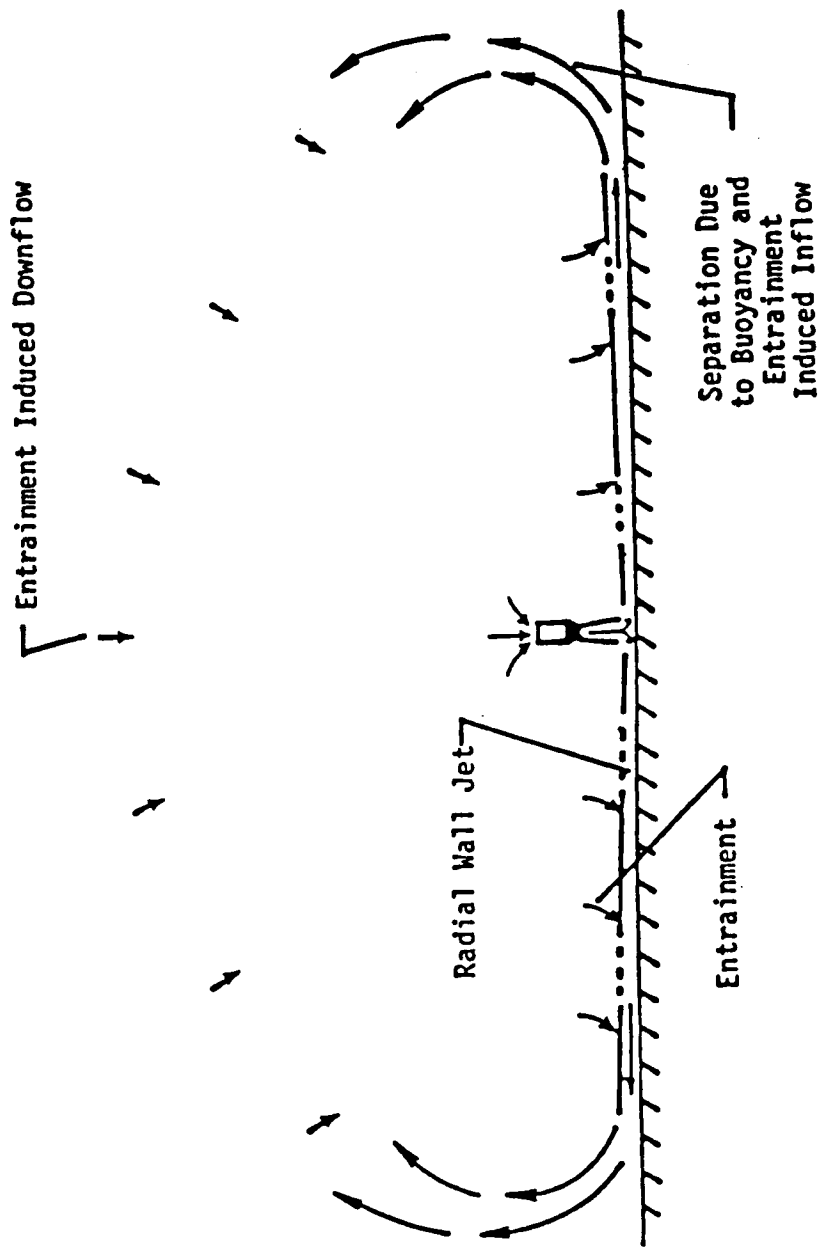


Figure 64.- Far field ingestion.

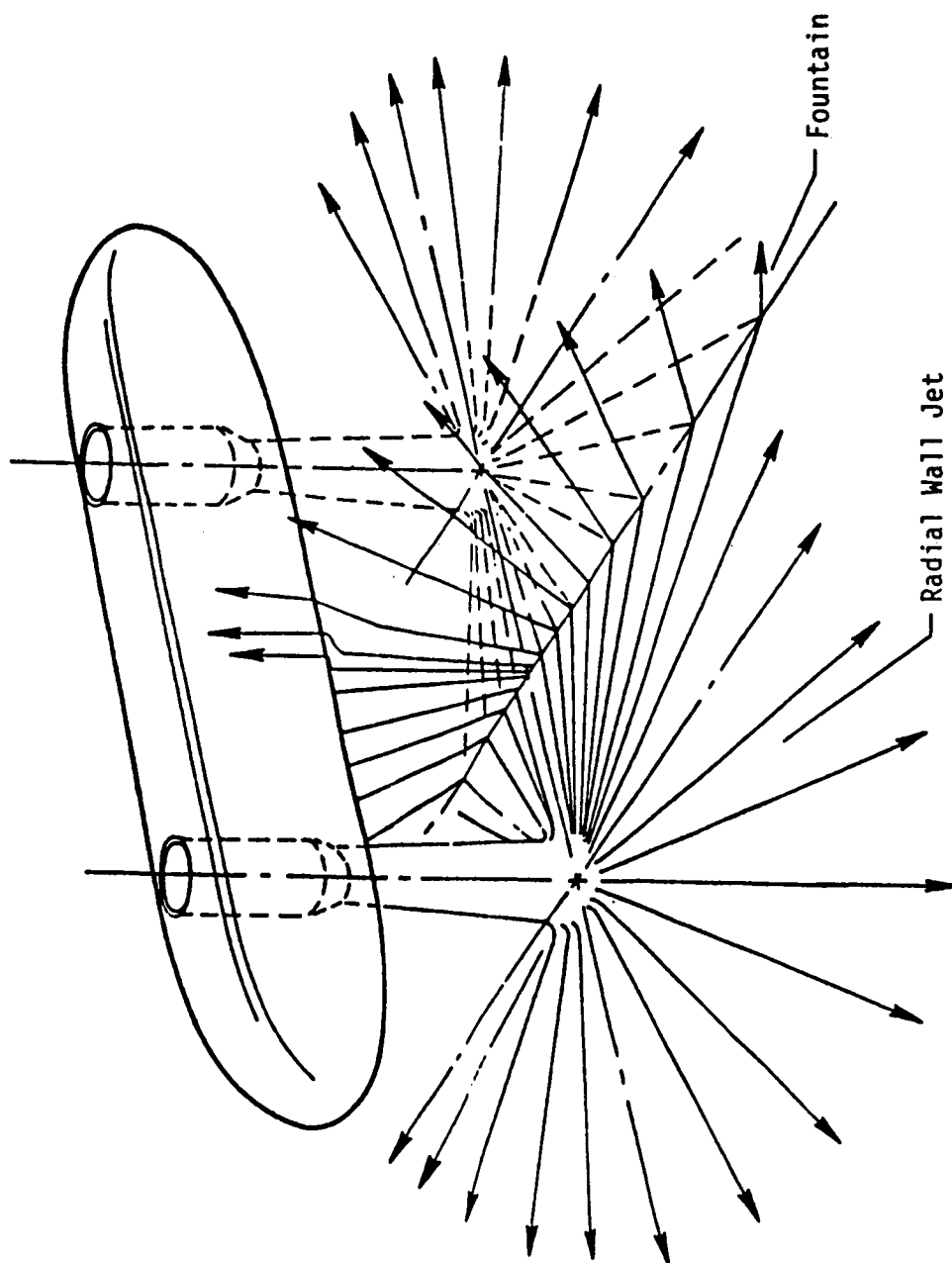


Figure 65. Fountain Flow Field

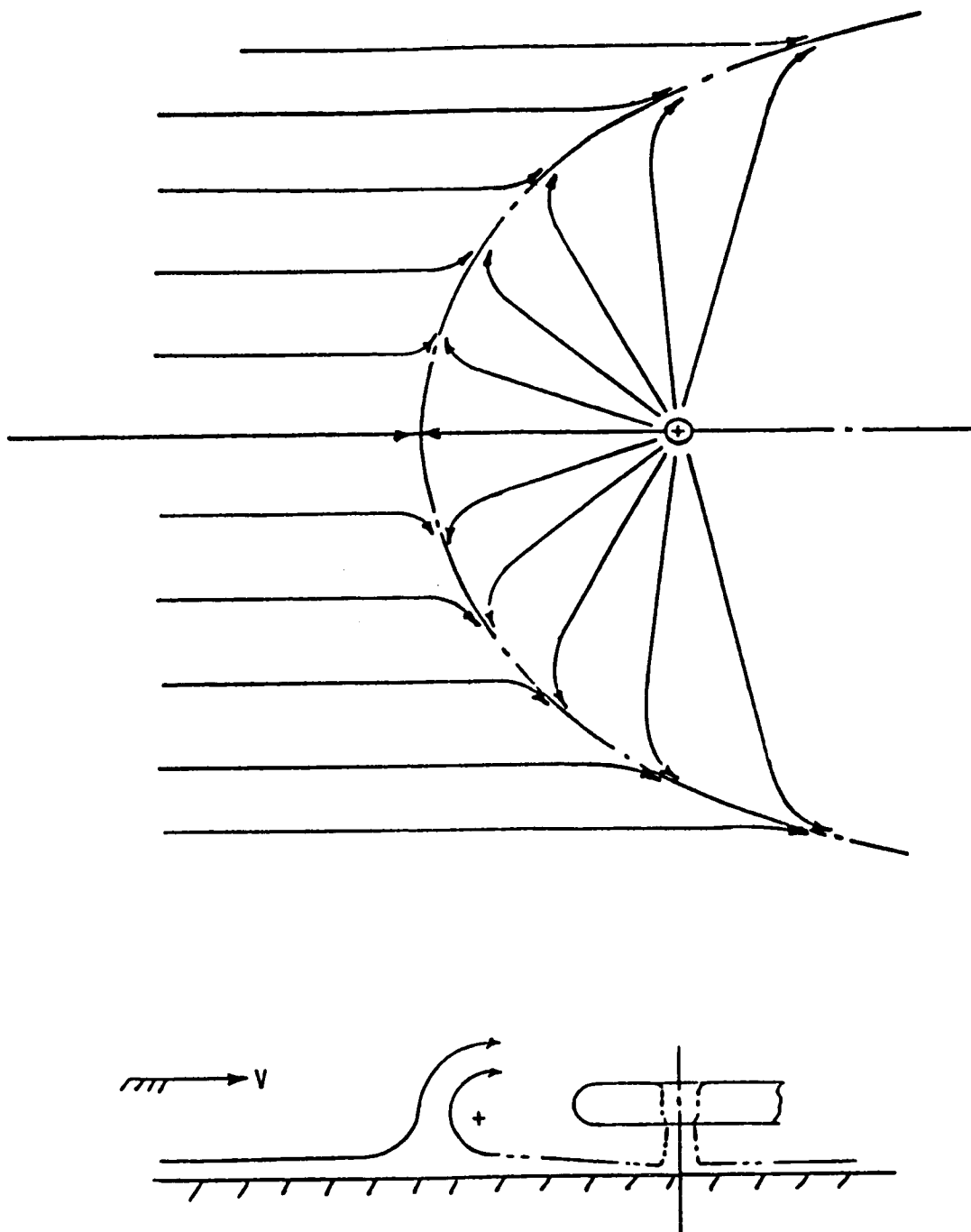


Figure 66.- Ground vortex flow field.

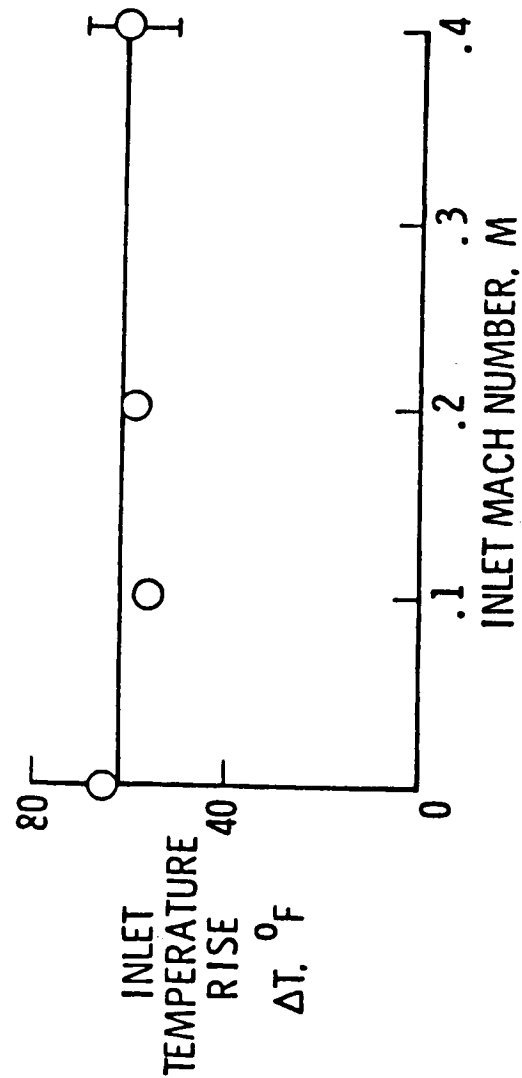
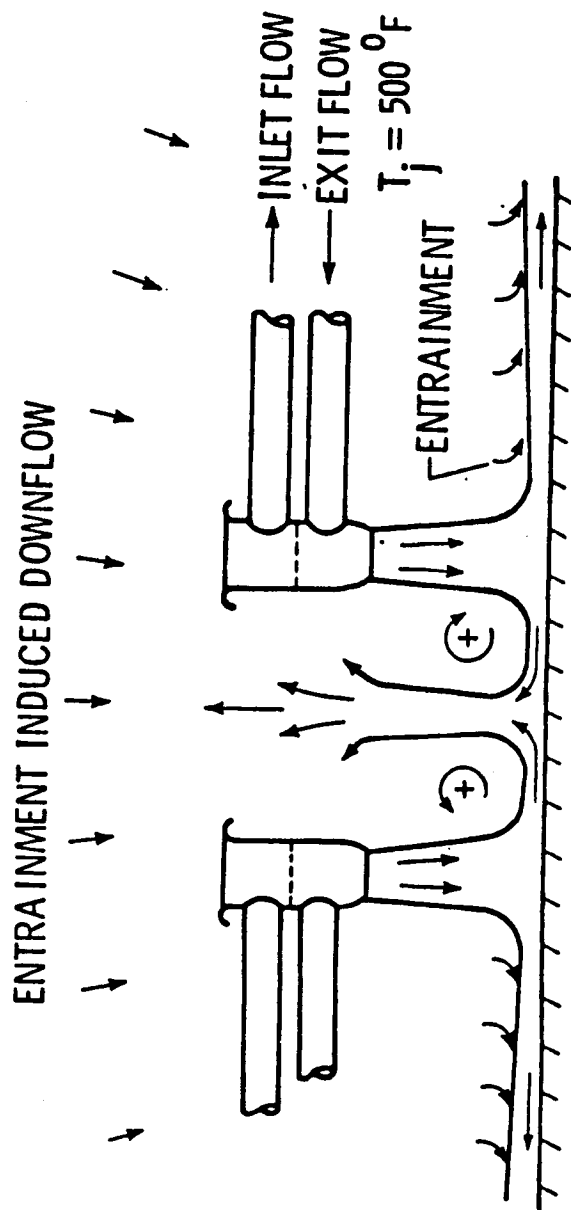


Figure 67.- Inlet temperature rise with two isolated jets. (Ref. 12)

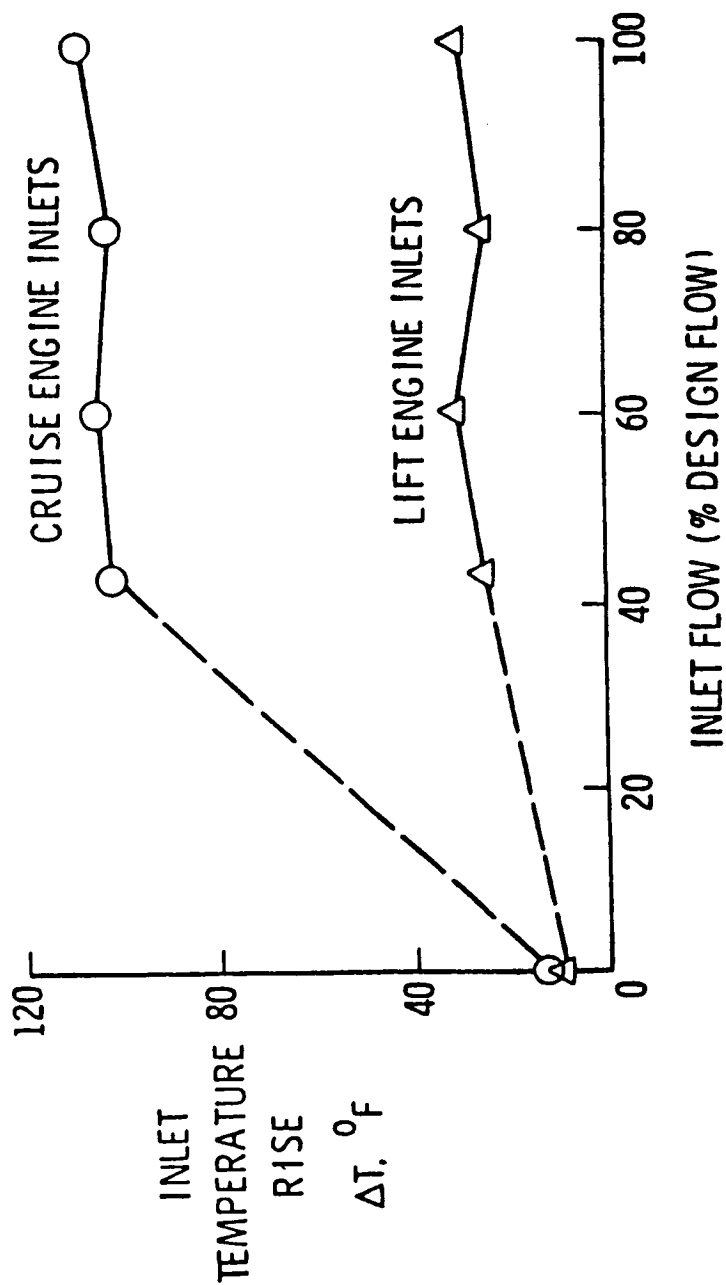
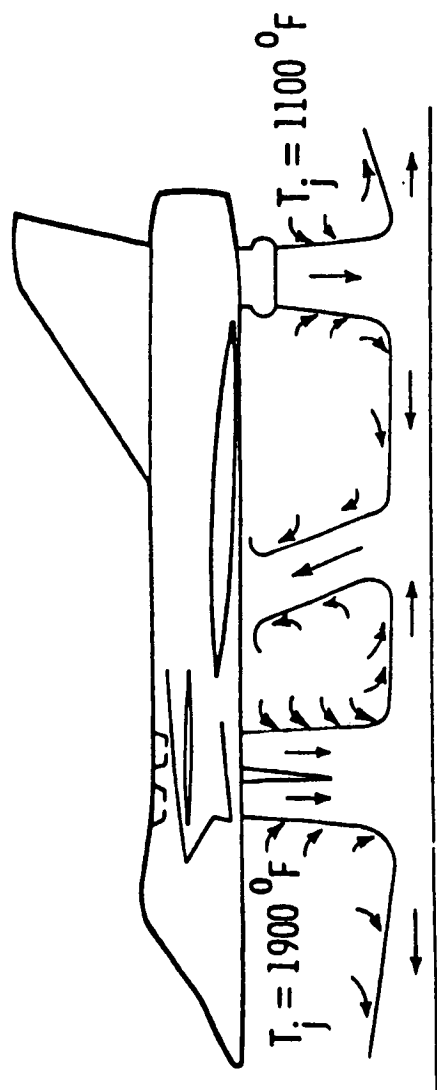


Figure 68.- Inlet temperature rise with fountain impingement. (Ref. 23)

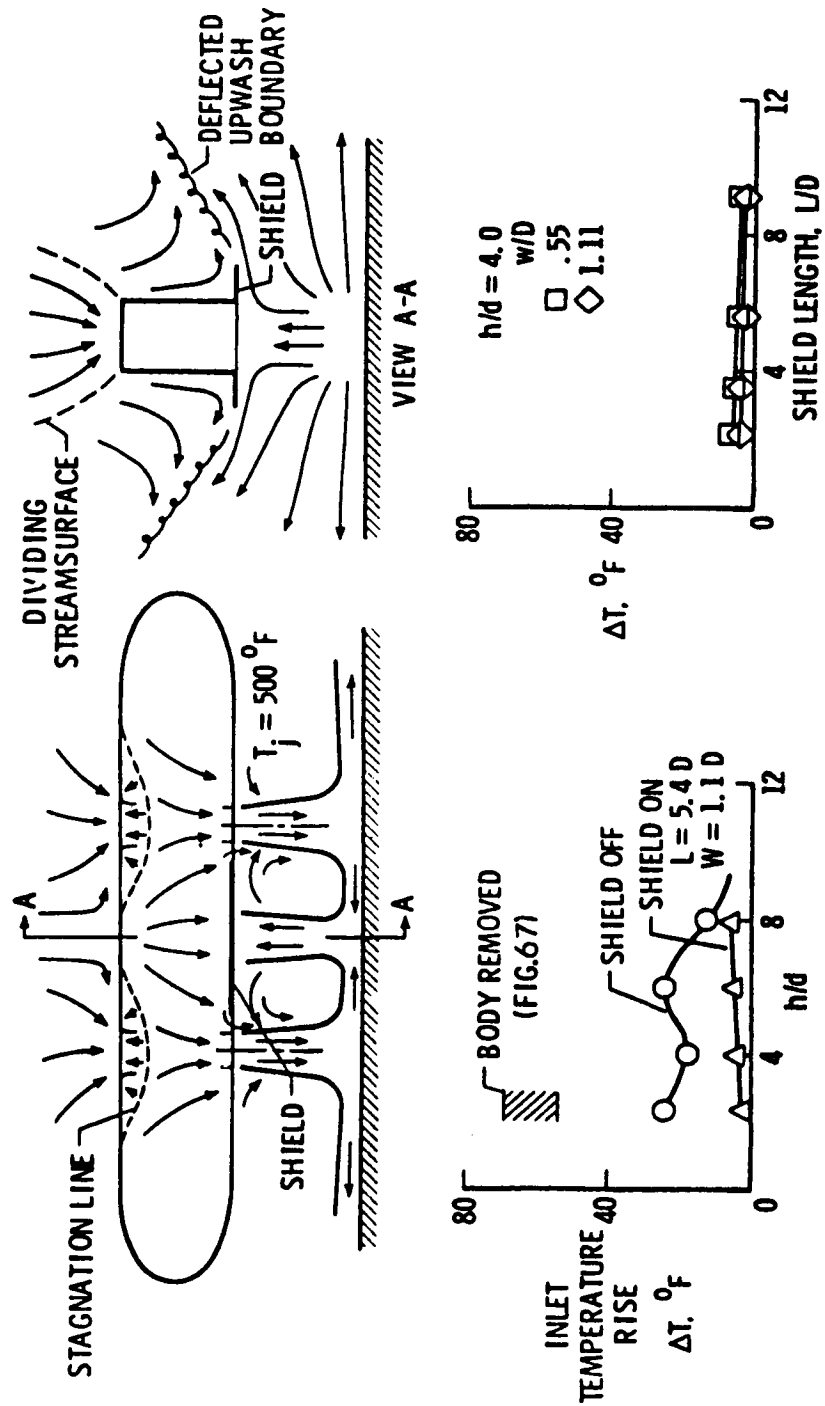


Figure 69.- Effect of exit plane shields. (Ref. 40)

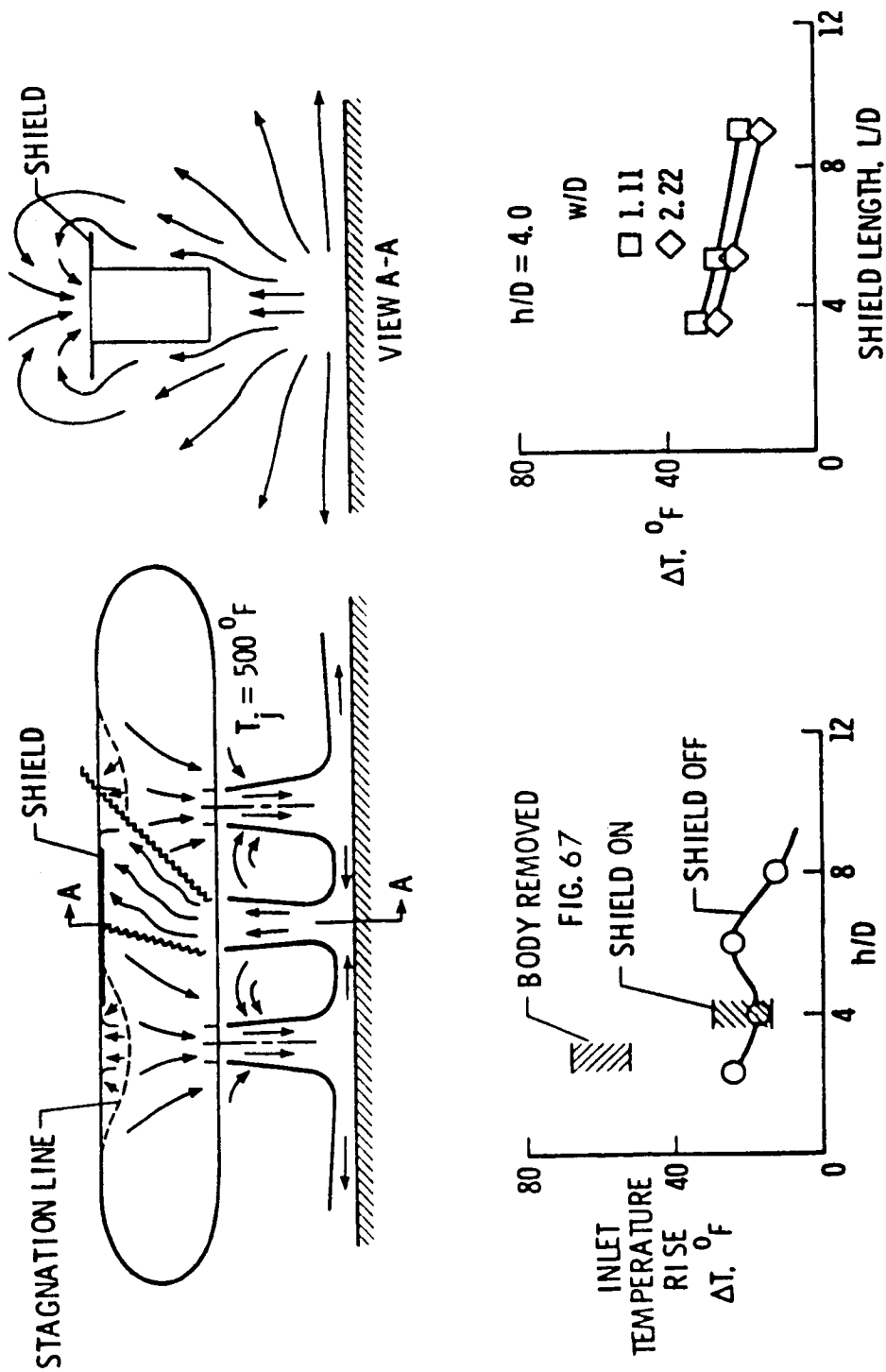


Figure 70.- Effect of inlet plane shields. (Ref. 40)



CONFIGURATION HAVING HIGH INGESTION  
 $h/D = 4.5$

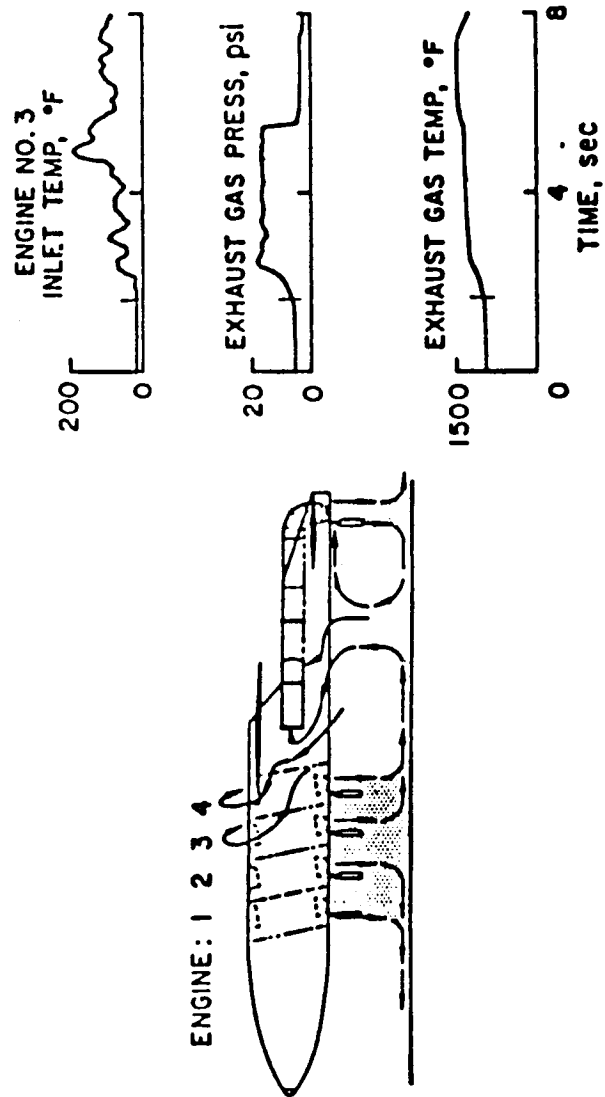


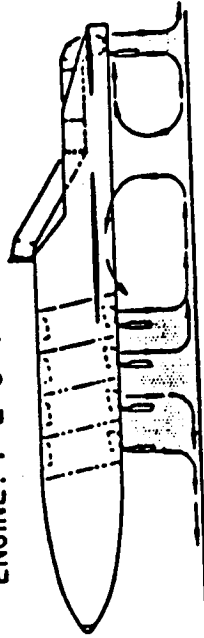
Figure 71.- Inlet temperature history for configuration having a high level of ingestion. (Ref. 41)

CONFIGURATION HAVING LOW INGESTION  
 $h/D = 4.5$

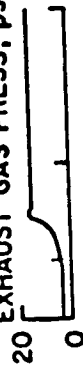
ENGINE NO. 3  
 INLET TEMP, °F



ENGINE: 1 2 3 4



EXHAUST GAS PRESS, psi



EXHAUST GAS TEMP, °F

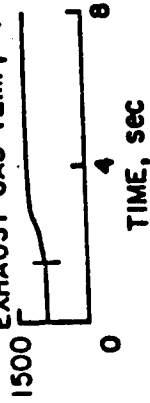


Figure 72.- Inlet time history for configuration having negligible ingestion. (Ref. 41)

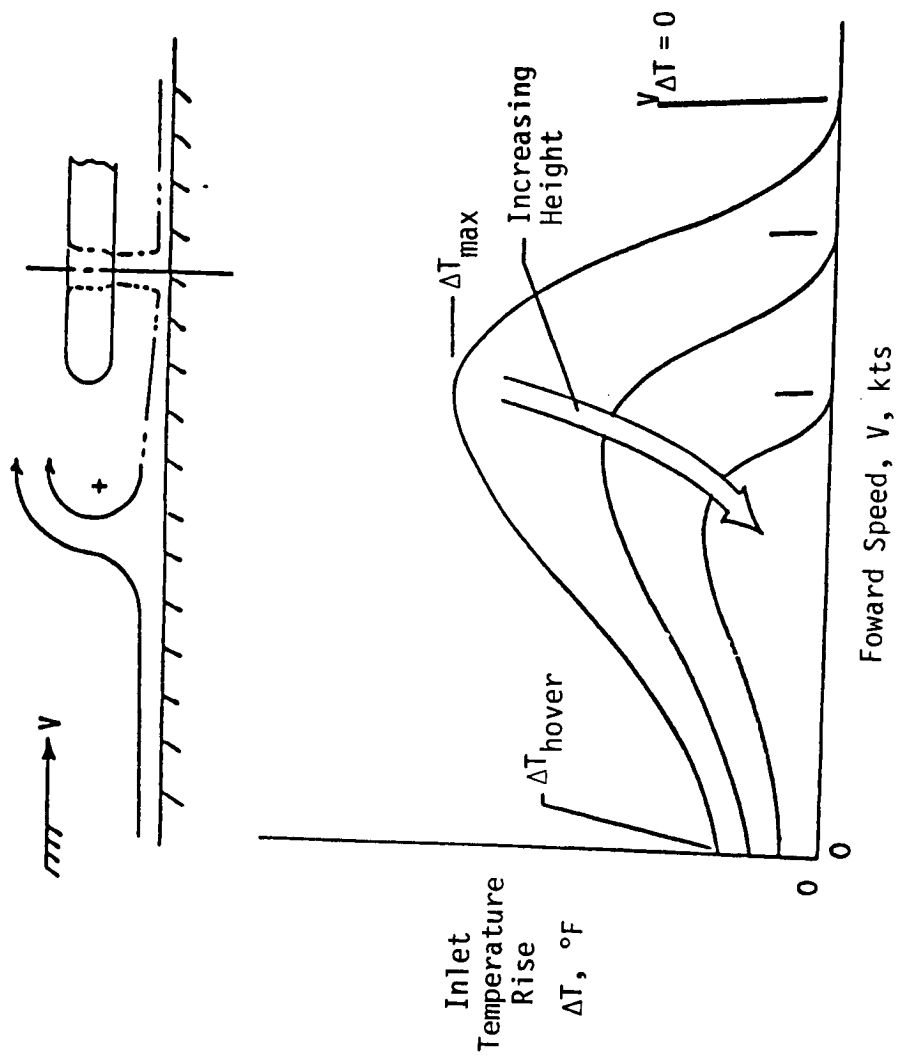


Figure 73.- Typical variation of inlet temperature rise with forward speed.

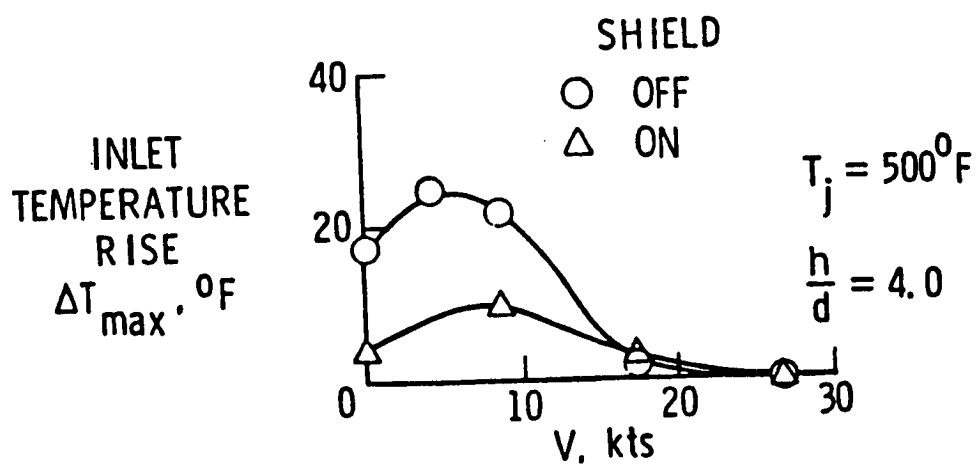
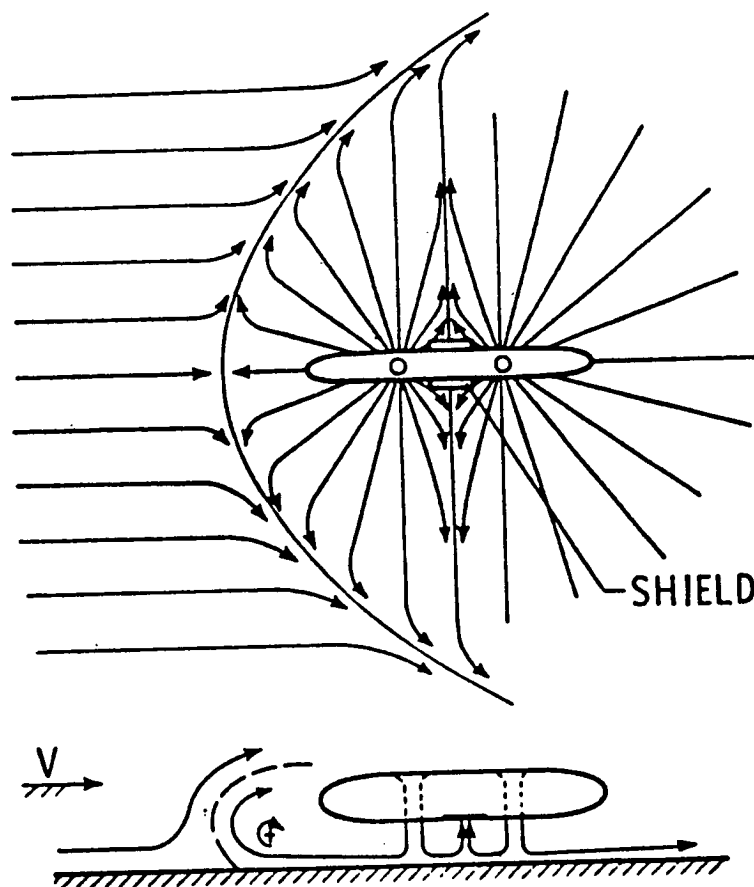


Figure 74.- Effect of free stream on configuration with two jets inline. (Ref. 40).

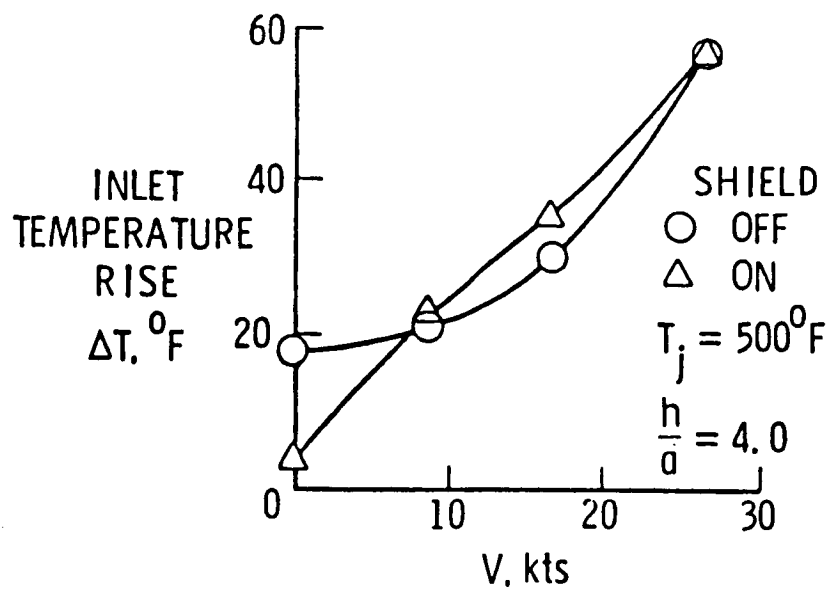
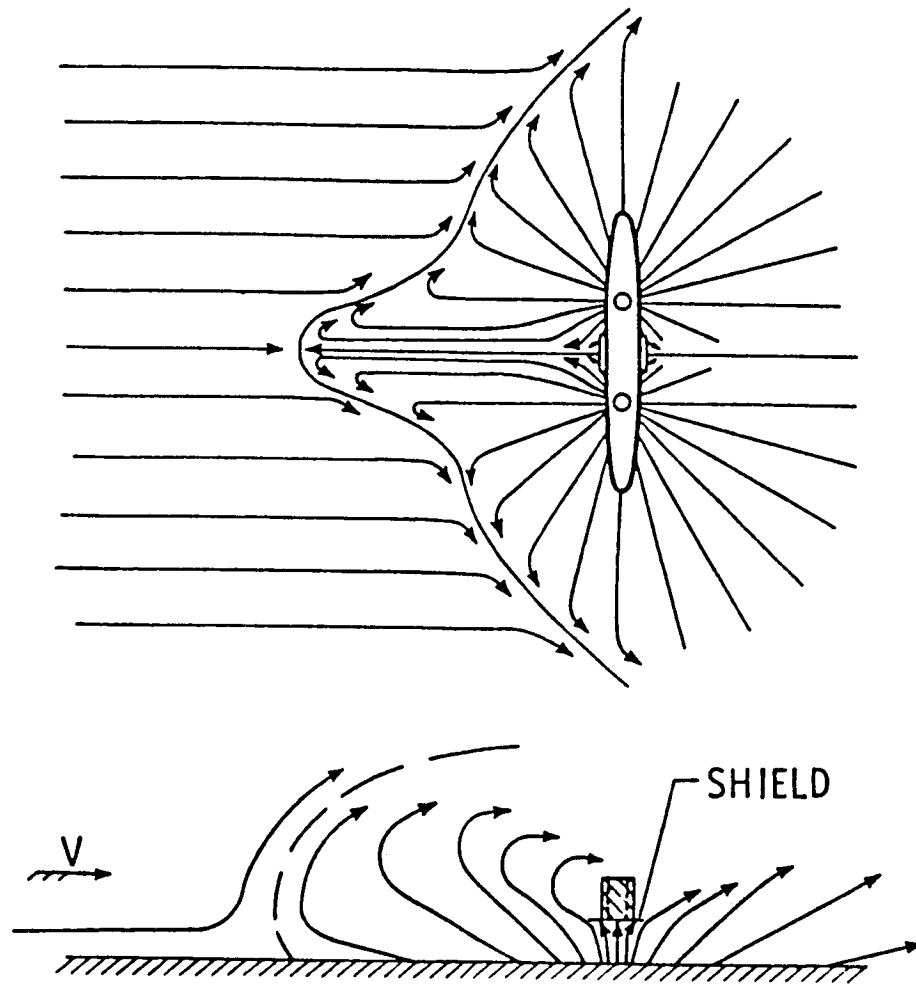


Figure 75.- Effect of free stream on side-by-side configuration. (Ref. 40)

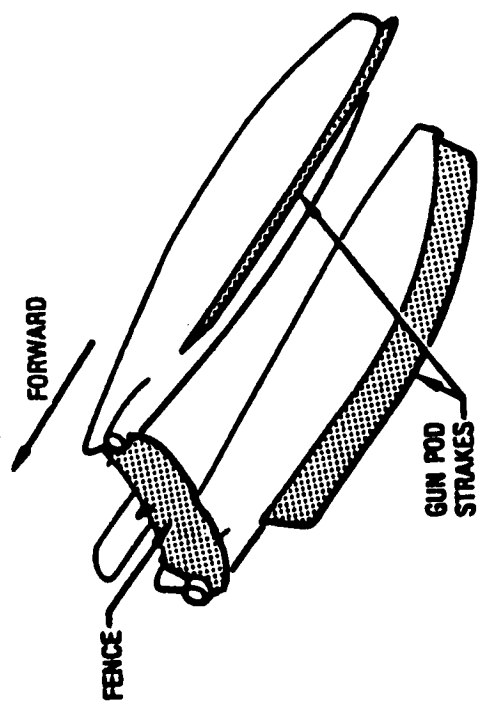


Figure 76.- Lift improvement devices on AV-8B. (Ref. 43)

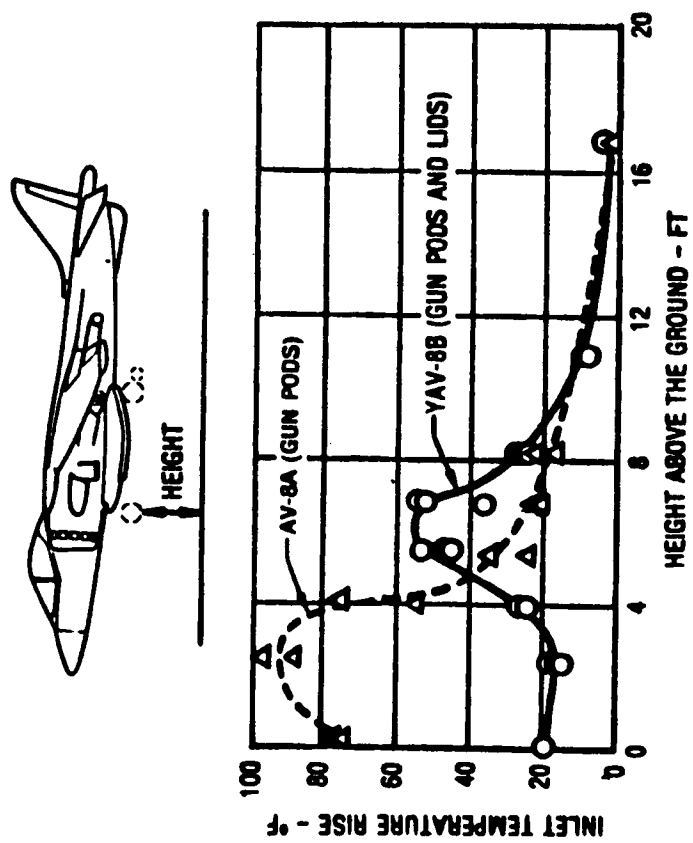


Figure 77.- Inlet temperature rise due to hot gas reingestion.

Static Scale Model Results Nozzles Vertical

(Ref. 43)

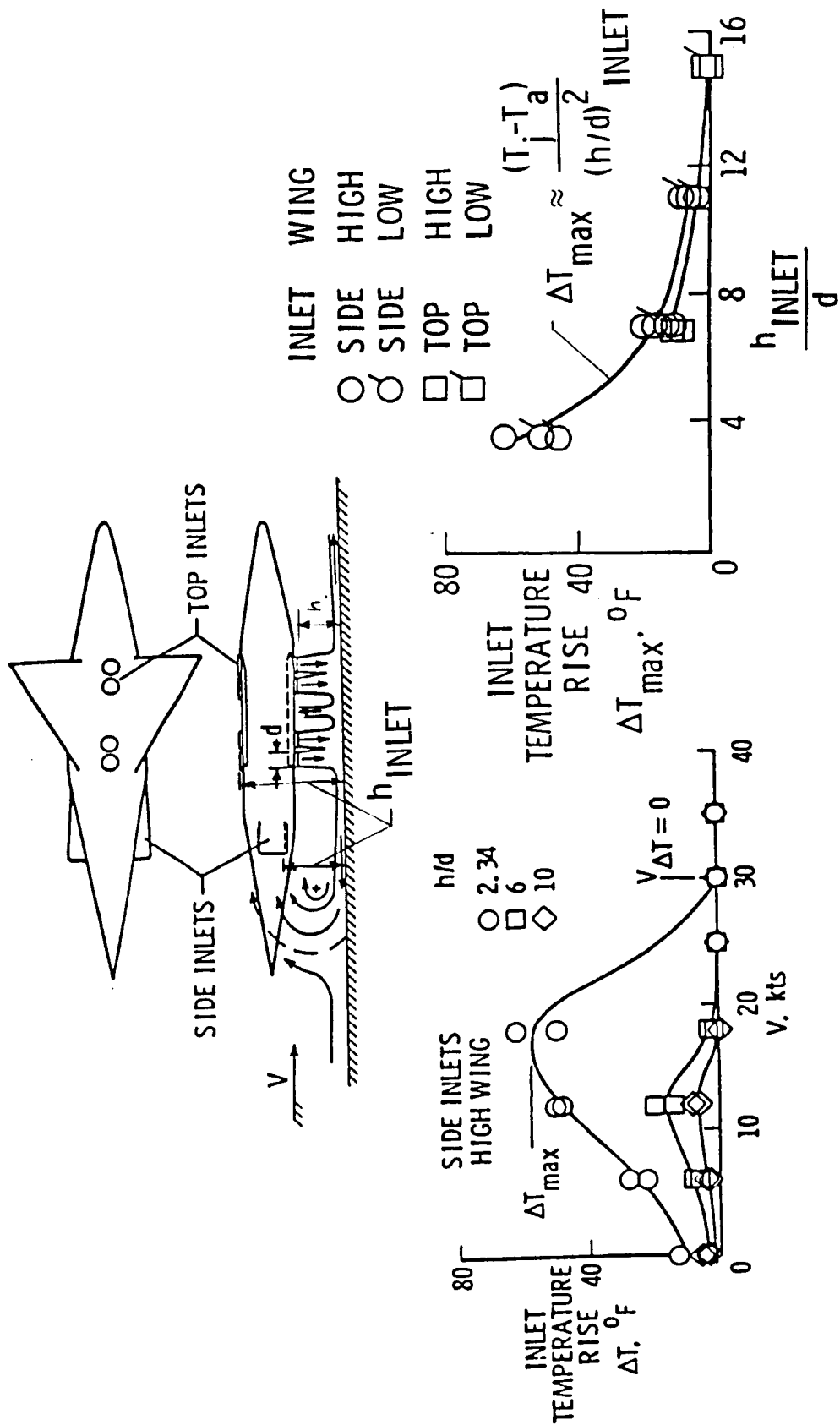


Figure 78.- Effect of height and velocity; four-jet in-line configuration. (Ref. 44)



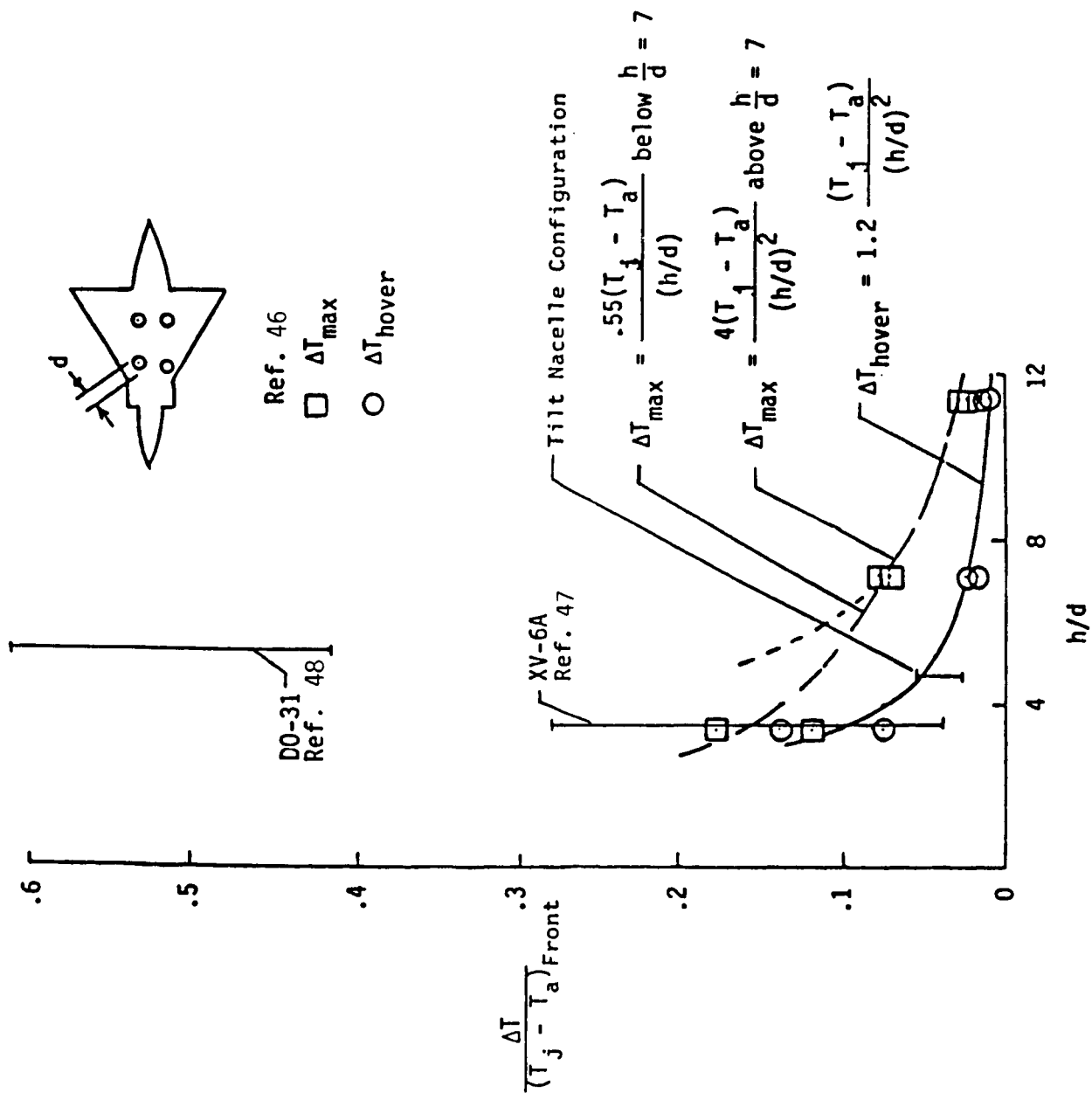


Figure 79.- Correlation of inlet temperature rise data, Ref. 45 configuration with side-by-side front jets.

# RECTANGULAR JET ARRANGEMENT

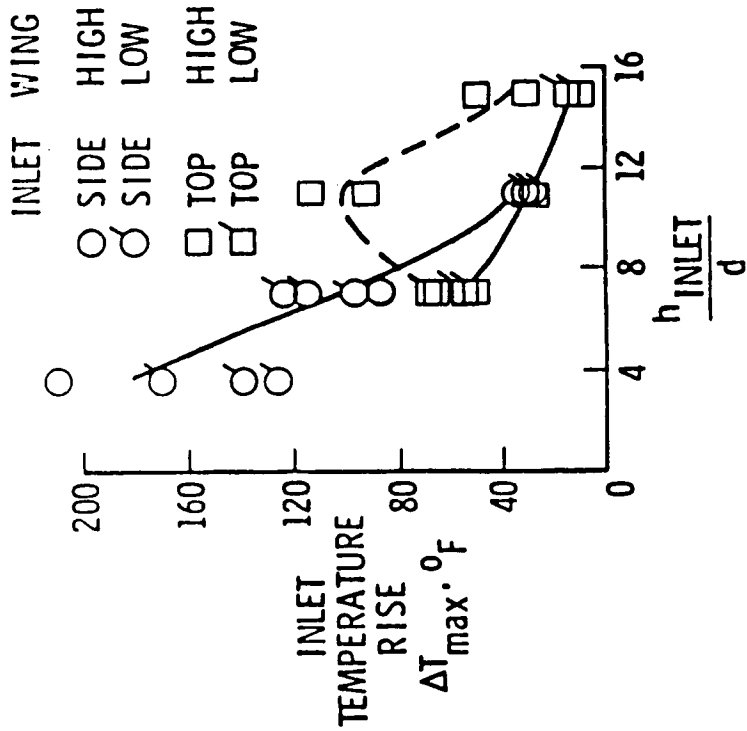
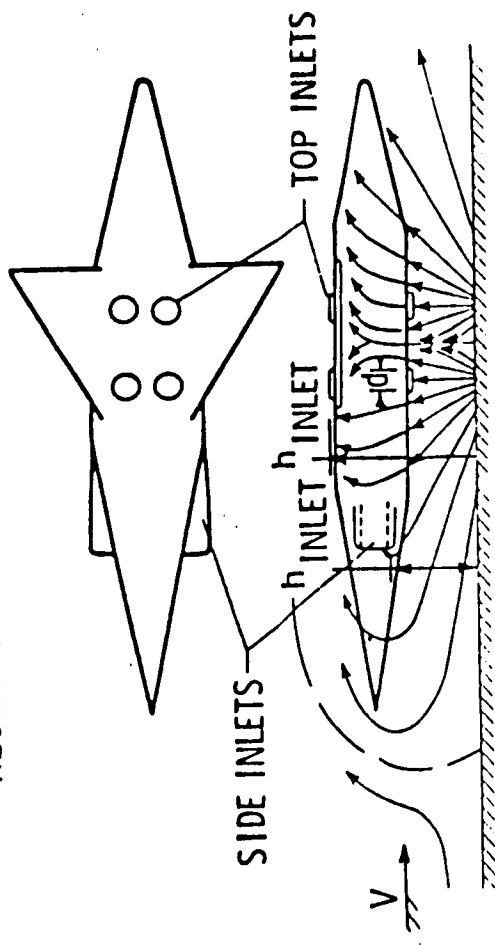


Figure 80.- Effect of inlet and wing location, Ref. 44; rectangular jet arrangement.

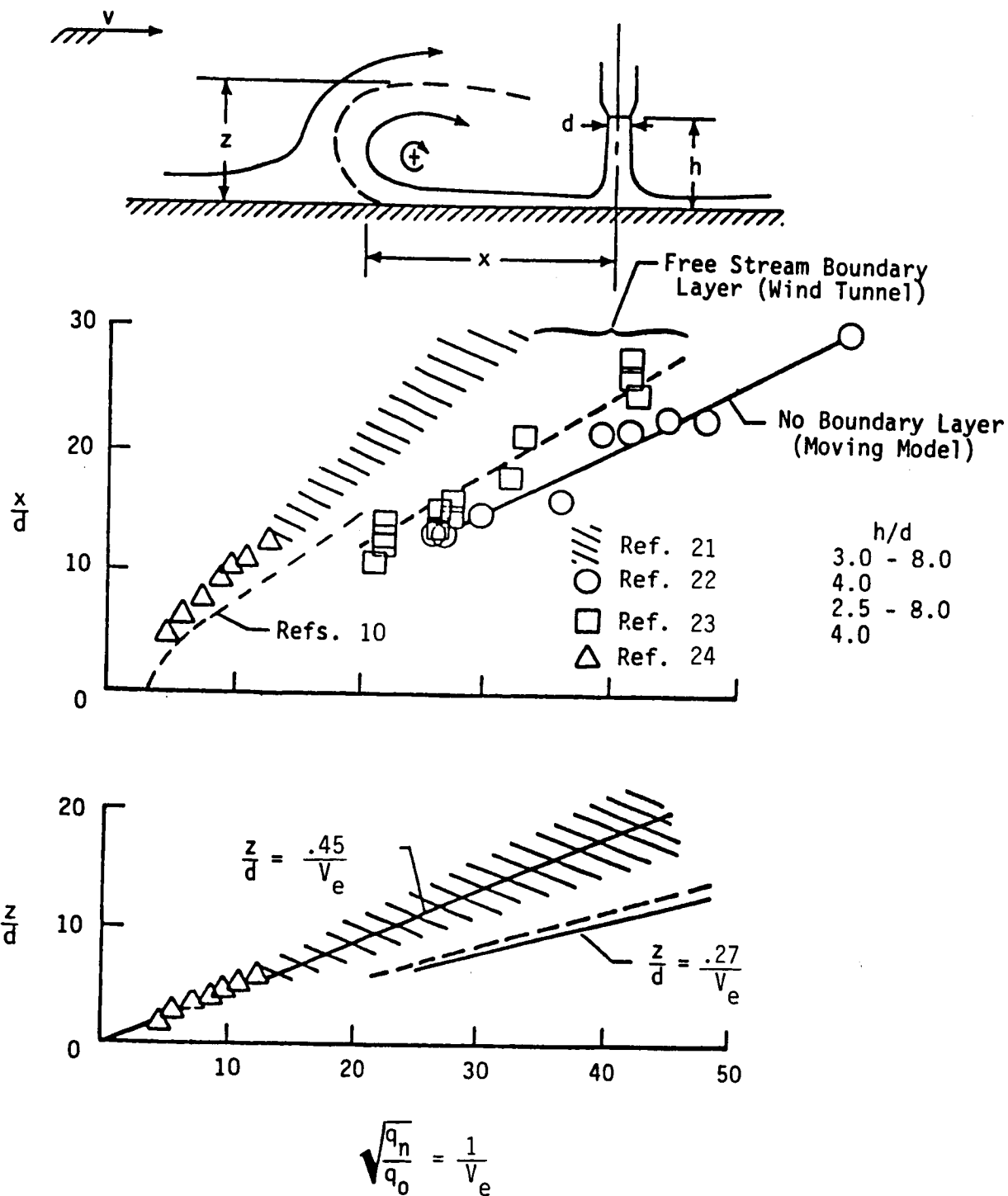


Figure 81- Size of Ground Vortex Recirculating Flow Region Generated by a Single Jet.

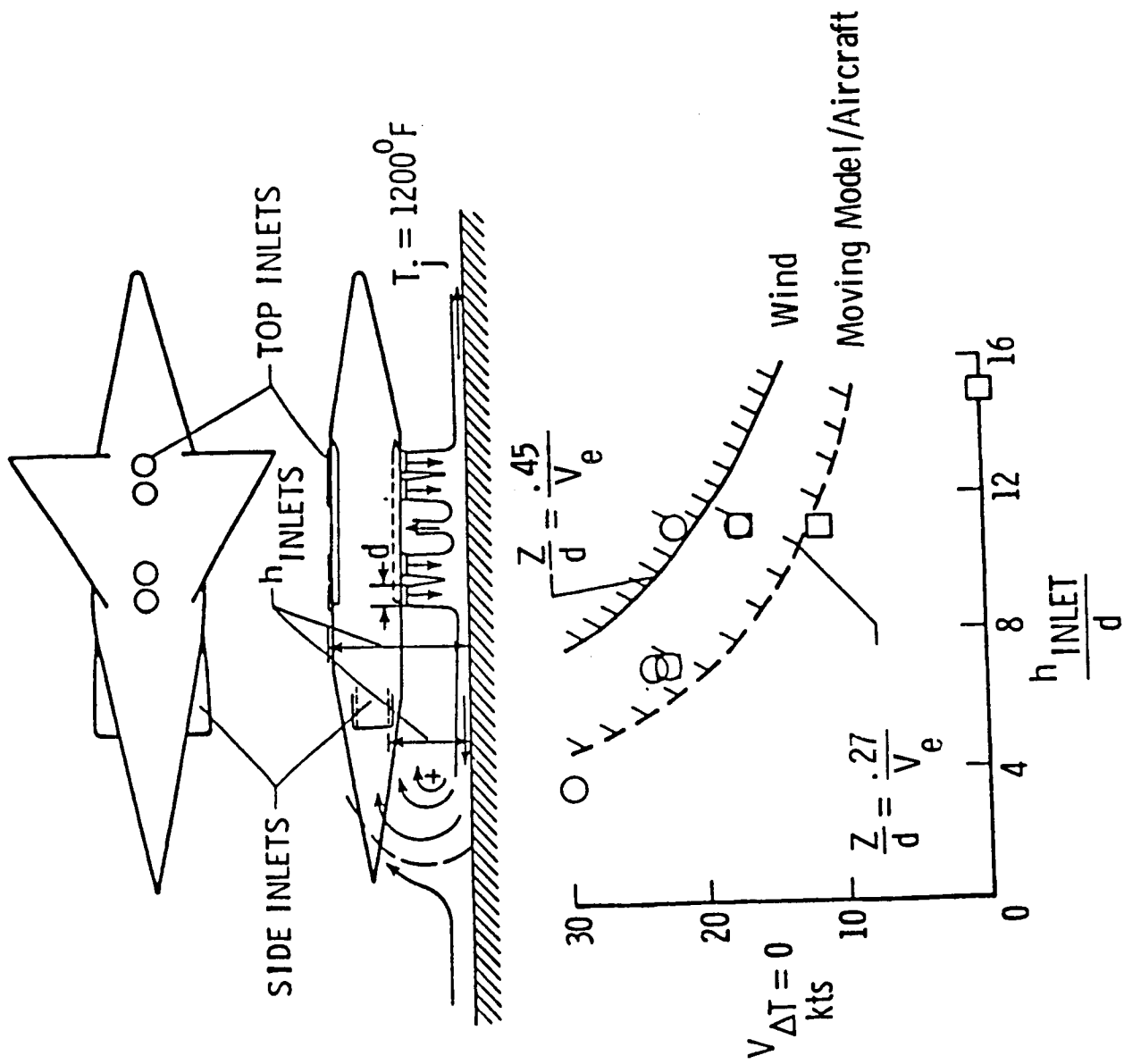


Figure 82.- Velocity required to avoid ingestion; in line jets. (Ref. 44)

# RECTANGULAR JET ARRANGEMENT

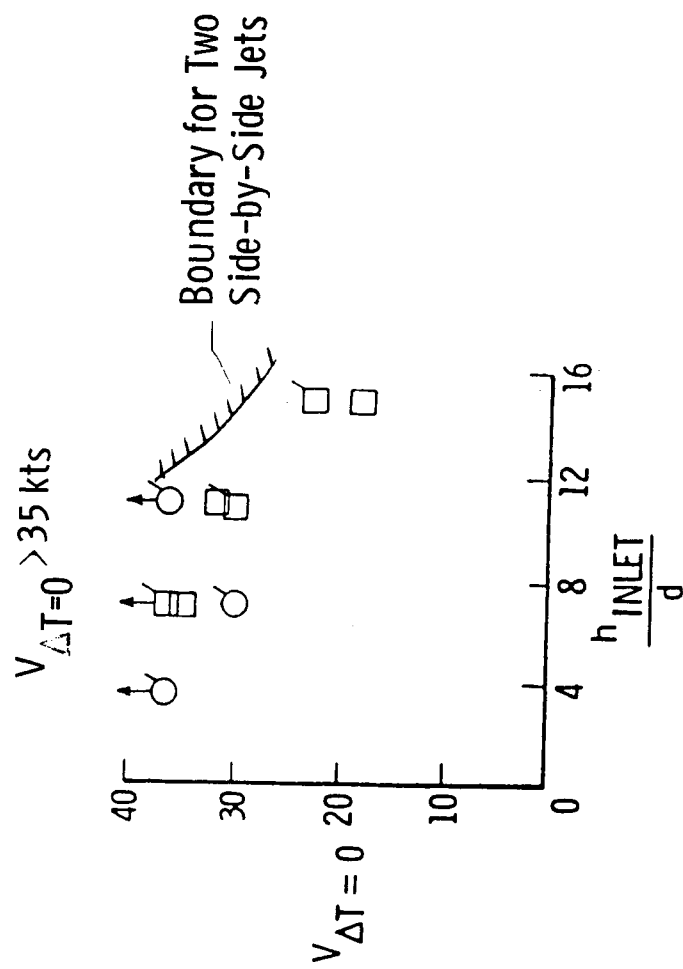
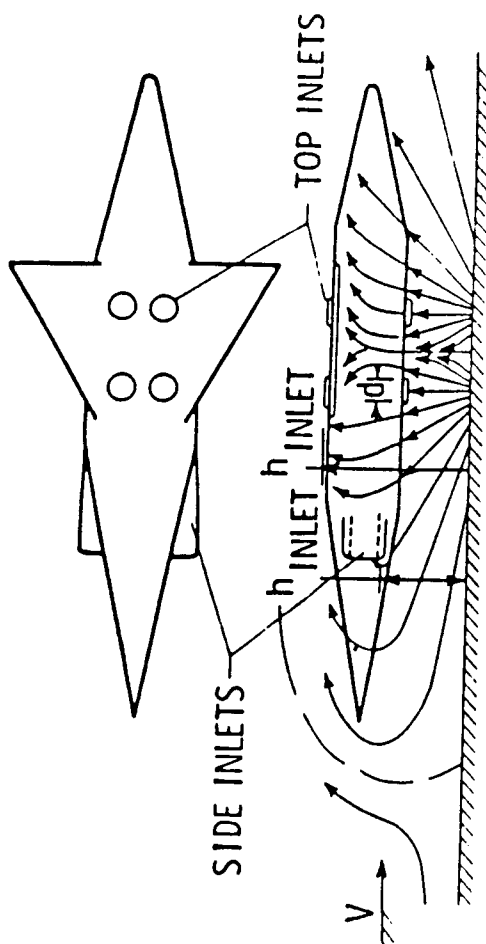


Figure 83.- Velocity required to avoid ingestion; configuration with forward fountain arm. (Ref. 44)

SEQUENCE PHOTOGRAPHS OF HOT-GAS CLOUD  
 FULL POWER, TOP INLET, SINGLE NOZZLE  
 ← 5-TO 8-KNOT WIND

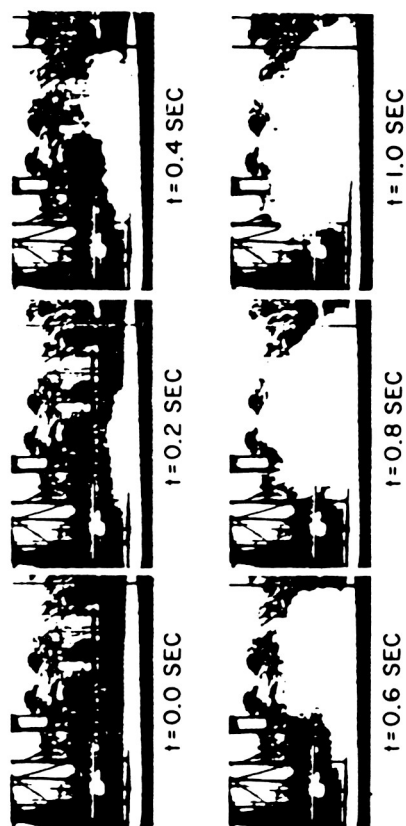
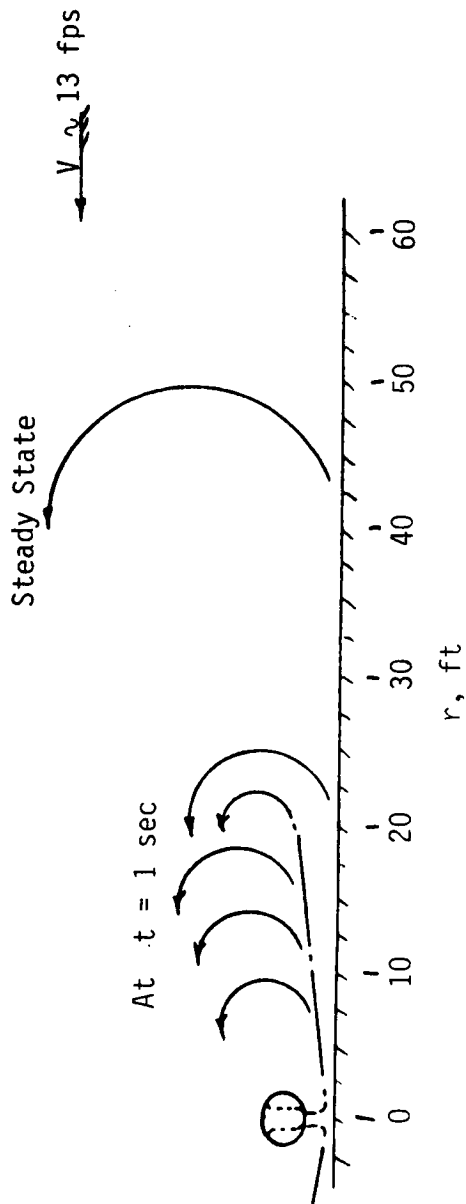
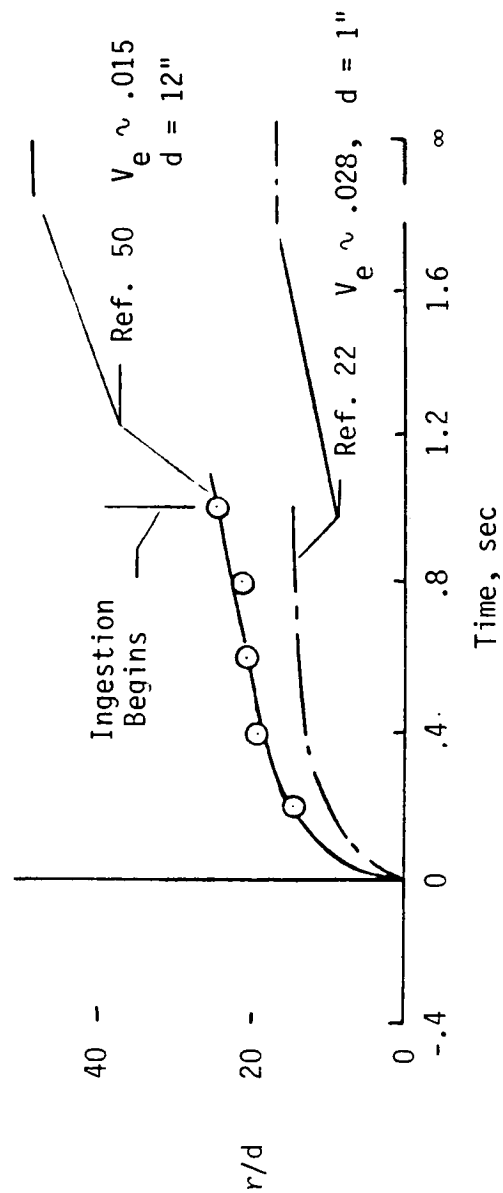


Figure 84.- Development of hot-gas cloud. (Ref. 50)

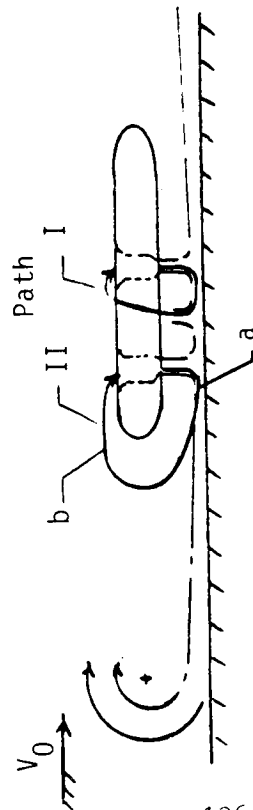


(a) Approximate flow field for configuration of Ref. 50.  
 $V_e \sim .015$ ,  $d = 12''$



(b) Time history of size.

Figure 85.- Growth of hot-gas cloud.



	Full Scale 1'	1/10 Scale .1'
Diameter		
Path I (Fountain)		
Distance	8' - 12'	.8' - 1.2'
Velocity $\rightarrow V_j$	Say 800 - 1200 fps	800 - 1200 fps
Time	.007 - .015 sec	.0007 - .0015 sec
Path II (Ground Vortex Flow)		
Distance	10 - 15'	1 - 1.5'
Velocity		
at a $\sim V_j$	1200 - 2000 fps	1200 - 2000 fps
at b $\sim V_0$	10 - 50 fps	10 - 50 fps
Time	.5 - 1.5 sec	.05 - .15 sec
Rate of Sink	$\sim 3$ fps	$\sim 30$ fps

Figure 86.- Time scaling considerations.



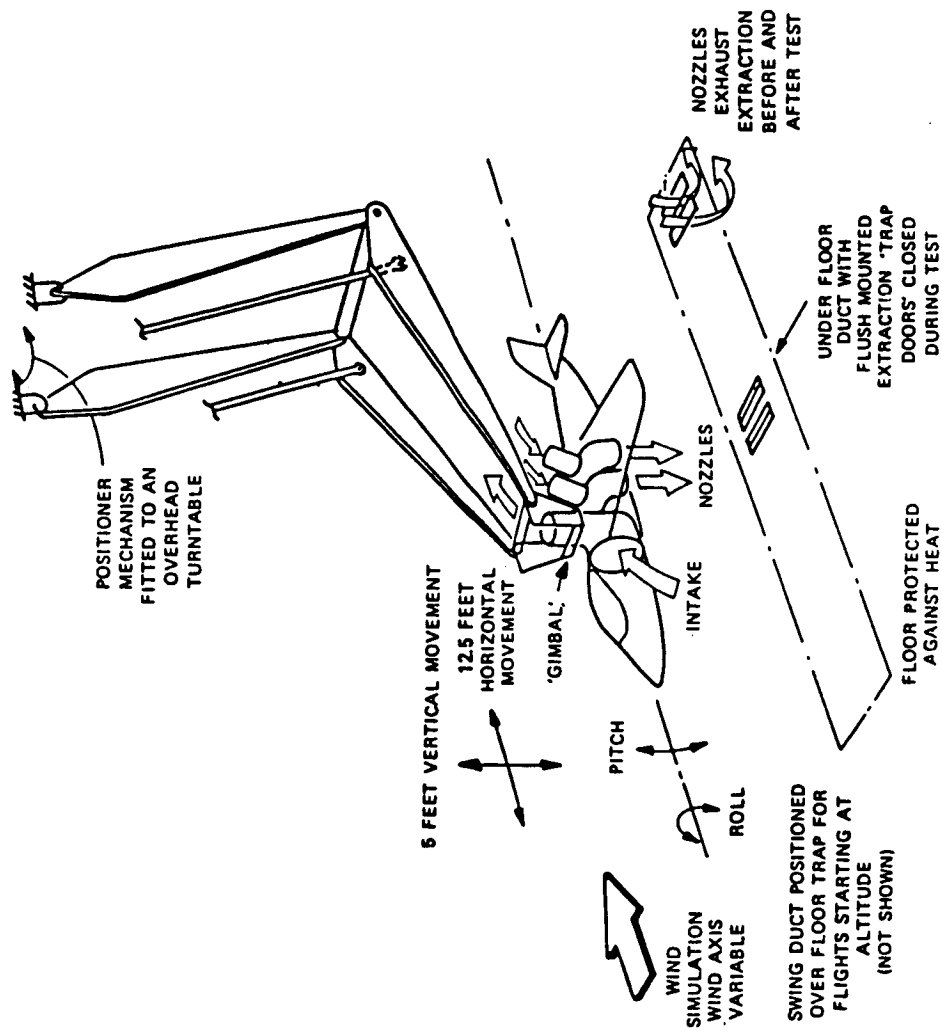


Figure 87.- British Aerospace Dynamic Hot-Gas Ingestion Test Rig, (Ref. 51).

$$\Delta T = k_1 (T_j - T_a) \quad \text{Abbott, Ref. 52}$$

$$\Delta T = k_2 (T_j - T_a) \left( \frac{T_j}{T_a} \right)^{-\frac{1}{2}} \quad \text{Milford, Ref. 53 and 54}$$

$$\Delta T = k_3 (T_j - T_a) \left( \frac{T_j}{T_a} \right)^{-n} \quad \text{Bore, Ref. 51}$$

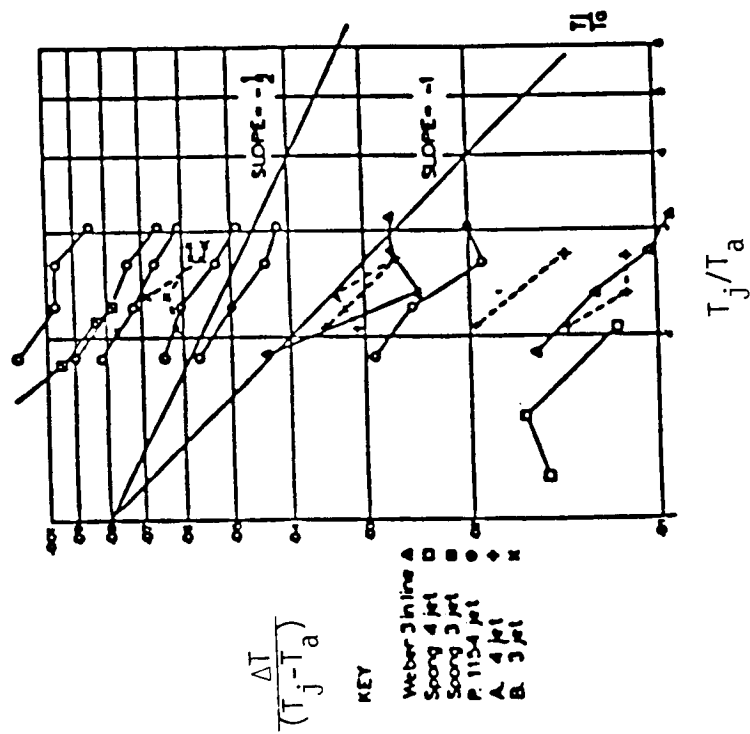


Figure 88.- Inlet temperature rise scaling.

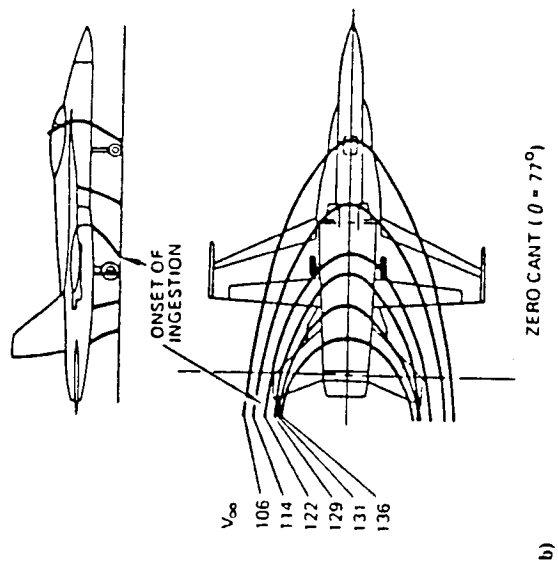
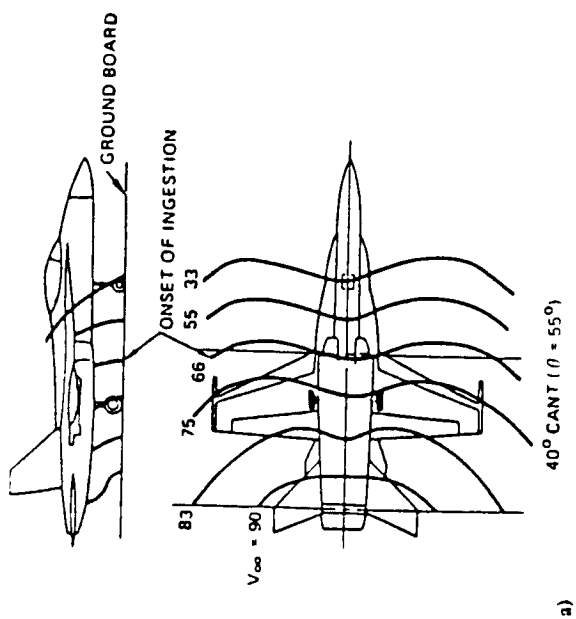
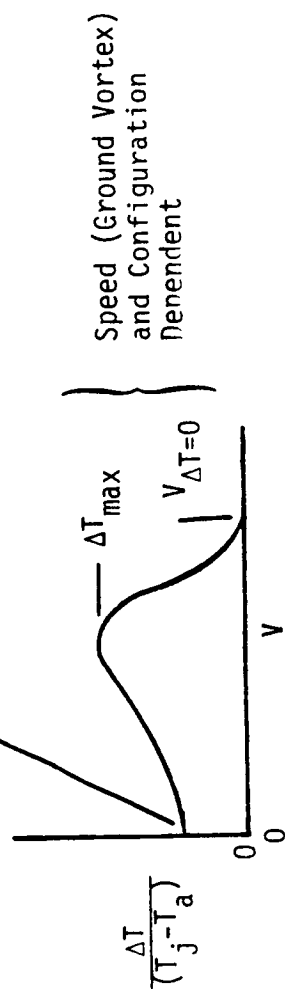


Figure 89.- Effect of lateral cant angle of thrust reverser flow on forward projection of hot gas flow. (Ref. 55)

Configuration (Fountain) Dependent



Vary

- Jet Configuration
  - Single Jet
  - Side-by-Side Jets
- Inlet Position
- Pressure Ratio
- Velocity Ratio
- Jet Deflection and Cant Angles

Temperature and Velocity Surveys

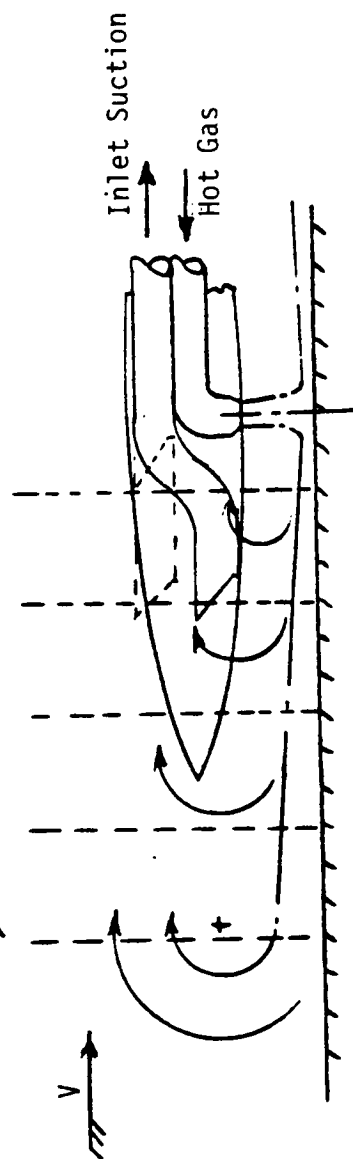
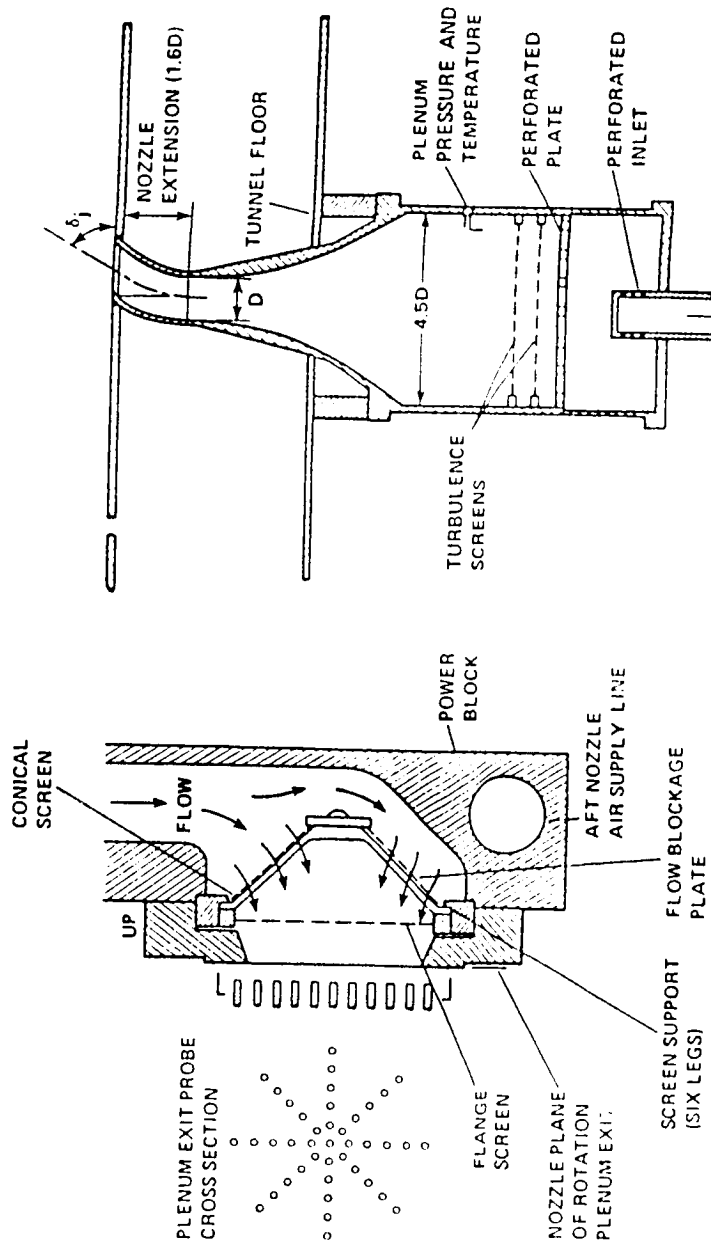


Figure 90.- Investigate rate of development and steady state flow field.



(a) Nozzle/Air-Feed design for limited space, (Ref. 19).

(b) Nozzle/Plenum-Chamber Design for good quality jet flow, (Ref. 57).

Figure 91.- Typical systems for using high pressure air for jet simulation. (Ref. 56)



ORIGINAL PAGE IS  
OF POOR QUALITY

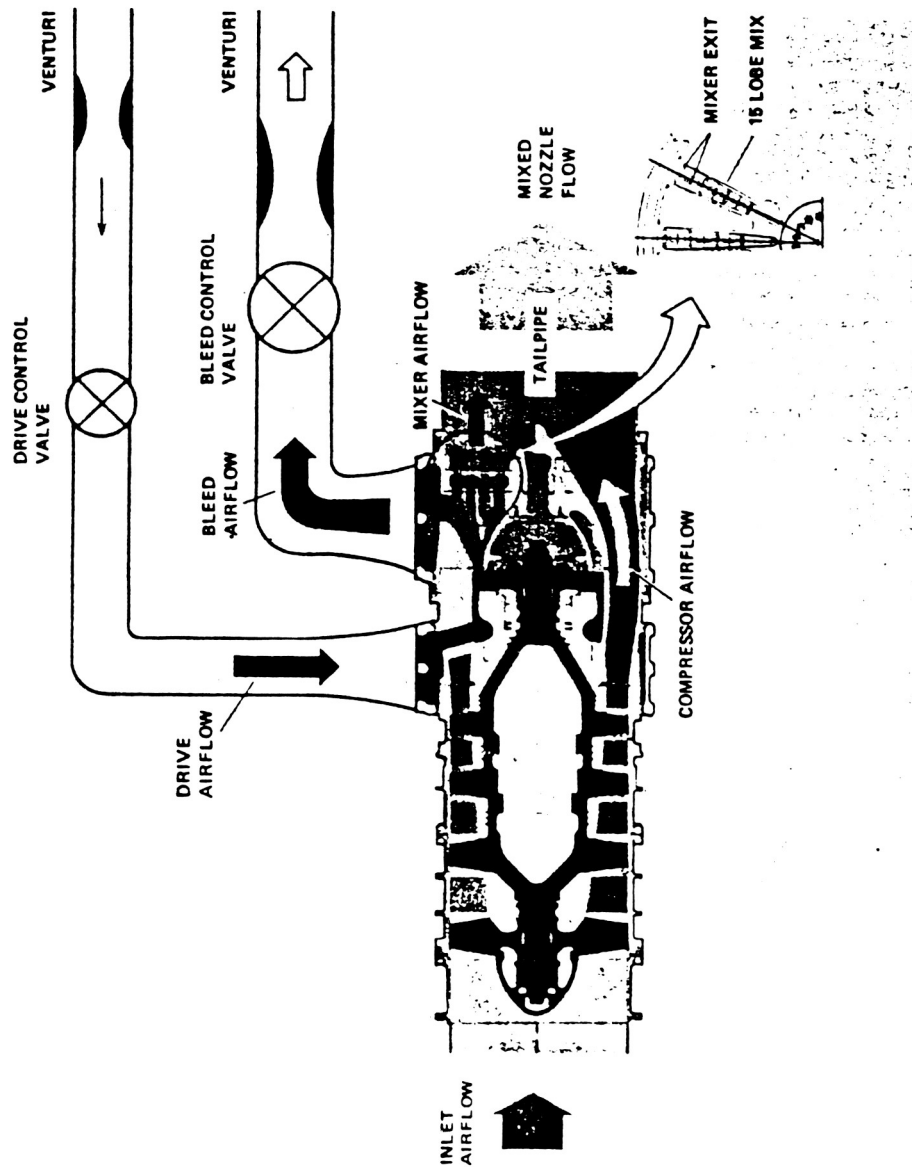


Figure 93.- Schematic of compact multission aircraft propulsion simulator. (Ref. 56)

$$h/d = 3$$

REFLECTION PLATE

O WITHOUT  
Δ WITH

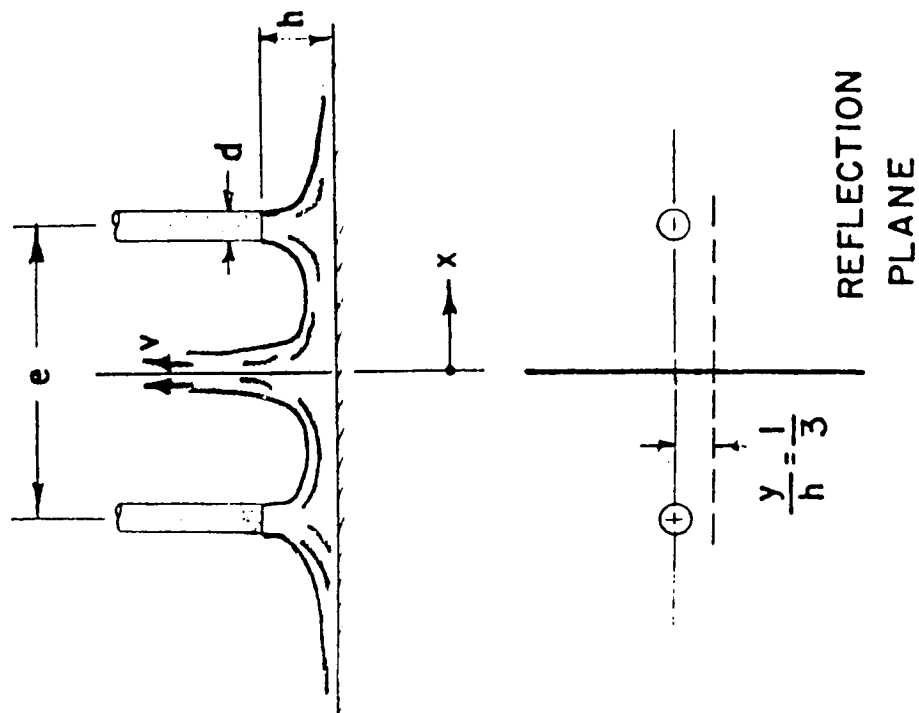
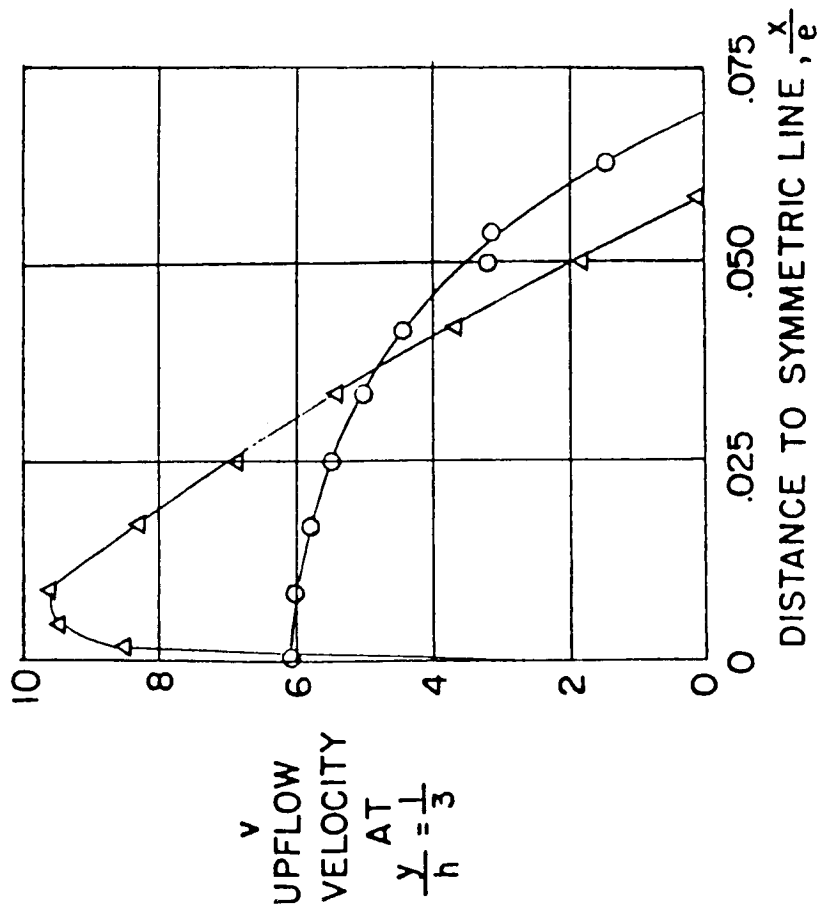


Figure 94.- Effect of a reflection plate on the measured upflow velocities in the fountain flow caused by two jets exiting vertically near the ground. (Ref. 58).



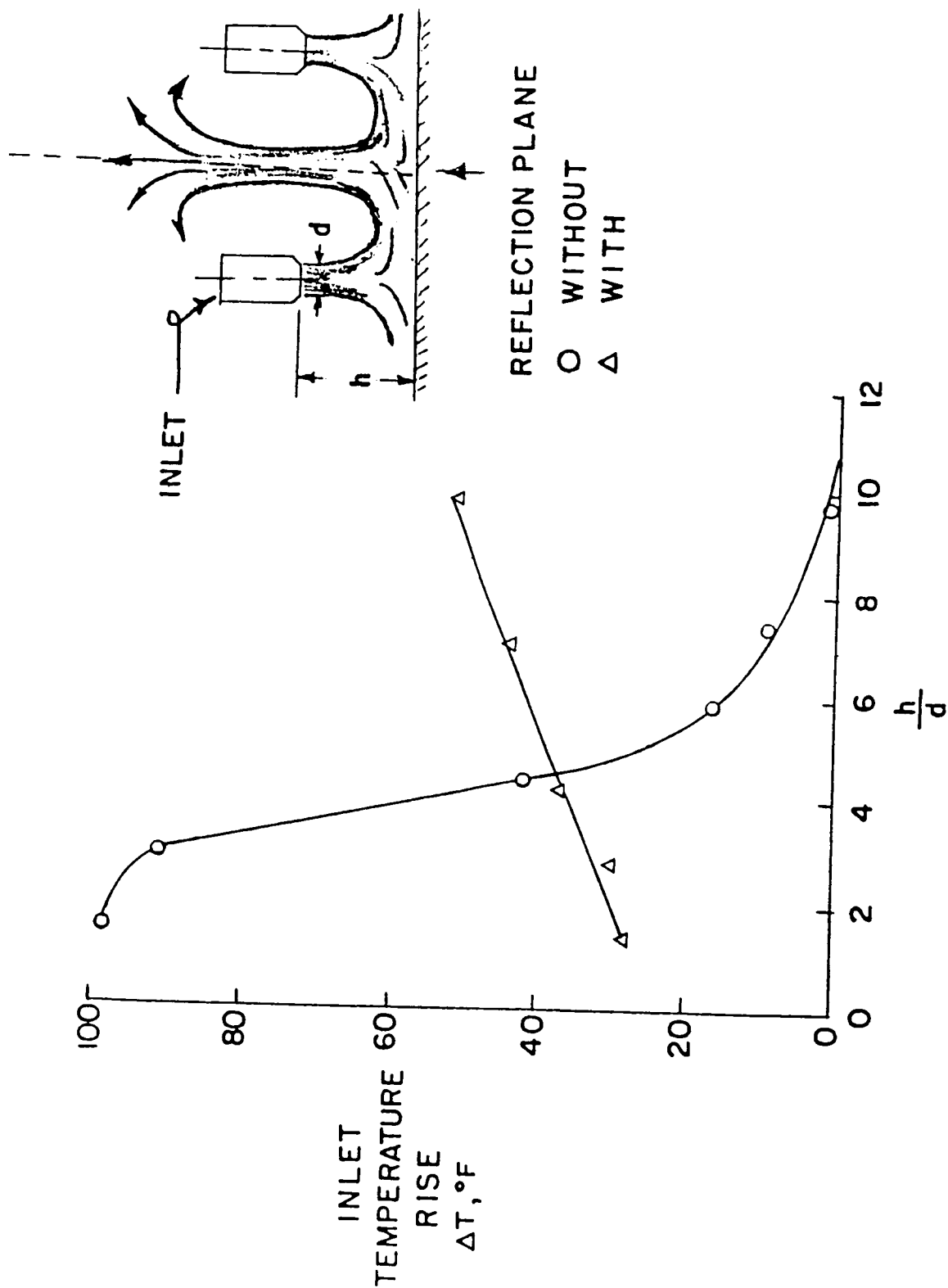


Figure 95.- Effect of a reflection plane on the measured inlet air temperature rise resulting from the fountain flow caused by two jets exiting vertically near the ground. (Ref. 59)